New Constructions of Optical codes, and Analysis for SAC - OCDMA Systems

Ph.D. Thesis

Mrs. Soma Kumawat
ID No. 2013REC9531

Department of Electronics and Communication Engineering
Malaviya National Institute of Technology Jaipur

Aug 2018

New Constructions of Optical codes, and Analysis for SAC - OCDMA Systems

Submitted in
fulfillment of the requirements for the degree of

Doctor of Philosophy

by

Mrs. Soma Kumawat
Id: 2013REC9531

Under the Supervision of

Dr. M. Ravi Kumar

Department of Electronics and Communication Engineering
Malaviya National Institute of Technology, Jaipur

Aug 2018

DECLARATION

I, Mrs. Soma Kumawat, declare that this thesis titled, "New Constructions of Optical codes, and Analysis for SAC - OCDMA Systems" and the work presented in it, are my own. I confirm that:

a. This work was done wholly or mainly while in candidature for a research degree at this university.

b. Where any part of this thesis has previously been submitted for a degree or any other qualification at this university or any other institution, this has been clearly stated.

c. Where I have consulted the published work of others, this is always clearly attributed.

d. Where I have quoted from the work of others, the source is always given. With the exception of such quotations, this thesis is entirely my own work.

e. I have acknowledged all main sources of help.

f. Where the thesis is based on work done by myself, jointly with others, I have made clear exactly what was done by others and what I have contributed myself.

Date

Mrs. Soma Kumawat
(2013rec9531)

CERTIFICATE

This is to certify that the thesis entitled " **New Constructions of Optical codes, and Analysis for SAC - OCDMA Systems**" being submitted by **Mrs. Soma Kumawat (2013rec9531)** is a bonafide research work carried out under my supervision and guidance in fulfillment of the requirement for the award of the degree of Doctor of Philosophy in the Department of Electronics and Communication Engineering, Malaviya National Institute of Technology, Jaipur, India. The matter embodied in this thesis is original and has not been submitted to any other University or Institute for the award of any other degree.

Place: Jaipur
Date:

Dr. M. Ravi Kumar
Associate Professor
Department of Electronics and Communication Engineering
Malaviya National Institute of Technology, Jaipur
India 302017.

Dedicated to

My Family

Acknowledgments

First of all, I would like to express my greatest gratitude to bharma baba, for His help and support during the course of life and the moment of truth. He give insight me to find a path to approach my destiny.

I would like to express my appreciation and sincere gratitude to my supervisor, Dr M. Ravi Kumar for his continuous support, encouragement and endless patience towards completing the research. These special thanks also dedicated to DREC members; Dr Vijay Janyani , Dr Ghanshyam Singh and Dr Ritu Sharma. for their invaluable guidance and constructive criticisms throughout the success of this thesis.

My sincere thanks to my lab mates Amit Garg, Nikhil Deep, Nitesh Kumar, Usha Mam, Sourbha Sahu, and Abhinav Bhatnagar for their help and support. I would like to thank Mr. Bipin Sir for their technical assistance in Optical lab. I am also thankful to all ECE department members for their direct and indirect support.

Without the love and support of my family, this would have been a very hard journey. I am dedicating this work to my husband Mr. Sudhir Mamoria; for giving me an unwavering love and support. I dare not even imagine how it would have been without you! I thank to my mother in law Mrs. Manju lata; for their appreciation and to believe in myself and support throughout the duration of Ph.D work. This is thanks to my daughter and son, Gauri Mamoria and Rishi Mamoria; for their patience throughout my work. A lot of thanks to my family for their continues support and huge appreciations towards my work. This dissertation was impossible without their support.

Lastly, I would like to thank all people who have helped and inspired me in the research contribution to this thesis.

Mrs. Soma Kumawat

List of Important Abbreviations

1D	One dimensional
2D	Two dimensional
BBS	Broad Band Sources
BD	Balanced Detection
BER	Bit Error Rate
CDMA	Code Division Multiple Access
CW	Constant Weight
CL	Constant Length
DD	Direct Detection
DW	Double Weight
EDW	Eahanced Double Weight
FCC	Flexible Cross Correlation
FBG	Fiber Bragg Gratings
IPCC	In Phase Cross Correlation
KS	Khazani Syed
LED	Light Emitting Diodes
MAI	Multiple Access Interference
MDW	Modified Double Weight
MZM	Mach Zehnder Modulator
MQC	Modified Quadratic Congruence
MFH	Modified Frequency Hopping
MS code	Multi Service code
OCDMA	Optical Code Division Multiple Access
PDs	Photo Detector
PIIN	Phase Induced Intensity Noise
PSD	Power Spectral Density

QoS	Quality of Service
RD code	Random Diagonal code
SAC	Spectral Amplitude Coding
SNR	Signal to Noise Ratio
S/S	Spectral/Spatial
VW	Variable Weight
WDMA	Wavelength Division Multiple Access
ZCC	Zero Cross Correlation
ZCCC	Zero Cross Correlation Code

List of Important Symbols

d_k	Data bit of the kth user
e	electron charge
$G(v)$	single sideband Power Spectral Density (PSD) of the source
(hv_0)	Photon energy
h	Planck's constant
I	Average photocurrent
P_{sr}	Effective power of a broadband source at the receiver
$\langle I^2_{PIIN} \rangle$	Phase-Induced Intensity Noise (PIIN)
$\langle I^2_{shot} \rangle$	Shot noise
$\langle I^2_{thermal} \rangle$	Thermal noise
τ_c	Coherence time
v	Linewidth of broadband source
$\mathcal{R}$	Responsivity
K_b	Boltzmanns constant
M	Basic matrix
N_B	Number of users of basic matrix
L_B	Code length of basic matrix
η	Quantum efficiency
T_n	Receiver noise temperature
B	Electrical bandwidth
R_L	Receiver Load resistor
λ_c	IPCC
L	Code length
W	Code weight
$\lfloor x \rfloor$	$Floor$(x)
$\lceil x \rceil$	$Ceil$(x)

List of Figures

List of Tables

Abstract

Spectral Amplitude Coding - Optical Code Division Multiple Access (SAC-OCDMA) systems are a type of OCDMA technique in which unique codes are mapped to different spectral lines of a broadband source. It eliminates the Multiple Access Interference (MAI) when codes with fixed In Phase Cross Corelation (IPCC) are used as address sequences. Double Weight (DW) codes are one of the code families reported for SAC-OCDMA systems. The property of these codes are that they have weight chips always in pairs. Due to that property, filtering requirements are reduced. These codes have ideal IPCC property. The code construction steps are easy to impelement. DW code structure is obtained only for weight two. The weight constraint inspires to develop codes with other weights. Modified Double Weight (MDW) code is also reported for even weights, greater than two. DW and MDW codes are limited to even weights. The code construction for odd weights greater than one is described and, that code is called Enhanced Double Weight (EDW) code. Khazani-Syed (KS) Code for even weights was constructed using combination of DW and MDW codes.

To generate a code for DW code family, first step is to construct a basic matrix. Depending on the number of users required in the code family, the basic matrix is repeated diagonally, known as mapping technique. Due to mapping, increment of code length is not constant. Even though mapping and crosscorrelation constraints are similar for all codes families of DW, they have different code construction algorithms, length and other properties. A generalised algorithm to construct these codes is a gap in literature which is investigated in this thesis with and without mapping.

A new generalized algorithm to construct EDW and MDW (PC1) like codes without mapping is proposed. The code construction is independent of mapping technique. Crosscorrelation value is equal to or less than 1 among all users. A single algorithm (PC1) is designed which provide the standardized formulation of code length, Signal to Noise Ratio (SNR) and Bit Error Rate (BER) for all weight greater than 2. It (PC1) designs code for Constant Length (CL) and Constant Weight (CW). The numerical results using balanced detection and direct detection are obtained and compared.

The above proposed codes are developed for CL and CW which are not suitable for multimedia services. Variable Weight (VW) algorithm (PC2) is proposed which is based on PC1. The cross correlation among all users is at most 1. This code construction algorithm ensures higher power at receiver for higher weight users. Lower weight users receive less power compared to higher weight users. The difference in received power translates as varying performance, and are useful for multimedia applications.

The above proposed codes are constructed without using mapping technique. The effect of mapping and to construct the single code construction algorithms with mapping for all weights are proposed and analysed. Like DW code families, Basic matrix is first constructed using proposed algorithm. The number of users for basic code matrix depends on the code weight and on a constant value. As size of basic matrix is changed, BER and code length of users are changed. All above described codes are 1 Dimensional (1D) which have a limitation of fewer users due to finite bandwidth of source. To solve this problem, 2 Dimensional (2D) code construction is also proposed using proposed 1D code. 2D code gives better performance with higher cardinality compared to 1D code. Khazani-Syed (KS) Code for odd weights construction is also proposed.

MAI can be removed from SAC-OCDMA system by using electrical subtraction, but Phase Induced Intensity Noise (PIIN) still remains. All the above codes suffer from PIIN. A code design with zero cross correlation (ZCC) property removes the effect of MAI and suppress the effect of PIIN. The code with the property of ZCC is called as Zero Cross Correlation Code (ZCCC). The code structure of ZCCC does not have any overlapping of wavelengths between any users. A new code with zero cross correlation, termed as Zero Cross Correlation Code (ZCCC) is proposed without mapping. Code construction algorithm is designed with any weight for any number of users having constant, or variable weights. Variable weight (VW) codes give different quality of service, and are useful for multimedia applications.

Key Words - SAC-OCDMA, DW, MDW, EDW, MAI, IPCC, ZCCC.

Contents

CHAPTER 1

Introduction and Review

1.1 Introduction

Optical networks provide the solution towards increased spectrum demand. The utilization of spectrum in proper and convenient manner is next raised question which is answered by different access techniques. They provide access and sharing of spectrum efficiently among different users. There are several access techniques such as Wavelength Division Multiple Access (WDMA) [1], Optical Time Division Multiple Access (OTDMA) [2], and Optical Code Division Multiple Access (OCDMA) [3, 4].

OCDMA has knocked the doors for future multiple access networks [3]. The basic concept of implementation of OCDMA is same as that of CDMA. The concept behind CDMA is to transmit the signature code in place of sending single one and same length zero sequences in place of sending single zero [5]. All the codes have same length but have unique pattern for different users. The patterns are defined according to chosen coding scheme. The autocorrelation function of a code gives a high peak. At receiver, a high peak is generated due to detection of desired code. On detection of a high peak, the receiver assumes the code was transmitted. OCDMA has many features such as; no need for centralized network control, number of codes decides the cardinality of a network, new user can easily be added to the networks, it does not require any scheduling, permitting asynchronous access with no waiting time, security against eavesdropping, supporting larger number of users, and provision for multimedia traffic. Therefore, OCDMA is a promising technology for next generation access network. On comparing with OTDMA and WDMA, where the transmission capacity can only be increased once, the total numbers of time or wavelength channels provide the capacity of system. On the other hand, OCDMA (at encoder fixed/variable) permits flexibility in capacity of system by generating codes to support network [6–9].

The performance of OCDMA systems is mainly affected by interference from other simultaneous users called Multi User Interference (MUI) or Multiple Access Interference (MAI) [10,11]. Spectral Amplitude Coding - OCDMA (SAC-OCDMA) systems are a type of the OCDMA technique in which unique codes are mapped to different spectral lines of a broadband source [12] [13]. It reduces the MAI when codes with fixed In Phase Cross Correlation (IPCC) are used as an address sequences. This reduction is realized by balanced detection of signals as shown in Figure 1.1. It also provides a low cost solution as it uses Broad Band Sources (BBS) like Light Emitting Diodes (LEDs).

1.2 Spectral Amplitude Coding (SAC) systems

Codes are represented as (N, L, W, λ_c), where N is number of users, L is code length, W is code weight and λ_c is IPCC. Code length (L) is total number of chips used by each user. Weight (W) represents the number of chips having value equal to unity. The IPCC between two codes is defined as $\lambda_c = \sum_{j=1}^{L} a_j d_j$ for two users codes $A = (a_1, a_2, a_3, ..., a_L)$ and $D = (d_1, d_2, d_3, ..., d_L)$ of code length (L). When λ_c= 1, it is considered that the code possesses ideal IPCC properties [14].

Figure 1.1 shows the block diagram of a SAC-OCDMA system. It employs transmitter and receiver pairs connected in a star configuration. The transmitter side incorporate light source, splitter, data generator, encoder, modulator and multiplexer. The light sources are BBS like LEDs and super luminescent diodes. The optical spectrum of BBS is divided into L number of chips. These chips are allocated according to the signature codes. At the encoder for each user, the code is generated by selecting the wavelengths from optical spectrum of the BBS. These signals are modulated by Mach Zehnder Modulator (MZM) according to given data. As, when the data bit is 1, chips are sent according to the signature code, and when the data bit is 0, no pulse is launched from the BBS. Codes from different users are combined before they are launched onto the optical fiber. The main components of receiver are filtering components and photodiodes. At receiver for balanced detection (BD) technique, the received signal splits into two arms. The upper arm of decoder uses the same wavelength structure as that of the encoder. For lower arm of decoder, wavelength structure is selected in such a way that it eliminates the MAI. Signals from upper arm and lower arm are sent to an

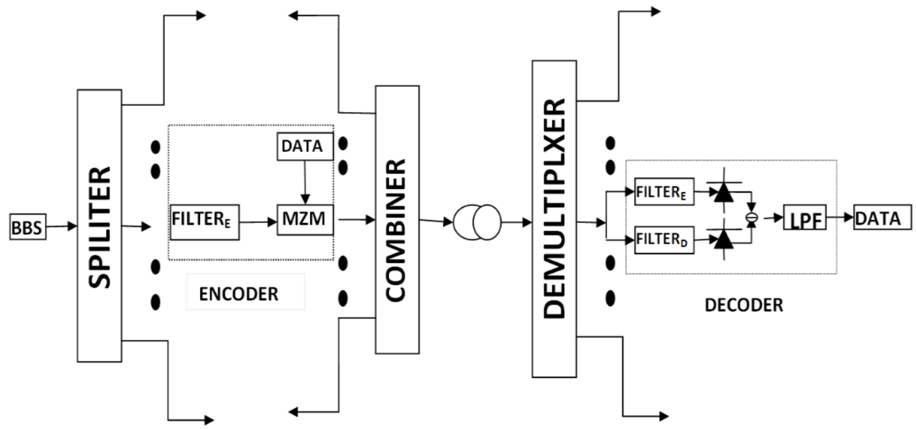

Figure 1.1: Block diagram of SAC-OCDMA system using BD technique.

electrical subtractor to cancel out the MAI.

MAI is the main factor which degrades the performance, especially when numbers of users are large. For SAC-OCDMA, MAI is only determined by the values of IPCC [15, 16]. One major advantage of such systems is that MAI can be eliminated when codes with fixed IPCC are used as address sequences. Nevertheless, such systems exhibit inherent PIIN (Phase-Induced Intensity Noise) due to spontaneous emission of the BBS that severely affects the overall system performance. To suppress the PIIN, the value of IPCC should be kept as small as possible [14]. Therefore, the codes with ideal IPCC become attractive. Many codes with ideal IPCC and other properties are reported for SAC-OCDMA systems.

1.3 Literature Survey

Spectral encoding is proposed using m-sequences codes in [12]. A single m-sequence code generates N user codes, simply by cyclic shifting of the single code N times. A $N \times N$ Hadamard matrix is used to generate codes for $(N-1)$ users [17]. The m-sequences and hadamard code are expressed as a (L, W, λ)= $(N, (N+1)/2, (N+1)/4)$ and $(N, N/2, N/4)$ respectively. These codes offer easy code construction, fixed IPCC and simple architecture. However, their performance is limited due to the large value of IPCC.

In [14] and [18], Modified quadratic congruence (MQC) $(P^2+1, P+1, 1)$ code families based on quadratic congruence code are investigated, where P is a prime number. However, there are only P^2 code sequences in a family with length $(P^2 + P)$. MQC has a limitation in code section due to its dependence on prime number for P. Modified frequency hopping (MFH) $(Q^2+Q, Q+1, 1)$ code families based on freguency hopping code is presented in [19], where $Q = p^n$ is a prime power. MFH code gives wider range in code selection on comparing with MQC code along with all its property. In [20], two algebraic construction methods for the balanced incomplete block design code are reported. In [21], three optical orthogonal codes construction are reported, based on mutually orthogonal latin squares or mutually orthogonal latin rectangles, integer lattice design and affine geometries. All these codes have algorithmic complexity such as projective geometry and block designs.

Partitioned partial prime codes are constructed using Kronecker Tensor product, multiplication operation, and matrix complement methods in [22]. Partitioned partial prime code family has low value of IPCC, flexible code length, and excellent orthogonality. Inspiteof these advantages, it has complex code construction, exists only for a prime number, and cross correlation calculation is time consuming. In [23], Diagonal permutation shifting code is proposed with fixed IPCC and short code length. It is constructed by using some simple algebraic ways and certain matrix operations. It has been derived from the prime code sequences based on Galois field. In [24] a code is reported with short code length named as Dynamic cyclic shift. It has cross correlation value between 1 and 0. It consists of two parts- weight and dynamic parts. The weight part is designed using the value of weight. The dynamic part is a set of zeros. The weight sequence and dynamic sequence are clubbed together to form a code, and on cyclic shifting other code sequences are generated. The cardinality of this system is limited by the condition that the number of users must equal the code length. Diagonal eigenvalue unity (DEU) code is constructed for any integer value of weight in [25]. Jordan block matrix is used to design the DEU code. Four combinations are designed using weight (W) and number of users (N). The combination are (even, odd), (odd, even), (odd, odd) and (even, even). Cross correlation is less than or equal to one. DEU code has higher code length. SW-Matrix Partitioning is introduced in [26] and compared to DEU codes. It has shorter code length compared to DEU code.

In [27], an algorithm is reported as Fixed Right Shifting code based on modified Jordan block matrix with algebraic methods. It constructs the codes by using different combinations of even and odd values of number of users and weight. Its cross correlation $\lambda_c \leq 1$. Code length is defined as $L = N(W-2) + W$. The minimum code weight is 3 for code construction. Matrix partitioning code is reported in [28]. It used the Arithmetic Sequence to construct the codes. Arithmetic Sequence is a sequence in which the next term originates by adding a constant to its predecessor, and the difference of any two successive numbers is a constant. Cross correlation is smaller than or equal to one. Code length is defined as $N \times W/2$. Any integer number of weight can be used in code construction. A Generalized Matrix Partitioning Code is reported which uses mathematical properties of matrix partitioning code in [29]. It defines the upper bounds and lower bounds for the code. By putting the value of g (set of codes) equals to 1, the matrix partitioning code is generated. Crosscorrelation is one in the same group and zero with codes in different groups. It is constructed for all natural numbers. Code length is $L = \frac{g(W \times N)}{2}$. Double Weight codes are one of the code families constructed for SAC-OCDMA systems in [30]. The families includes the code construction of Double Weight (DW) [30], Modified Double Weight (MDW) [30], and Enhanced Double Weight (EDW) [31]. These codes have ideal IPCC property. The code construction steps are easy to implement. They have weight chips always in pairs which required less filtering component. Khazani-Syed (KS) Code for even weights was constructed in [32]. It is a combination of DW and MDW codes. Weight constraint with different algorithms are main difficult with these codes.

The Flexible Cross Correlation (FCC) codes are reported with property of flexible cross correlation. The code lengths are shorter for these codes which turn in higher cardinality. FCC eliminates the effect of MAI. Random Diagonal (RD) code is reported in [33]. Code construction is divided in two parts - code and data. At data part, it designs zero cross correlation code of weight 1. Code part consists of basics and weight parts. Weight part is responsible for increasing number of weights. It constructs code with shorter length. Cross correlation value is greater than zero and depends on weight and number of users. Code is designed for weight greater than 2. In [34], FCC Code is reported using tridiagonal code matrix. In [35], Sequential Algorithm code is reported with FCC property. It generates code set of any desired cross correlation properties with smallest code length for the given number of users. It used tridiagonal matrix code property to constructed code for any given number of users and weights. Drawback of FCC codes is higher value of cross correlation which leads to more PIIN. On the other hand, the codes constructed by FCC have shorter code length compared to fixed cross correlation codes.

MAI can be removed from SAC-OCDMA system by using electrical subtraction, but PIIN still remains. Thus, PIIN can severely affect the overall system performance. All the above codes suffer from PIIN. The code design with zero cross correlation (ZCC) property removes the effect of MAI and suppresses the effect of PIIN.

The code with the property of zero cross correlation is called as Zero Cross Correlation Code (ZCCC). The code structure of ZCCC does not have any overlapping of wavelengths between any users. The ZCCC is reported with Constant Weight code construction in [36]. The ZCCC code construction along with LED Spectrum slicing is explained in [37]. These codes are using mapping technique to provide codes for higher number of users. Multi diagonal Code [38] and modified Zero Cross Correlation Code [39] are reported with ZCC property. The MAI is completely eliminated by using codes with ZCC property but at the price of longer code length. Longer code length requires wide band sources.

Enhanced Multi Diagonal code is invented in [40]. It improves the code property of multi diagonal and RD codes. It defined two matrices, data and code matrices as RD code. Data matrix is a diagonal matrix of size $N \times N$. It has zero cross correlation between all rows. Code matrix used chip combination (1 2 1) as DW code. This combination is repeated diagonally. Cross correlation of chip combination is 1. Code length is $L = N + [N(W - 2) + 1]$. Code is designed for weight greater than 2.

All of the above described coding schemes have fixed code length and weight, and are not suitable for multimedia services. Thus, coding techniques with variable code weights and code lengths are required. The code weight indicates the amount of power sent by each code. Higher code weight means higher transmitted power and vice versa. Variable Weight (VW) optical orthogonal code to support multimedia services with different Quality of Service (QoS) was reported in [41]. VW Khazani Syed (KS) code was reported in [42]. KS code is designed only for even weights. It uses mapping technique to obtain codes for higher number of users for same weight and variable weight. Experimental and simulation results of VW KS code was done for SAC OCDMA system in [43]. In [44], hybrid fixed-dynamic weight assignment technique is reported for VW KS code. Comparison of various detection techniques for KS code is reported in [45]. VW Random Diagonal (RD) Code is reported in [46] for triple play service. RD code is designed for weights greater than 2. It uses two segments as code and data to obtain codes. Data segment has zero cross correlation. The code segment is responsible for cross correlation and its value is high. To obtain the codes for variable weight, RD code uses the mapping technique. A code construction is reported for Multi Service (MS) code in [47] for fixed weight, and variable QoS obtained by varying the number of codes in basic matrix.

All above described codes are 1 Dimensional (1D) which have a limitation of fewer users due to finite bandwidth of source. To solve this problem, Two Dimensional (2D) codes in Spectral/Spatial (S/S) domain have been reported. All the reported 2D codes extend the number of codes in spatial domain in which, each spectral component is split according to spatial code of that user.

The 2D M-matrices codes are reported in [48]. The performance of M-matrices codes were affected by high value of cross correlation. To further increase the number of users along with performance and improve structure of system, Permuted M-matrices code was given in [49]. It used the cyclic property of Arrayed Waveguide Grating routers together with M-sequence code. The permuted M-matrix code allowed a greater number of users [49]. The cross correlation value of 2D M-matrix codes is high resulting in inefficient performance. The 2D perfect difference codes were proposed in [50] to provide low cross correlation value. In [51], the 2D Diluted Perfect Difference codes were proposed to further increase performance of 2D PD codes. The DPD codes used the dilution method on the spectral and spatial codes. It has IPCC property. It reduces the effect of PIIN resulting in improved system performance along with number of users.

The Quadratic Congruence Code Matrices were constructed as 2D code in [52] with IPCC property to reduce MAI. In [53], the 2D Spatial division multiplexing-Balanced Incomplete Block Design codes were reported with spatial division multiplexing technique. The 2D Extended M Sequence/Extended Perfect Difference codes with a low IPCC value is given in [54]. Design of optical line terminal and optical network units were also described. Extended perfect difference code provided orthogonal property in spatial domain. The 2D hybrid codes also reported MAI cancellation property in [55]. The code has the property of spectral orthogonality. The spectral orthogonality was used to reduce the PIIN induced from the other users.

1.3.1 Motivation

OCDMA is promising technology for next generation access networks. Although, it has one major limitation, MAI. As the cardinality of system increases, MAI and Bit Error Rate (BER) increases. The MAI of system is removed and eliminated by using SAC-OCDMA systems [12, 15]. However, developing codes with good properties is a challenging task in the optical CDMA and SAC-OCDMA systems. To design a code with higher cardinality, better performance and less noise is an open task. The challenging points in designing are; MAI increases as cardinality increases, PIIN and other noises increase the BER, code to support various traffic demands, extension of codes in other dimensions. These points are motivating to develop code families for SAC-OCDMA systems.

The **objective** of the thesis can be stated as: To develop suitable codes for SAC-OCDMA system with desirable cross correlation properties, flexibility in implementation of algorithms, to support multimedia communication requirements, and efficient detection techniques. To simplify the system architectures to make it cheaper, and to improve the performance by reducing BER.

1.4 Contributions

The overall contributions of the thesis can be summarized below.

- Proposed and analysed Generalized Optical Code construction for Enhanced and Modified Double Weight like Codes without mapping for SAC-OCDMA systems.

- Proposed and analysed variable weight code using Generalized Optical Code construction for Enhanced and Modified Double Weight like Codes for multimedia communication systems.

- Design of a new code construction for Double Weight (DW) code families for all weights with mapping.

- 2D code construction of a new algorithm for DW code families.

- Proposed code construction of Zero Cross Correlation Code (ZCCC) for constant weight and variable weight.

- Proposed 2D code design using existing DW code families.
- Proposed Khazani-Syed (KS) code design for odd weights.
- Analysis of different detection techniques.

1.5 Organization of the Thesis

The remainder of the thesis is organized as follows.

Chapter 2 describes the code construction algorithms reported for DW code families along with available work done in literature and followed with gaps in literature. An odd weight construction of KS code is also introduced in this chapter. It is followed with 2D code construction by using reported 1D DW codes.

Chapter 3 proposes the algorithm to construct generalized codes for Enhanced and Modified Double Weight like Codes without mapping for SAC-OCDMA systems. Constructed code is compared with reported EDW and MDW codes. It designs code for Constant Length (CL) and Constant Weight (CW). A single algorithm is implemented with standardized formulation of code length, SNR and BER for all weights greater than 2.

A Variable Weight (VW) code construction algorithm is explained for generalized code in Chapter 4. Generalized code is explained in Chapter 3 for CL and CW. To obtain different BER, VW algorithm is needed in which weight is varied. Variation of weights provides different BER for different services. It is designed for any number of users for weight greater than 2. It does not use mapping technique to obtain more users. The cross correlation value of atmost 1 is obtained between any two users. Code construction begins with the highest weight.

A new algorithm is developed for DW code families with mapping is presented in Chapter 5. A single code construction algorithm is proposed with mapping for all weights. It also has standardized formulation of code length, SNR and BER for all weights. The major code construction steps are similar to DW code families like construct basic matrix and use mapping technique. It describes the effect of mapping on code performance. 2D code is also constructed by using 1D code construction. 2D code gives better performance with higher number of users compare to 1D code.

Chapter 6 proposes an algorithm to construct CW and VW codes with ZCC property. The constructed code is named as ZCCC. It does not use mapping technique to obtain codes for higher number of users. It eliminates the PIIN theoretically. Finally Chapter 7 summarizes the thesis with conclusions and future work.

CHAPTER 2

DW code families for SAC-OCDMA systems

2.1 Introduction

Double weight (DW) code was first introduced by Aljunid et al. in [30] in 2004. It was proposed for constant weight 2. It has simple and easy code construction along with ideal IPCC and shorter length. It also reduces the number of required filters due to number of chips occuring in pairs. Many advanced versions of this code have been reported resently. Evolution in DW code families from its introduction to persent is surveyed and presented in Section 2.2.

2.2 DW code families

2.2.1 1D codes

Code construction for 1 Dimensional (1D) codes for DW code families begin with constructing basic matrix (M) of size ($N_B \times L_B$) and weight (W). N_B and L_B denotes number of users and code length for basic matrix. Number of users (N_B) in basic matrix depends on particular code. Basic matrix is repeated diagonally to obtain number of users (N). This method to obtain N users code is known as mapping [30, 31, 56–58]. The cross correlation (λ_c) is equal to 1 for users inside basic matrix (M) and 0 for users outside basic matrix (M).

DW code structure [30] is obtained only for weight two. The weight constraint inspires to develop codes with other weights. Modified Double Weight (MDW) code is also reported in [30] for even weights greater than two. It explains code design for $W = 4$ only. For higher even weights construction, the chips combination of $(1, 2, 1)$ is kept for every three columns in M. Code construction steps are not outlined in [30] for MDW code. In [59], formulation of MDW code in terms of matrix is explained and described by using examples. In [60], generalised formulation is developed for MDW code without using matrix and mapping technique. A general equation is also given for code length calculation.

DW and MDW codes are limited to even weights. Code construction for odd weight greater than one is described in [31] and, the code is named as Enhanced Double Weight (EDW) code. Code construction steps are not outlined in [31] for EDW code. In [61,62], formulation of EDW code in terms of matrix is explained and described by using examples. The reconstruction of EDW code is reported for higher weights in [61].

Code Construction

DW code

1. Construction of basic matrix (M) using a fixed weight of 2 as described in [30] is shown below

$$M = \begin{bmatrix} 1 & 1 & 0 & \text{Code 1} \\ 0 & 1 & 1 & \text{Code 2} \\ \hline 1 & 2 & 1 & \text{Sum} \end{bmatrix}. \tag{2.1}$$

2. Chips follow (1,2,1) patterns.

3. Mapping of M to obtain N users are done as

$$\text{Mapping}- : \begin{bmatrix} M & 0 & ..... & 0 \\ 0 & M & ..... & 0 \\ .. & .. & .. & .. \\ 0 & 0 & ..... & M \end{bmatrix}_{N \times L} \tag{2.2}$$

4. Code length is defined as $L = \begin{cases} \frac{3N}{2}, & \text{for N is even} \\ \frac{3N}{2} + \frac{1}{2}, & \text{for N is odd} \end{cases}$

MDW code

1. For MDW code using even weight greater than 2, basic matrix is constructed as given in [59]

$$M = \begin{bmatrix} A & B \\ C & D \end{bmatrix}$$

where, A consists of a zeros matrix of size $1 \times 3 \sum_{j=1}^{\frac{W}{2}-1} j$, B is a matrix of size $1 \times 3(\frac{W}{2})$ in which Z_2 is repeated $(\frac{W}{2})$ times, C is the basic matrix for the next lower weight $(W-2)$, and D is a matrix of size $\frac{W}{2} \times \frac{W}{2}$ expressed as:

$$\begin{bmatrix} 0 & 0 & Z_3 \\ 0 & Z_3 & 0 \\ Z_3 & 0 & 0 \end{bmatrix}$$

where $Z_1 = [0\ 0\ 0]$; $Z_2 = [1\ 1\ 0]$; $Z_3 = [0\ 1\ 1]$. Chips follow the (1,2,1) patterns.

2. Mapping is used to obtain N users from basic matrix, as shown in Eq. (2.2).

3. Code length for $(W = 4)$ is defined as

$$L = (3N) + \frac{8}{3}\left[sin(N*180)/3\right]^2.$$

EDW code

1. For EDW code [62] using odd weight greater than 1, basic matrix is constructed as

$$M = [R_1 R_2 ......R_W]$$

Where, R is matrix of size $W \times \frac{\sum_{j=1}^{W} j}{W}$.

Each R matrix has columns sum [2, 2 ... 1] in such a way sum 2 appear $\frac{W-1}{2}$ times. Chips follows the (2,..,2,1) patterns.

2. To obtain N users codes, mapping is used as explained in Eq. (2.2).

3. Code length $(W = 3)$ is defined as

$L = (2N) + \frac{8}{3}\left[sin\frac{(N+1)180}{3}\right]^2 \frac{4}{3}\left[sin\frac{N*180}{3}\right]^2 + \frac{4}{3} * \left[sin\frac{(N+2)*180}{3}\right]^2.$

Table 2.1: The comparison of DW code families

Code	Existence	Weight	Size of B_M	Code length (L_B)
DW	2	2	2×3	3
MDW	even number > 2	even	3×9 for ($W = 4$)	9 for ($W = 4$)
EDW	odd number > 1	odd	3×6 for ($W = 3$)	6 for ($W = 3$)

The other parameters for these codes are studied as: Performance of EDW code is analysed for multirate transmission in [62]. The system parameters for EDW code are examined by using Optisys 6.0 software. The parameters are number of users, fiber length, bit rate, spacing of chips and transmitted power in [63]. The point to multipoint Fiber to the home access network is designed for EDW code by using OptiSystem 7.0 software in [64]. In [65], Stimulated Brillouin Scattering effect is observed on system by using EDW code. MDW code performance is observed for multirate transmission in [66]. This technique was implemented in local area environment using ring network [67]. In [68], parallel and serial Fiber Bragg Gratings (FBG) constructions are used to set encoder and decoder structure using MDW code. EDW code performance is evaluated by using Direct Detection (DD) technique [56]. The AND detection technique for EDW code is simulated in [69]. The effect of Non Return to Zero and Return to Zero data format on BER using AND detection technique and MDW code is explained in [70]. A comparison between different detection techniques for EDW and MDW codes are presented in [71]. Single photo diode detection is proposed for EDW code in [72] and for MDW code in [73].

2.2.2 2D codes

1D code have a limitation of lower cardinality due limited bandwidth and MAI. To overcome the limitation, 1D code is extended to 2 Dimensions

(2D) code. 2D codes have combination of two algorithms, one applied in each dimension. The 2D code is developed from 1D MDW and 1D DW codes in [74], [75], [76] and [77]. In [76], the Avalanche Photo Diode is used to enhance the performance and cardinality. Due to PIIN reduction, cardinality of 2D code is improved compared to 1D code. Simulation results are shown in [75], [77]. The 2D code developed from 1D MDW and DW codes designed only for even weights. To resolve weight limitation, it is hybrid with others such as Flexible Cross Correlation in [78], [79]. In [80], 2D MDW code is simulated and compared for Non Return to Zero and Return to Zero data formats. The 2D code is developed by combining 1D EDW codes and M-sequence codes in [81]. In [82], 2D Extended-EDW code is constructed by 1D EDW codes. The Time hopping Enhanced Double Weight is reported in [83] by merging EDW wavelength spreading into 2D time hopping scheme.

Literature gap -: These algorithms have different construction for different weights and varying calculation of code length, SNR and BER with weight. Generalized algorithm is a gap in literature for all weights with standardized formulation of BER, SNR and code length.

2.3 New construction based on above codes

The section is divided into 2 subsections. Subsection 2.3.1 explains the code construction algorithm for KS code using odd and even weights. Subsection 2.3.2 describe the code construction algorithm for 2D code.

2.3.1 Odd weight construction for KS code

KS code construction is reported only for even weights. It is a combination of two code construction algorithms, MDW code and DW code. The odd weight code construction for KS code is proposed. Proposed algorithm is a combination of previously proposed KS code (for even weight) and identity matrix. It designs the codes for all weights. Algorithm steps are-

- Choose weight [EVEN (W_E) / ODD (W_O)].

  1. If weight is even W_E.

     (a) The first row of matrix is filled with X from the left upto the number of ones equal to weight.

     (b) The second row is filled with Y diagonally, so column sum [1 2 1] is obtained for every three columns.

     (c) Fill all empty spaces with Z.

     (d) Repeat steps a to c from second row, until all rows obtain number of ones equal to weight.

     Where, $X = [1\ 1\ 0]$, $Y = [0\ 1\ 1]$ and $Z = [0\ 0\ 0]$.

  2. Else, weight is odd W_O.

     (a) Construct basic matrix A of next smaller weight $(W_O - 1)$.

     (b) Construct identity matrix B of size $B_m \times B_m$, where $B_m = \lfloor \frac{W}{2} \rfloor + 1$. Where $\lfloor x \rfloor$ is floor function.

     (c) An identity matrix is concatenated with basic matrix of next smaller weight as

$$\text{Basic matrix} = [A|B] \tag{2.3}$$

- Number of users (N_B) in basic matrix is $\lfloor w/2 \rfloor + 1$ for even and odd weights.

- Code lengths are defined as

For even weight,

$$L_E = 3\sum_{1}^{\lfloor W/2 \rfloor} i. \tag{2.4}$$

For odd weight,

$$L_O = 3\sum_{1}^{\lfloor W/2 \rfloor} i + \left\lfloor \frac{W}{2} \right\rfloor + 1. \tag{2.5}$$

- The basic matrix is repeated $\lceil N/N_B \rceil$ number of times, where $\lceil x \rceil$ is ceil function.
- Total code length is $L_E\lceil N/N_B \rceil$ and $L_O\lceil N/N_B \rceil$ for even and odd weights respectively.

Code construction example of weight 3 is as follows.

1. Weight is odd.
2. Number of users N_B in basic matrix B_m is $\lfloor W/2 \rfloor + 1 = 2$.
3. First basic matrix of next lower weight is constructed.
4. Basic matrix of $(W-1) = 2$ is constucted as
   (a) The first row is filled with X.
   (b) The second row is filled with Y.
   (c) Basic matrix is

$$B_{m_E} = \begin{bmatrix} 1 & 1 & 0 \\ 0 & 1 & 1 \end{bmatrix}$$

5. Construct identity matrix of size $B_m \times B_m$.
   (a) $B_m = \lfloor \frac{W}{2} \rfloor + 1 = 2$.
   (b) Identity matrix of size 2×2 is

$$B_{m_O} = \begin{bmatrix} 1 & 0 \\ 0 & 1 \end{bmatrix}$$

6. Attach both matrix as

$$B_m = \begin{bmatrix} 1 & 1 & 0 & 1 & 0 \\ 0 & 1 & 1 & 0 & 1 \end{bmatrix}$$

7. $L_O = 3\sum_1^{\lfloor W/2 \rfloor} i + \lfloor \frac{W}{2} \rfloor + 1 = 5.$

BER Anaysis

Figure 2.1 shows the block diagram of system setup for KS code. At the transmitter, the code sequences are generated by selecting wavelengths as per given code from Broadband Source (BBS). These selected wavelengths are modulated by MZM as per data. The output of each user is combined and sent to the optical fiber. At receiver, balanced detection technique is used to detect data. The received signal is divided into two parts, upper part and lower part. The upper part has same wavelength structure as an encoder. The wavelength structure of lower part of decoder is defined according to binary sum of columns. The output photodetector is sent to electrical subtractor to remove MAI.

Let the jth component of the kth proposed code is $H_k(j)$. The correlation function of upper part is given as

$$\sum_{j=1}^{L} H_k(j) \cdot H_l(j) = \begin{cases} W & k = l \quad \text{same user at basic matrix} \\ 1 & k \neq l \quad \text{other users at basic matrix} \\ 0 & k \neq l \quad \text{other users outside basic matrix} \end{cases} \tag{2.6}$$

The cross-correlation function of lower part of decoder is obtained as

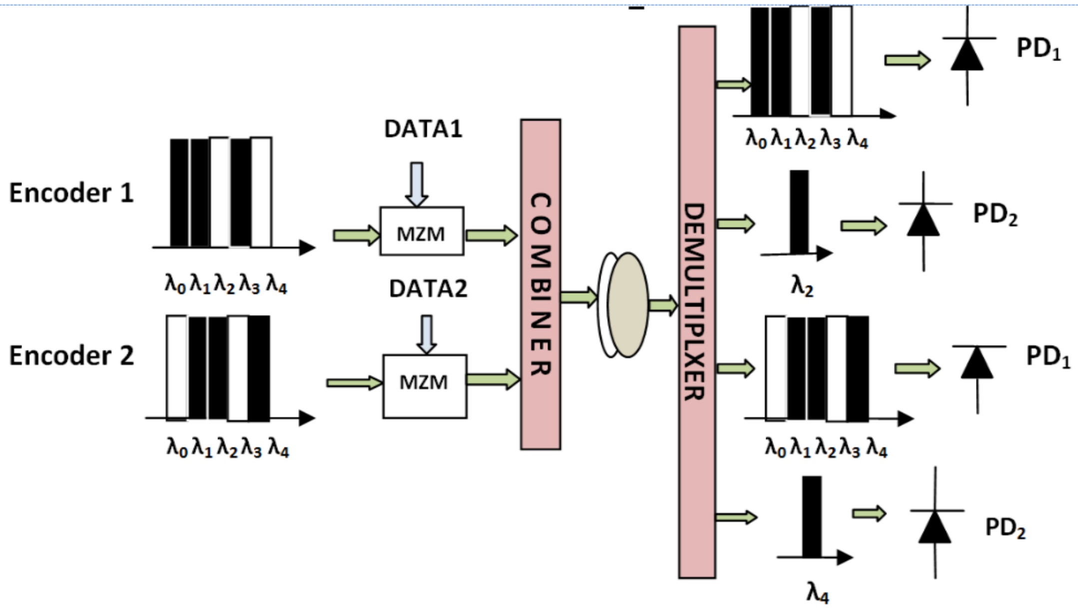

Figure 2.1: System block diagram of KS code for encoder and decoder.

1. Ex-ORing desired user with interfering user.

$$H_Z(j) = \sum_{j=1}^{L} H_k(j) \oplus H_l(j)$$

$\oplus$ denotes the Ex-OR function.

2. H_Z is AND with given interfering user [57].

$$H_Y(j) = H_Z(j) \cdot H_l(j)$$

where $\cdot$ denotes the AND function.

$$H_Y(j) = \begin{cases} 0 & k = l \quad \text{same user at basic matrix} \\ (W-1) & k \neq l \quad \text{other users at basic matrix} \\ 0 & k \neq l \quad \text{other users outside basic matrix} \end{cases} \tag{2.7}$$

3. Correlation function is given as

$$\frac{\sum_{j=1}^{L} H_k(j)\cdot H_Y(j)}{(W-1)} = \begin{cases} 0 & k=l \quad \text{same user at basic matrix} \\ 1 & k\neq l \quad \text{other users at basic matrix} \\ 0 & k\neq l \quad \text{other users outside basic matrix} \end{cases} \tag{2.8}$$

Photodiodes are used to detect optical power in upper and lower parts. Outputs of two photodiodes are sent to an electrical subtractor to cancel out MAI.

To analyse BER of the system, the Gaussian approximation with following assumptions [14], [18] are considered as.

- Each light source is ideally unpolarized and its spectrum is flat for given bandwidth $[v_0-\Delta v/2, v_0+\Delta v/2]$, where v_0 is the central optical frequency and Δv is optical source bandwidth.
- Each bit stream is synchronized for each user.
- Spectral width of each frequency component is identical.
- The received power is the same for each user.

The above assumptions are used for mathematical simplification. At receiver, selected wavelengths from both parts are incident upon a photo-detector, the phase noise of the fields causes an intensity noise term in the photo-detector output. The coherence time of a thermal source [18] is given by

$$\tau_c = \frac{\int_0^\infty G^2(v)d(v)}{\left[\int_0^\infty G(v)d(v)\right]^2}. \tag{2.9}$$

In the above equation, $G(\upsilon)$ is the single sideband Power Spectral Density (PSD) of the source [25, 57, 58].

The variance of photocurrent due to the detection of an ideally unpolarized thermal light, which is generated by spontaneous emission, can be written as

$$\langle I^2 \rangle = \langle I^2_{shot} \rangle + \langle I^2_{PIIN} \rangle + \langle I^2_{thermal} \rangle \tag{2.10}$$

Where

- Phase-Induced Intensity Noise (PIIN) is

$$\langle I^2_{PIIN} \rangle = I^2 B \tau_c. \tag{2.11}$$

- Shot noise is

$$\langle I^2_{shot} \rangle = 2eIB. \tag{2.12}$$

- Thermal noise is

$$\langle I^2_{thermal} \rangle = \frac{4K_b T_n B}{R_L}. \tag{2.13}$$

The PSD of the received optical signals can be written as [25, 57, 58]:

$$r(\upsilon) = \frac{P_{sr}}{\Delta\upsilon} \sum_{k=1}^{N} d_k \sum_{j=1}^{L} C_k(j) rec(j) \tag{2.14}$$

Where d_k is the data bit of the kth user, P_{sr} is effective power of a broadband source at the receiver and $rec(i)$ function in Eq.(2.14) is explained in terms of unit step function $u(\upsilon)$ as shown in Eqs. (2.15) and (2.16)

$$rec(j) = u\left[\upsilon - \upsilon_0 - \frac{\Delta\upsilon}{2L}(-L + 2j - 2)\right] - u\left[\upsilon - \upsilon_0 - \frac{\Delta\upsilon}{2L}(-L + 2j)\right] \tag{2.15}$$

$$rec(j) = u\left[\frac{\Delta\upsilon}{L}\right] \tag{2.16}$$

At PD_1 of kth receiver, total power is calculated as

$$P(PD_1) = \int_0^\infty G_1(\upsilon)d\upsilon = \int_0^\infty \left[\frac{P_{sr}}{\Delta\upsilon}\sum_{k=1}^{N_B} d_k \sum_{j=1}^{L} H_k(j)H_l(j)\left\{u\left[\frac{\Delta\upsilon}{L}\right]\right\}\right]d\upsilon.$$

$$= \frac{P_{sr}}{\Delta\upsilon}\frac{\Delta\upsilon}{L}\sum_{k=1}^{N_B} d_k \sum_{j=1}^{L} H_k(j)H_l(j). \tag{2.17}$$

Using correlation function from Eq. (2.6), Eq. (2.17) is written as

$$P(PD_1) = \frac{P_{sr}W}{L} + \frac{P_{sr}}{L}\sum_{k=1,k\neq p}^{N_B} d_k. \tag{2.18}$$

At PD_2 of kth receiver, total power is calculated as

$$P(PD_2) = \int_0^\infty G_2(\upsilon)d\upsilon = \int_0^\infty \left[\frac{P_{sr}}{\Delta\upsilon}\sum_{k=1}^{N_B} d_k \sum_{j=1}^{L} H_k(j)H_l(j)\left\{u\left[\frac{\Delta\upsilon}{L}\right]\right\}\right]d\upsilon$$

$$P(PD_2) = \frac{P_{sr}}{\Delta\upsilon}\frac{\Delta\upsilon}{L}\sum_{k=1}^{N_B} d_k \sum_{j=1}^{L} H_k(j)H_k(j) \tag{2.19}$$

Using correlation property given in Eq. (2.8), Eq. (2.19) leads to

$$P(PD_2) = \frac{P_{sr}}{L}\sum_{k=1,k\neq p}^{N_B} d_k \tag{2.20}$$

The received signal is the difference between photocurrents, which is expressed as $I = I_1 - I_2$. I_1 and I_2 are currents at photodiodes.

$$I = \mathcal{R}P(PD_1) - \mathcal{R}P(PD_2) \tag{2.21}$$

Here $\mathcal{R} = \eta e/(hv_0)$ is the responsivity as given in [18], and η is the quantum efficiency of photodiode. e is the electron's charge, and (hv_0) is the photon energy, where h is Planck's constant.

Replacing the values of $P(PD_1)$ and $P(PD_2)$ of total power incident at input of PD_1 and PD_2 from Eqs. (2.18) and (2.20) into Eq. (2.21), the recevied signal is

$$I = \frac{\mathcal{R}P_{sr}W}{L} \tag{2.22}$$

The shot noise is

$$\langle I^2_{shot}\rangle = 2eB(I_1 + I_2) = 2eB\mathcal{R}\left[P(PD_1) + P(PD_2)\right] \tag{2.23}$$

Eqs. (2.18) and (2.20) are substituted in Eq. (2.23).

$$\langle I^2_{shot}\rangle = \frac{2eB\mathcal{R}P_{sr}(W + 2(N_B - 1))}{L} \tag{2.24}$$

The approximation is used $\sum_{k=1}^{N} H_k(j) \approx \frac{NW}{L}$ as given in [18]. The PIIN is

$$\langle I^2_{PIIN}\rangle = BI_1^2\tau_{c1} + BI_2^2\tau_{c2} = B\mathcal{R}^2\left[\int_0^\infty G_1^2(\upsilon)d\upsilon + \int_0^\infty G_2^2(\upsilon)d\upsilon\right] \tag{2.25}$$

Eqs. (2.18) and (2.20) are substituted in Eq. (2.25), PIIN is

$$\langle I^2_{PIIN}\rangle = \frac{B\mathcal{R}^2P_{sr}^2NW}{L^2\Delta\upsilon}[W + 2(N_B - 1)] \tag{2.26}$$

Noise power, $\langle I^2\rangle$ as given in Eq. (2.10) is expressed as

$$\langle I^2\rangle = \frac{2eB\mathcal{R}P_{sr}(W + 2(N_B - 1))}{L} + \frac{B\mathcal{R}^2P_{sr}^2NW(W + 2(N_B - 1))}{L^2\Delta\upsilon} + \frac{4K_bT_nB}{R_L}. \tag{2.27}$$

The probability of sending bit 1 is half, Eq. (2.27) leads to

$$\langle I^2 \rangle = \frac{P_{sr}eB\mathcal{R}(W+2(N_B-1))}{L} + \frac{B\mathcal{R}^2P_{sr}^2NW[W+2(N_B-1)]}{2L^2\Delta\upsilon} + \frac{4K_bT_nB}{R_L} \tag{2.28}$$

The Signal to Noise Ratio (SNR), as defined in [14, 18, 25, 30, 31, 56–58, 84, 85], of SAC-OCDMA systems can be written as

$$SNR = (I)^2/\langle I^2 \rangle. \tag{2.29}$$

Put values from Eqs. (2.22) and (2.28) in Eq. (2.29), SNR is

$$SNR = \frac{\left(\frac{\mathcal{R}P_{sr}W}{L}\right)^2}{\frac{P_{sr}eB\mathcal{R}(W+2(N_B-1))}{L} + \frac{B\mathcal{R}^2P_{sr}^2NW[W+2(N_B-1)]}{2L^2\Delta\upsilon} + \frac{4K_bT_nB}{R_L}}. \tag{2.30}$$

The BER is calculated by using Gaussian approximation from SNR as given in

$$BER = \frac{1}{2}erfc\sqrt{(SNR/8)}. \tag{2.31}$$

Numerical Results

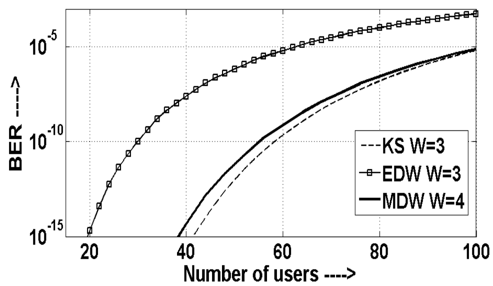

Figure 2.2: BER versus number of users.

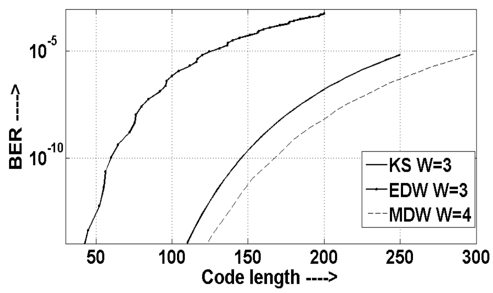

Figure 2.3: BER versus code length.

Comparison of KS code (W=3), MDW code (W=4) and EDW code (W=3).

Table 2.2: The Parameters used for BER calculation

Parameter	Value
Linewidth of broadband source (Δv)	3.75 THz
Electrical bandwidth (B)	311 MHz
Broadband effective power (P_{sr})	-10dBm
Quantum efficiency (η)	0.6
Operating wavelength (λ_0)	1550 nm
Receiver noise temperature	300 K
Receiver Load resistor	1030 Ω
Electron charge (e)	$1.6 \times 10^{-19} C$
Planck's constant (h)	$6.66 \times 10^{-34} J/s$
Boltzmann's constant (K_b)	$1.38 \times 10^{-23} J/K$

The relevant parameters used for numerical analysis, are listed in Table 2.2. Figure 2.2 is plotted for the BER versus number of users. It compare the BER for different codes, EDW ($W = 3$), MDW ($W = 4$) and KS code ($W = 3$) at a data rate of 622 Mbps using balanced detection. At BER of 10^{-12}, number of users are 25, 47 and 50 respectively for EDW code, KS code and MDW code. The variation of results for same weights are due to difference in code length. Required code length for KS code and EDW code are 250 and 200 respectively at 100 number of users as shown in Fig. 2.3. KS code gives improve performance with greater code length. But it give comparable performance with MDW code. KS code gives less BER with shorter length and less weight.

2.3.2 Proposed 2D code construction from DW code families

2D code construction is proposed using 1D DW code families which includes all weights. To construct 2D code, different combination of codes are used such as DW/DW, DW/EDW, DW/MDW, EDW/MDW, EDW/EDW, MDW/MDW. Proposed 2D code is represented as C_{gh} where g and h denotes the number of codes used in spectral and spatial domain respectively. C_{gh} is given as $X_g^T Y_h$. Where X_g and Y_h are 1D codes represented as $X_g = x_0, x_1, x_2, ..., x_{(L_x-1)}$ and $Y_h = y_0, y_1, y_2, ..., y_{(L_y-1)}$. Where, L_x and L_y are code lengths of 1D code. Code weights are represented as W_x and W_y for X_g and Y_h respectively. The cross correlation is defined as

$$R_{gh}^{(d)} = \sum_{i=o}^{L_x-1} \sum_{j=0}^{Ly-1} C^{(d)} C_{gh}. \tag{2.32}$$

Where $C^{(d)}$ is denoted as characteristic matrices $d(0,1,2,3)$,

$C^{(0)} = X_g^T Y_h$, $C^{(1)} = \overline{X_g^T} Y_h$, $C^{(2)} = X_g^T \overline{Y_h}$, and $C^{(3)} = \overline{X_g^T}\,\overline{Y_h}$. Here, X_g^T is transpose function of X_g. $\overline{X_g^T}$ and $\overline{Y_h}$ are complements of X_g^T and Y_h respectively.

The MAI elimination is obtained using Table 2.5 as follows

$$R_{g,h}^{(0)} - \frac{R_{g,h}^{(1)}}{(W_y-1)} - \frac{R_{g,h}^{(2)}}{(W_x-1)} + \frac{R_{g,h}^{(3)}}{(W_x-1)(W_y-1)} = \begin{cases} K_x K_y & \text{same user or } g=0, h=0 \\ 0 & \text{other users of same basic matrix} \\ 0 & \text{other users of other basic matrix} \end{cases} \tag{2.33}$$

Due to mapping technique, the interfering users belong to their own basic matrix users. From other users, they have no interferences. N_{B_g} and N_{B_h} represent number of users in basic matrix.

Performance analysis of code

The variance of photocurrent [24] can be written as given in Eq. (2.10). As in [54], [51], and Section 2.3.1, the Gaussian approximation is applied to

Table 2.3: 2D code construction using DW codes.

	[1 1 0]	[0 1 1]
1	1 1 0	0 1 1
1	1 1 0	0 1 1
0	0 0 0	0 0 0
0	0 0 0	0 0 0
1	1 1 0	0 1 1
1	1 1 0	0 1 1

Table 2.4: 2D code construction using DW and EDW codes.

	[0 0 1 1 0 1]	[0 1 0 0 1 1]	[1 1 0 1 0 0]
1	0 0 1 1 0 1	0 1 0 0 1 1	1 1 0 1 0 0
1	0 0 1 1 0 1	0 1 0 0 1 1	1 1 0 1 0 0
0	0 0 0 0 0 0	0 0 0 0 0 0	0 0 0 0 0 0
0	0 0 0 0 0 0	0 0 0 0 0 0	0 0 0 0 0 0
1	0 0 1 1 0 1	0 1 0 0 1 1	1 1 0 1 0 0
1	0 0 1 1 0 1	0 1 0 0 1 1	1 1 0 1 0 0

Table 2.5: Cross correlation values for 2D code.

	$R^{(0)}(g,h)$	$R^{(1)}(g,h)$	$R^{(2)}(g,h)$	$R^{(3)}(g,h)$
$g=0\bigcap h=0$	K_xK_y	0	0	0
$g=0\bigcap h\neq 0$	W_x	$W_x(W_y-1)$	0	0
$g\neq 0\bigcap h=0$	W_y	0	$W_y(W_x-1)$	0
$g\neq 0\bigcap h\neq 0$	1	(W_y-1)	(W_x-1)	$(W_x-1)(W_y-1)$

system. The PSD of the received optical signals can be written as

$$r(f)=\frac{P_{sr}}{W_y\Delta f}\sum_{U=1}^{U}d(u)\sum_{i=0}^{(L_x-1)}\sum_{j=0}^{(L_y-1)}a_{ij}(u)F(f,i) \tag{2.34}$$

Here $d(u)$ is the data bit of the uth user, P_{sr} is effective power of a BBS at the receiver, $a_{i,j}(u)$ is element of uth user code and $F(f,i)$ function in Eq.(2.34) is explained in terms of unit step function $u(f)$ as shown in Eqs.(2.35).

$$F(f,i)=u\left[f-f_0-\frac{\Delta f}{2L_x}(-L_x+2i)\right]-u\left[f-f_0-\frac{\Delta f}{2L_x}(-L_x+2i+2)\right] \tag{2.35}$$

PSDs of optical signals at PDs of the receiver can be written as

$$S_0(f) = \frac{P_{sr}}{W_y \Delta f} \sum_{u=0}^{U} d(u) \sum_{i=0}^{L_x-1} \sum_{j=0}^{L_y-1} a_{ij}^{(0)} a_{ij}(u) F(f,i) \quad (2.36)$$

$$S_1(f) = \frac{P_{sr}}{W_y (W_y - 1) \Delta f} \sum_{u=0}^{U} d(u) \sum_{i=0}^{L_x-1} \sum_{j=0}^{L_y-1} a_{ij}^{(1)} a_{ij}(u) F(f,i) \quad (2.37)$$

$$S_2(f) = \frac{P_{sr}}{W_y (W_x - 1) \Delta f} \sum_{u=0}^{U} d(u) \sum_{i=0}^{L_x-1} \sum_{j=0}^{L_y-1} a_{ij}^{(2)} a_{ij}(u) F(f,i) \quad (2.38)$$

$$S_3(f) = \frac{P_{sr}}{W_y (W_x - 1)(W_y - 1) \Delta f} \sum_{u=0}^{U} d(u) \sum_{i=0}^{L_x-1} \sum_{j=0}^{L_y-1} a_{ij}^{(3)} a_{ij}(u) F(f,i) \quad (2.39)$$

Using Table 2.5, The effect of MAI is split into three parts, i.e., $g = 0 \bigcap h \neq 0$, $g \neq 0 \bigcap h = 0$ and $g \neq 0 \bigcap h \neq 0$. The interfering users for these parts are $(N_{B_h} - 1)$, $(N_{B_g} - 1)$, and $(N_{B_h} - 1) \times (N_{B_g} - 1)$ respectively. The ensemble average of the interference amount for three groups are as

$$A_1 = \frac{(U-1)(N_{B_h} - 1)}{gh - 1} \quad (2.40)$$

$$A_2 = \frac{(U-1)(N_{B_g} - 1)}{gh - 1} \quad (2.41)$$

$$A_3 = \frac{(U-1)(N_{B_h} - 1)(N_{B_g} - 1)}{gh - 1} \quad (2.42)$$

Set $d(u) = 1$ for worst case analysis [55] and use PSDs of PDs to calculate the output currents of each PDs as

$$I_0 = \mathcal{R} \int_0^{\infty} S_0(f) df \quad (2.43)$$

$$I_0 = \frac{\mathcal{R}P_{sr}}{W_y L_x}\left[K_x K_Y + \frac{W_x(U-1)(N_{B_h}-1)}{gh-1} + \frac{W_y(U-1)(N_{B_g}-1)}{gh-1} + \frac{(U-1)(N_{B_h}-1)(N_{B_g}-1)}{gh-1}\right] \quad (2.44)$$

$$I_1 = \mathcal{R}\int_0^\infty S_1(f)df \quad (2.45)$$

$$I_1 = \frac{\mathcal{R}P_{sr}}{W_y L_x}\left[\frac{W_x(U-1)(N_{B_h}-1)}{gh-1} + \frac{(U-1)(N_{B_h}-1)(N_{B_g}-1)}{gh-1}\right] \quad (2.46)$$

$$I_2 = \mathcal{R}\int_0^\infty S_2(f)df \quad (2.47)$$

$$I_2 = \frac{\mathcal{R}P_{sr}}{W_y L_x}\left[\frac{W_y(U-1)(N_{B_g}-1)}{gh-1} + \frac{(U-1)(N_{B_h}-1)(N_{B_g}-1)}{gh-1}\right] \quad (2.48)$$

$$I_3 = \mathcal{R}\int_0^\infty S_3(f)df \quad (2.49)$$

$$I_3 = \frac{\mathcal{R}P_{sr}}{W_y L_x}\left[\frac{(U-1)(N_{B_h}-1)(N_{B_g}-1)}{gh-1}\right] \quad (2.50)$$

The average output photocurrent of the receiver is

$$I = I_0 + I_1 + I_2 + I_3 = \frac{\mathcal{R}P_{sr}W_x}{L_x} \quad (2.51)$$

The shot noise is written as

$$I_{shot} = 2eB(I_0 + I_1 + I_2 + I_3). \quad (2.52)$$

The PIIN is given as

$$I_{PIIN} = \frac{BLx}{2v}\left((I_0 - I_2)^2 + (I_1 - I_3)^2\right) \quad (2.53)$$

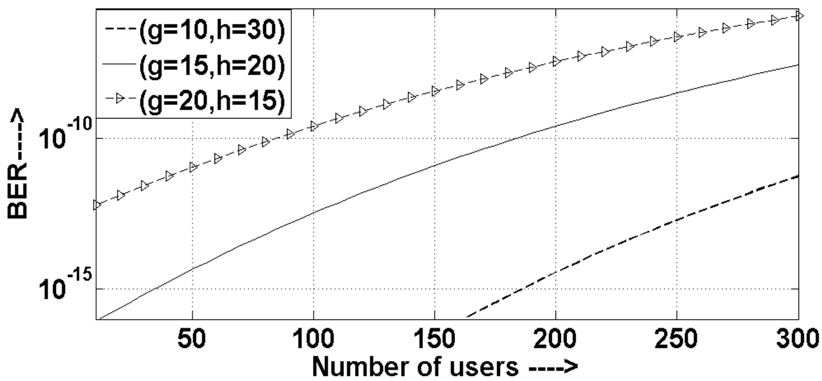

Figure 2.4: BER is compared for different value of g and h for proposed 2D code.

The SNR is calculated as per written in Eq. (2.29), and BER from SNR is expressed as given in Eq. (2.31).

Numerical Results

2D code reduces PIIN which turns to reduce BER, and increases cardinality. Because of that Electrical bandwidth (B) of system set to 1024 MHz results are shown and compared at 10^{-9} and 10^{-12}. Figure 2.4 depicts the affect of varying number of codes at spectral and spatial dimension on BER. The weight of the code is set to value $W_x = 2, W_y = 2$. The total number of users is chosen to be 300. The number of codes for both dimension are taken as $(g = 20, h = 15)$, $(g = 15, h = 20)$, and $(g = 10, h = 30)$. At BER of 10^{-12}, number of users obtained are 17, 111 and 270 for codes $(g = 20, h = 15)$, $(g = 15, h = 20)$, and $(g = 10, h = 30)$ respectively. As the value of spatial codes h is increased and spectral codes g is decreased, BER performance is improved. Numerical result shows that BER is decreased as h is maximized and g is minimized.

2.4 Summary

A survey on Double Weight code families is presented. The DW code family is one of the code families proposed for SAC-OCDMA systems to reduce MAI. These codes have ideal IPCC property. Code construction steps are easy to implement. They have weight chips always in pairs which reduce number of filtering element. Odd weight implementation of KS code is also introduced in chapter. 2D code construction using DW code families are also introduced. However, DW codes family have different constructions of basic matrix, generalised formulation of code length and BER is not presented, and have limitation of weight.

CHAPTER 3

Generalized Optical Code construction for Enhanced and Modified Double Weight like Codes without mapping

3.1 Introduction

To generate a code for DW code family, first step is to construct a basic matrix. Depending on the number of users required in the code family, the basic matrix is repeated diagonally, known as mapping technique. Due to mapping, increment of code length is not constant. Its increment is dependent on the size of basic matrix and required number of additional users. For example, if basic matrix has size (3×9) where users are 3 and code length is 9. For 3 additional users, code length becomes 18. Even though mapping and crosscorrelation constraints are similar for all codes families of DW, they have different code construction algorithms, length and other properties. A generalised algorithm to construct these codes is a gap in literature which is investigated in Chapters 3, 4 and 5, with and without mapping.

A new generalized algorithm to construct EDW and MDW like codes without mapping for any weight greater than 2 is proposed. The code construction is independent of mapping technique. It maintains crosscorrelation value of atmost 1 ($\lambda_c \leq 1$) between all the N users. A single code construction algorithm is designed for all weights greater than 2. For each additional user, code length increment is constant. For example, if code length for 3 users is 9 then for 4 users it is 12, for 5 users it is 15 and so on (increment of 3 for each user).

3.2 Code Construction

The section is divided into 2 subsections. 3.2.1 explains the code construction algorithm. 3.2.2 contains the code construction example.

3.2.1 Algorithm

The value of weight (W) and number of users (N) are chosen. Code length is given as $L = N(W-1)$ for W and N.

Basic Matrix (M) of size $2 \times (W-1)$ is constructed as follows.

$$M = \begin{bmatrix} R_1 \\ R_2 \end{bmatrix} = \begin{bmatrix} \lfloor \frac{W-2}{2} \rfloor 0s & \lfloor \frac{W+1}{2} \rfloor 1s \\ \lfloor \frac{W}{2} \rfloor 1s & \lfloor \frac{W-1}{2} \rfloor 0s \end{bmatrix}_{2\times(W-1)} \tag{3.1}$$

The complete code set is represented by matrix U of size $N \times L$ for N users. The construction of U involves 3 steps in which an intermediary matrix U^*

is first constructed. M is repeated $N-1$ times in U^* as shown below.

$$U^* = \begin{bmatrix} R_1 & .. & .. & .. & .. & .. \\ R_2 & R_1 & .. & .. & .. & \vdots \\ \vdots & R_2 & R_1 & .. & .. & \vdots \\ \vdots & \vdots & \vdots & \ddots & \ddots & \vdots \\ \vdots & \vdots & \vdots & \ddots & R_1 & \vdots \\ .. & .. & .. & .. & R_2 & .. \end{bmatrix} \tag{3.2}$$

To completely fill all columns, basic matrix rows R_1 and R_2 are added to last row and first row of last column of matrix U^* respectively as shown below.

$$U^{**} = \begin{bmatrix} R_1 & .. & .. & .. & .. & & R_2 \\ R_2 & R_1 & .. & .. & .. & .. & \vdots \\ \vdots & R_2 & \ddots & \ddots & \ddots & \ddots & \vdots \\ \vdots & \vdots & \ddots & \ddots & \ddots & \ddots & \vdots \\ \vdots & \vdots & \ddots & \ddots & \ddots & R_1 & \vdots \\ .. & .. & .. & .. & .. & R_2 & R_1 \end{bmatrix}_{N\times L} \tag{3.3}$$

The complete code set is obtained by filling up empty places in U^{**} with zeros.

$$U = \begin{bmatrix} R_1 & 0 & 0 & .. & .. & .. & R_2 \\ R_2 & R_1 & 0 & .. & .. & .. & 0 \\ 0 & R_2 & 0 & .. & .. & .. & \vdots \\ \vdots & \vdots & \vdots & \ddots & \ddots & \ddots & \vdots \\ \vdots & \vdots & \vdots & \ddots & \ddots & R_1 & 0 \\ 0 & 0 & 0 & .. & .. & R_2 & R_1 \end{bmatrix}_{N\times L} \tag{3.4}$$

Algorithm is stated as:

- Choose W, N and calculate the code length L.
- Construct M as per Eq. (3.1).
- Repeat M in U^* as per Eq. (3.2).
- R_1 and R_2 are added to U^{**} as per Eq. (3.3) and empty places in U^{**} are filled with zeros to complete code construction for all users.

3.2.2 Code construction example

Weight ($W = 3$)

1. Let number of users are $N = 3$. Code length is calculated as $L = N(W - 1) = 3(2) = 6$.
2. Size of matrix is defined as $2 \times (3 - 1) = 2 \times 2$. Matrix is created as

$$M = \begin{bmatrix} R_1 \\ R_2 \end{bmatrix} = \begin{bmatrix} \lfloor \frac{3-2}{2} \rfloor 0s & \lfloor \frac{3+1}{2} \rfloor 1s \\ \lfloor \frac{3}{2} \rfloor 1s & \lfloor \frac{3-1}{2} \rfloor 0s \end{bmatrix}_{2\times 2} = \begin{bmatrix} 1 & 1 \\ 1 & 0 \end{bmatrix}_{2\times 2}$$

3. M is repeated 2 times as

$$U^* = \begin{bmatrix} 1 & 1 & .. & .. & .. & .. \\ 1 & 0 & 1 & 1 & .. & .. \\ .. & .. & 1 & 0 & .. & .. \end{bmatrix}_{N\times L} .$$

4. Matrix upper row R_1 and lower row R_2 is put in last and first row of last column respectively as

$$U^{**} = \begin{bmatrix} 1 & 1 & .. & .. & 1 & 0 \\ 1 & 0 & 1 & 1 & .. & .. \\ .. & .. & 1 & 0 & 1 & 1. \end{bmatrix}_{3\times 6} .$$

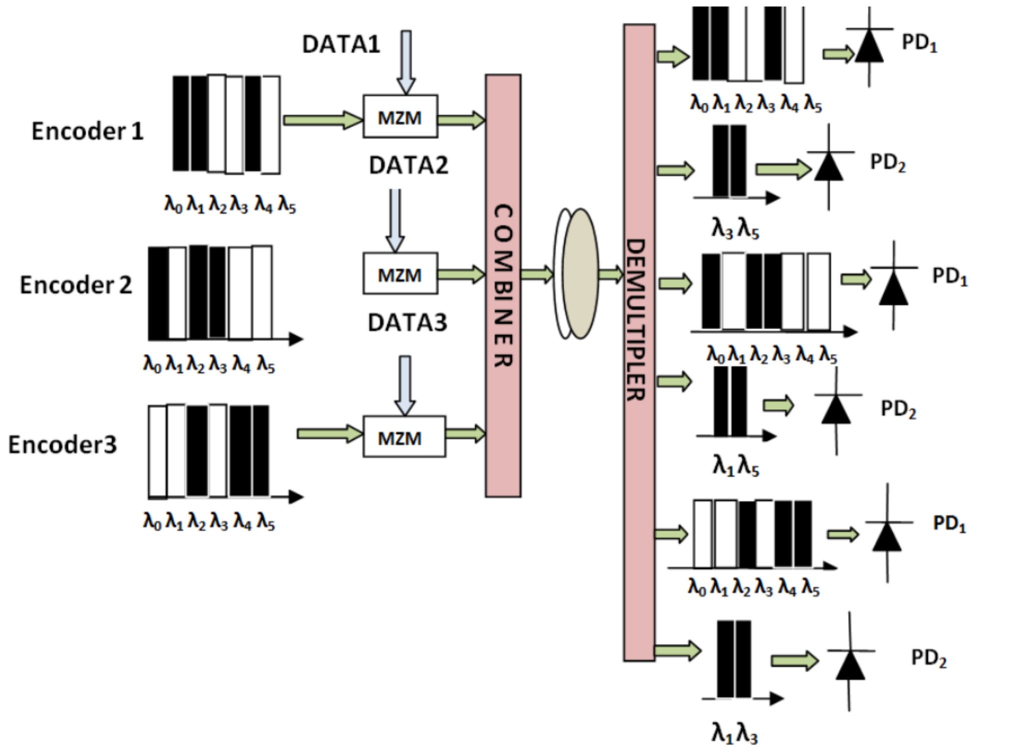

Figure 3.1: SAC-OCDMA system setup for $W = 3$ using Balanced Detection for generalized code.

Remaining places are filled with zeros.

$$U = \begin{bmatrix} 1 & 1 & 0 & 0 & 1 & 0 \\ 1 & 0 & 1 & 1 & 0 & 0 \\ 0 & 0 & 1 & 0 & 1 & 1 \end{bmatrix}_{3\times 6}.$$

3.3 SAC-OCDMA system

The implementation of SAC-OCDMA system using balanced detection technique for $W = 3$ using generalized code is shown in Fig.3.1. At the encoder for each user, the code is generated by selecting the wavelengths from optical signal of the broadband source. The wavelengths are selected according to the code to be transmitted over the channel. These signals are modulated by MZM according to given data. Codes from different users are combined by using mod-2 sum before they are launched onto the optical fiber.

At receiver, the received signal divides into two arms. The upper arm of decoder uses the same wavelength structure as that of the encoder. In the lower arm of decoder, wavelength structure is given according to binary sum of columns of matrix U.

For an example of weight, $W = 3$, and number of users, $N = 3$, U matrix is given as

$$\begin{array}{c} Wavelengths \\ user1 \\ user2 \\ user3 \\ -- \\ Sum \end{array} \begin{bmatrix} \lambda_0 & \lambda_1 & \lambda_2 & \lambda_3 & \lambda_4 & \lambda_5 \\ 1 & 1 & 0 & 0 & 1 & 0 \\ 1 & 0 & 1 & 1 & 0 & 0 \\ 0 & 0 & 1 & 0 & 1 & 1 \\ -- & -- & -- & -- & -- & -- \\ 0 & 1 & 0 & 1 & 0 & 1 \end{bmatrix}. \tag{3.5}$$

The binary sum of all columns of matrix U gives $W - 2$ non-overlapping wavelengths for each user. The non-overlapping wavelengths which are not present in desired user are used to eliminate the MAI at lower arm of decoder.

Photodiodes are used to detect the filtered optical signal. An electrical subtractor between the two arms is used to cancel out the MAI.

3.4 Balanced Detection Technique

Let $C_k(j)$ be the jth element of the kth proposed code sequence. At balanced receiver, the proposed code exhibits different code properties in the upper and lower arms of detector depending on particular detection technique.

In case of upper arm, detector has same structure as an encoder. The autocorrelation function of a desired user gives a high peak of W. Cross correlation of interfering users with desired user is atmost 1. Correlation function for upper arm is explained as

$$\sum_{j=1}^{L} C_k(j) \cdot C_l(j) = \begin{cases} W & k = l \quad \text{same user} \\ 1 & k \neq l \quad l = k \pm 1 \\ 0 & k \neq l \quad \text{other users} \end{cases} \tag{3.6}$$

In case of lower arm, the $W-2$ non-overlapping wavelengths are denoted by $C_Z(j)$ as shown in Section 3.3. The method to reject the MAI from interfering users is explained below. The product of $C_Z(j)$ and codes of interfering users $(l = k \pm 1)$ is considered first as

$$C_X(j) = \sum_{j=1}^{L} (C_Z(j) \cdot C_l(j)). \tag{3.7}$$

Correlation function for lower arm is given as

$$\sum_{j=1}^{L} C_k(j) \cdot C_X(j) = \begin{cases} 0 & k = l & \text{same user} \\ (W-2) & k \neq l & l = k \pm 1 \text{ interfering users} \\ 0 & k \neq l & \text{other users} \end{cases} \tag{3.8}$$

$$\frac{\sum_{j=1}^{L} C_k(j) \cdot C_X(j)}{(W-2)} = \begin{cases} 0 & k = l \quad \text{same user} \\ 1 & k \neq l \quad l = k \pm 1 \\ 0 & k \neq l \quad \text{other users} \end{cases} . \tag{3.9}$$

An electrical subtractor between the two arms is used to cancel out the MAI as

$$\sum_{j=1}^{L} C_k(j)\cdot C_l(j) - \frac{\sum_{j=1}^{L} C_k(j)\cdot C_X(j)}{(W-2)} = \begin{cases} W & k=l \quad \text{same user} \\ 0 & k\neq l \quad l=k\pm 1 \\ 0 & k\neq l \quad \text{other users} \end{cases}. \tag{3.10}$$

To analyse BER, the Gaussian approximation with assumptions are taken as per given in Section 2.3.1.The coherence time of a thermal source [18] is given in Eq. (2.9). The variance of photocurrent [24] can be written as given in Eq. (2.10). The PSD of the received signals is written as given in Eq. (2.14). The total power incident at the input of photodetector, PD_1 of kth receiver during one bit period can be written as

$$P(PD_1) = \int_0^\infty G_1(v)dv = \int_0^\infty \left[\frac{P_{sr}}{\Delta v}\sum_{k=1}^{N} d_k \sum_{j=1}^{L} C_k(j)C_l(j)\left\{u\left[\frac{\Delta v}{L}\right]\right\}\right]dv.$$

$$= \frac{P_{sr}}{\Delta v}\frac{\Delta v}{L}\sum_{k=1}^{N} d_k \sum_{j=1}^{L} C_k(j)C_l(j). \tag{3.11}$$

Using upper arm property of correlation function given in Eq. (3.6), Eq. (3.11) simplifies to

$$P(PD_1) = \frac{P_{sr}W}{L} + \frac{P_{sr}}{L}\sum_{k=1,k\neq l}^{N} d_k. \tag{3.12}$$

The total power incident at the input of photodetector, PD_2 of kth receiver during one bit period can be written as

$$P(PD_2) = \int_0^\infty G_2(v)dv = \int_0^\infty \left[\frac{P_{sr}}{\Delta v}\sum_{k=1}^{N} d_k \sum_{j=1}^{L} C_k(j)C_X(j)\left\{u\left[\frac{\Delta v}{L}\right]\right\}\right]dv$$

$$P(PD_2) = \frac{P_{sr}}{\Delta \upsilon} \frac{\Delta \upsilon}{L} \sum_{k=1}^{N} d_k \sum_{j=1}^{L} C_k(j) C_X(j) \tag{3.13}$$

Using lower arm property of correlation function given in Eq. (3.9), Eq. (3.13) simplifies to

$$P(PD_2) = \frac{P_{sr}}{L} \sum_{k=1, k \neq l}^{N} d_k \tag{3.14}$$

The received signal of specific user is given by the difference between photocurrents I_1 and I_2, which is expressed as $I = I_1 - I_2$. I_1 and I_2 are currents at photodiodes of upper and lower branch respectively.

$$I = \mathcal{R}P(PD_1) - \mathcal{R}P(PD_2) \tag{3.15}$$

Substituting the expressions of $P(PD_1)$ and $P(PD_2)$ of total power incident at input of PD_1 and PD_2 from Eqs. (3.12) and (3.14) into Eq. (3.15), the received signal is

$$I = \frac{\mathcal{R}P_{sr}W}{L} \tag{3.16}$$

The shot noise power is given as

$$\langle I_{shot}^2 \rangle = 2eB(I_1 + I_2) = 2eB\mathcal{R}\left[P(PD_1) + P(PD_2)\right] \tag{3.17}$$

By substituting the values in Eq. (3.17) from Eqs. (3.12) and (3.14), shot noise is

$$\langle I_{shot}^2 \rangle = \frac{2eB\mathcal{R}P_{sr}(W+4)}{L} \tag{3.18}$$

The following approximation is used as per the methodology given in [58]

$$\sum_{k=1}^{N} C_k(j) \approx \frac{NW}{L} \tag{3.19}$$

. The PIIN power can be written as

$$\langle I_{PIIN}^2 \rangle = BI_1^2 \tau_{c1} + BI_2^2 \tau_{c2} = B\mathcal{R}^2 \left[\int_0^\infty G_1^2(\upsilon) d\upsilon + \int_0^\infty G_2^2(\upsilon) d\upsilon \right] \quad (3.20)$$

By substituting values in Eq. (3.20) from Eqs. (3.12) and (3.14), PIIN is

$$\langle I_{PIIN}^2 \rangle = \frac{B\mathcal{R}^2 P_{sr}^2 NW}{L^2 \Delta \upsilon} [W + 4] \quad (3.21)$$

Noise power, $\langle I^2 \rangle$ as given in Eq. (2.10) is expressed as

$$\langle I^2 \rangle = \frac{2eB\mathcal{R}P_{sr}(W+4)}{L} + \frac{B\mathcal{R}^2 P_{sr}^2 NW(W+4)}{L^2 \Delta \upsilon} + \frac{4K_b T_n B}{R_L}. \quad (3.22)$$

Noting that the probability of sending bit 1 at any time for each user is half [58], Eq. (3.22) leads to

$$\langle I^2 \rangle = \frac{P_{sr} eB\mathcal{R}(W+4)}{L} + \frac{B\mathcal{R}^2 P_{sr}^2 NW[W+4]}{2L^2 \Delta \upsilon} + \frac{4K_b T_n B}{R_L} \quad (3.23)$$

Substituting from Eqs. (3.16) and (3.23) in Eq. (2.29), SNR is expressed as

$$SNR = \frac{\left(\frac{\mathcal{R}P_{sr}W}{L}\right)^2}{\frac{eB\mathcal{R}P_{sr}(W+4)}{L} + \frac{B\mathcal{R}^2 P_{sr}^2 NW(W+4)}{2L^2 \Delta \upsilon} + \frac{4K_b T_n B}{R_L}}. \quad (3.24)$$

The BER using Gaussian approximation from SNR is expressed as given in Eq. (2.31).

3.5 Direct Detection Technique

The implementation of SAC-OCDMA system using DD for $W = 3$ and $N = 3$ (generalized code) is shown in Fig.3.2. DD uses the non-overlapping wave-

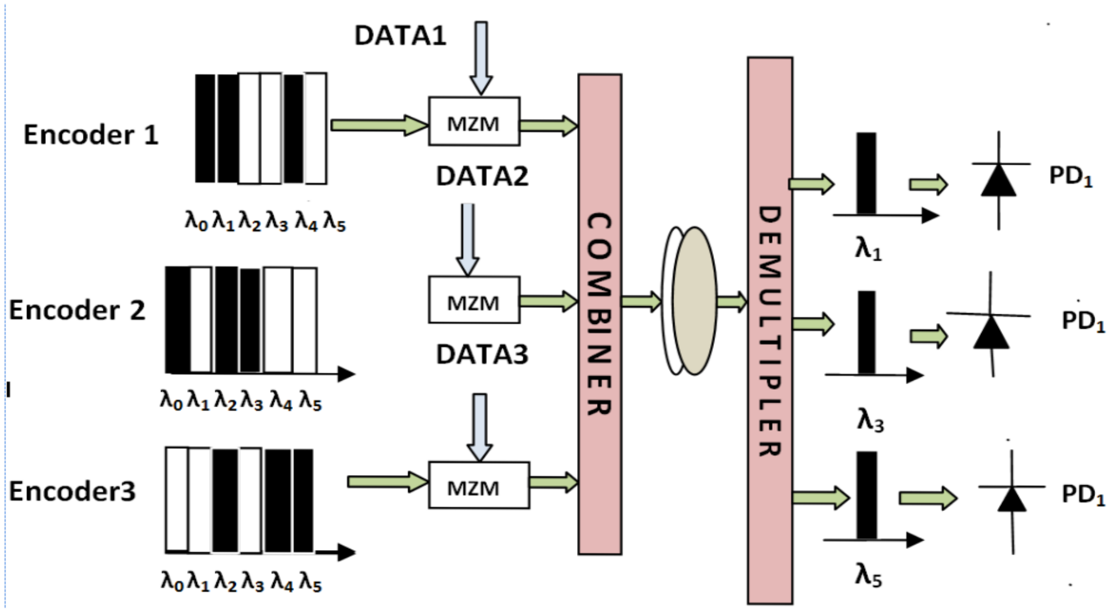

Figure 3.2: SAC-OCDMA system setup for $W = 3$ using DD for generalized code.

lengths in its detection process. Non-overlapping wavelengths are calculated by mod-2 sum of all users as shown in Eq. (3.5). At receiver, the non-overlapping wavelengths, which are unique for each user are selected and sent to photo diode. It requires a single photo detector for detecting the wavelengths without any subtractor as used in balanced detection (Section 3.3). PIIN is theoretically eliminated on detecting non-overlapping wavelengths. This results in reduced complexity of receiver along with performance improvement.

For BD, signal is divided into two parts which are detected and converted into electrical signal, which is followed by electrical subtractor. BD technique require more processing and more components as compare to DD. In DD, only single photodiode need to detect signal. DD requires less components which turn to reduce cost of recevier. DD requires less processing which leads to less complexity at recevier [56, 85].

Let $C_k(j)$ be the jth element of the kth proposed code sequence. The $W-2$ non-overlapping wavelengths for each user from $C_Z(j)$ is selected by product of $C_Z(j)$ and with desired user. Correlation function is given as

$$C_X(j) = \sum_{j=1}^{L}(C_Z(j) \cdot C_k(j)) = \begin{cases} W-2 & k = l \quad \text{same user} \\ 0 & k \neq l \quad \text{other users} \end{cases}. \tag{3.25}$$

For BER analysis, the Gaussian approximation and all other assumptions are same as used in Section 2.3.1. The variance of photocurrent due to the detection of an ideally unpolarized thermal light can be written as [56, 85]:

$$\langle I^2 \rangle = \langle I^2_{shot} \rangle + \langle I^2_{thermal} \rangle. \tag{3.26}$$

here $\langle I^2_{shot} \rangle$, and $\langle I^2_{thermal} \rangle$ are Shot noise and Thermal noise respectively. The expressions of $\langle I^2_{shot} \rangle$, and $\langle I^2_{thermal} \rangle$ are as given in Eqs. (2.12),(2.13). The PSD of the received optical signal is expressed in Eq. (2.14)

After selecting non-overlapping wavelengths, total power incident at the input of photodiode of kth receiver during one bit period can be given as

$$\int_0^\infty G(\upsilon)d\upsilon = \int_0^\infty \left[\frac{P_{sr}}{\Delta\upsilon}\sum_{k=1}^{N} d_k \sum_{j=1}^{L} C_k(j)C_X(j)\left\{u\left[\frac{\Delta\upsilon}{L}\right]\right\}\right]d\upsilon$$

$$= \frac{P_{sr}}{\Delta\upsilon}\frac{\Delta\upsilon}{L}\sum_{k=1}^{N} d_k \sum_{j=1}^{L} C_k(j)C_X(j). \tag{3.27}$$

Using correlation property given in Eq. (3.25), Eq. (3.27) can be written as

$$\int_0^\infty G(\upsilon)d\upsilon = \frac{P_{sr}(W-2)}{L}. \tag{3.28}$$

The photo current generated by the incident optical power is given by

$$I = \mathcal{R}\int_0^\infty G(v)dv. \tag{3.29}$$

Put the value from Eq. (3.28) into Eq. (3.29) for total power incident at input of PD. The resultant photo current is

$$I = \frac{\mathcal{R}P_{sr}(W-2)}{L}. \tag{3.30}$$

By substituting the values in Eq. (2.10) from Eq. (3.30), shot noise is

$$\langle I_{shot}^2 \rangle = 2eB\mathcal{R}\left(\frac{P_{sr}(W-2)}{L}\right) \tag{3.31}$$

Noise power, $\langle I^2 \rangle$ is expressed as:

$$\langle I^2 \rangle = 2eB\mathcal{R}\left[\frac{P_{sr}(W-2)}{L}\right] + \frac{4K_bT_nB}{R_L} \tag{3.32}$$

Noting that the probability of sending bit 1 at any time for each user is half [58], Eqs. (3.32) leads to

$$\langle I^2 \rangle = eB\mathcal{R}\left[\frac{P_{sr}(W-2)}{L}\right] + \frac{4K_bT_nB}{R_L} \tag{3.33}$$

Substituting from Eqs. (3.30), (3.33) in Eq. (2.29), SNR is expressed as

$$SNR = \frac{(\frac{\mathcal{R}P_{sr}(W-2)}{L})^2}{eB\mathcal{R}\left[\frac{P_{sr}(W-2)}{L}\right] + \frac{4K_bT_nB}{R_L}} \tag{3.34}$$

The Bit Error Rate (BER) is calculated as given in Eq. (2.31).

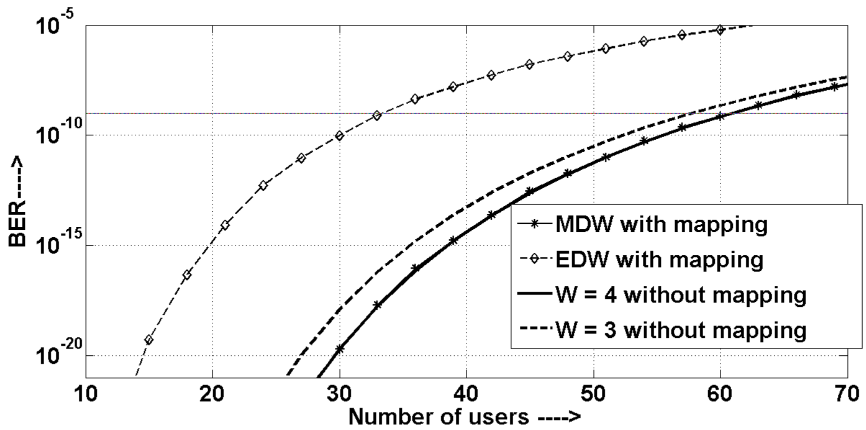

Figure 3.3: Comparision of MDW and EDW code with Generalized code.

3.6 Numerical Results

To calculate the numerical results, the relevant parameters are listed in Table 2.2.

Figure 3.3 depicts the BER versus number of users for EDW ($W = 3$), MDW ($W = 4$) and generalized code for ($W = 3, 4$) at a data rate of 622 Mbps using balanced detection. At BER of 10^{-9}, number of users are 61 and 58 for $W = 3$ and $W = 4$ respectively for generalized code. The number of users for EDW ($W = 3$) and MDW ($W = 4$) are 34 and 61 respectively. The variation of results are due to difference in code length which depends on the number of users and its dependency on mapping for EDW and MDW which affects the BER performance. The BER for EDW and MDW depends on the size of basic matrix. BER changes on varying the size of basic matrix which further changes the length of code on increasing number of users. The designing of code without mapping eliminates the effect of basic matrix dimensions on BER.

BER is plotted against number of users when weight is varying from 3 to 6 using balanced detection for generalized code as shown in Fig.3.4. At

BER of 10^{-9}, number of users are 57, 61, 63 and 64 for $W = 3, 4, 5$ and 6 respectively. As the weight is increased auto correlation peak value (W) increases which reduces the error probability. Resultant number of users for same BER is increased along with increased code length. As the weight is increased, the number of pulses per code increases which in turn increases the signal power per user. As a result SNR and hence BER improves.

Figure 3.5 depicts the affect of datarate on BER at constant value of $W = 4$ using balanced detection for generalized code. BER is plotted against number of users (N) with increasing data rate. Number of users are 34, 19 and 10 for data rate 1.25 Gbps, 2.5 Gbps and 5 Gbps respectively at BER of 10^{-9}. As the data rate of the system is increased, BER is increased for system which degrades the number of supportable users for same BER. This happens due to increase in required bandwidth which increases the noise in system. Hence number of users are reduced on increasing data rate as shown in Figure 3.5.

Balanced detection and DD are two different detection techniques. Both are different ways to detect code for each user. Balanced detection use various techniques to select wavelengths for lower arm such as complementary technique, AND technique, and Ex-OR technique. For generalized code, binary sum technique is used for theoretical and numerical results. For DD, binary sum technique is used to select the non-overlapping wavelengths. These non-overlapping wavelengths after filtering are sent to the photodiode. The middle term of denominator of Eq. (3.24) is due to PIIN for BD. Similar expression for DD is not required as in Eq. (3.34). Further weight factor in SNR expressions for BD and DD are different.

BER is plotted against number of users for balanced detection and DD using generalized code for $W = 6$ as shown in Fig.3.6. Number of users are

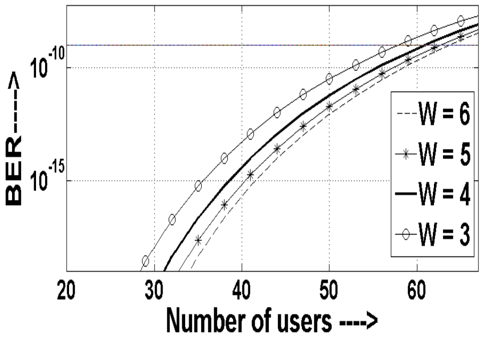

Figure 3.4: Comparison of BER for different weights using Generalized code.

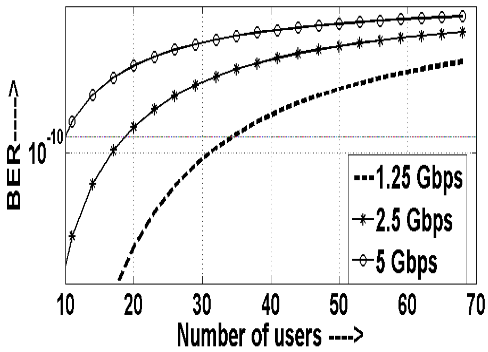

Figure 3.5: Comparison of datarate for $W = 4$ using generalized code.

64 and 71 for balanced detection and DD respectively at BER of 10^{-9}. Due to elimination of PIIN for DD, performance is improved and, the receiver complexity and cost of receiver design is reduced.

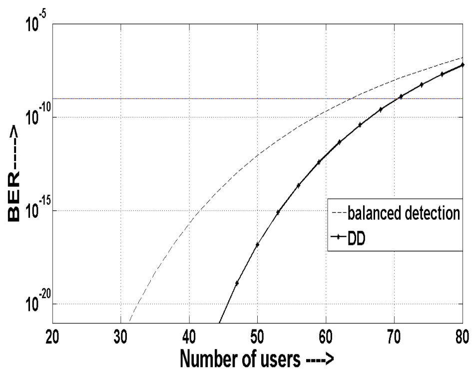

Figure 3.6: Comparison of BER for detection techniques ($W = 6$) using generalized code.

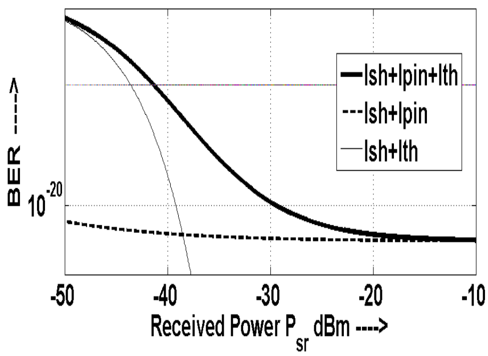

Figure 3.7: BER (PIIN, shot and thermal noise) versus received power (P_{sr}) at $N = 15$ and $W = 4$ using balanced detection.

Figure 3.7 illustrates the BER (PIIN, Shot and thermal noise) versus received power using balanced detection for $N = 15$ and $W = 4$. As shown in Fig. 3.7, the main factor which degrades system performance is PIIN using balanced detection. It occurs due to fluctuations in intensity of the received signal which results in variance of the received signal. It cannot be improved by increasing the transmitted power. PIIN also depends on the number of interfering users and increases with increasing interfering users. On the other hand, shot noise reduces with increase in received power.

3.7 Summary

A new generalized algorithm to construct EDW and MDW like codes without mapping for any weight greater than 2 is proposed. Code construction is independent of mapping technique. The proposed algorithm is for Constant Length (CL) and Constant Weight (CW). The code length increment is constant for each additional user. First, it constructs a basic matrix for particular weight. Secondly, it is repeated for each row upto $(N-1)$ times. Lastly, rows of basic matrix is added and all empty spaces are filled with zeros. It maintains crosscorrelation value of atmost 1 ($\lambda_c \leq 1$) between any two of the users. The numerical results using balanced detection and direct detection are obtained and compared.

CHAPTER 4

Variable Weight Construction using Generalized code

4.1 Introduction

The codes with fixed code length and weight are not suitable for multimedia services. Thus, coding techniques with variable code weights and code lengths are required. The code weight indicates the amount of power sent by each code. Higher code weight means higher transmitted power and vice versa. Variable Weight (VW) algorithm is proposed which is based on Generalized Optical Code construction for Enhanced and Modified Double Weight codes as discussed in Chapter 3. The proposed algorithm can be used for any combination of weights greater than 2. The cross correlation between any two users is at most 1. This code construction algorithm ensures higher power at receiver for higher weight users. Lower weight users receive less power compared to higher weight users. The difference in received power translates as varying performance, and is useful for multimedia applications.

4.2 Code Construction

4.2.1 Algorithm

The fundamental equations to find the basic matrix is based on as given in Section 3.2. The steps involved in code construction using proposed algorithm are given below

1. The cardinality or total number of users (N_{max}) is given by

$$N_{max} = \sum_{i=1}^{N} N_{W_i} \tag{4.1}$$

   N_{W_i} represents number of users with weight 'W_i'. The value of W_i must be greater than 2.

2. For all weights, basic matrix (M_{W_i}) of size $2 \times (W_i - 1)$ is constructed as

$$M_{W_i} = \begin{bmatrix} R_1^{(W_i)} \\ R_2^{(W_i)} \end{bmatrix} = \begin{bmatrix} \lfloor \frac{W_i-2}{2} \rfloor 0s & \lfloor \frac{W_i+1}{2} \rfloor 1s \\ \lfloor \frac{W_i}{2} \rfloor 1s & \lfloor \frac{W_i-1}{2} \rfloor 0s \end{bmatrix}_{2\times(W_i-1)} \tag{4.2}$$

   W_i is any of the weights from W_1 to W_N.

3. Code construction starts from highest weight (W_N) and ends with lowest weight (W_1).

4. Basic matrix of highest weight (W_N) is repeated ($N_{W_N} + 1$) times as

$$U = \begin{bmatrix} R_1^{(W_N)} & .. & .. & .. & .. \\ R_2^{(W_N)} & R_1^{(W_N)} & .. & .. & .. \\ .. & R_2^{(W_N)} & R_1^{(W_N)} & .. & .. \\ .. & .. & \ddots & .. & .. \\ .. & .. & \ddots & R_2^{(W_N)} & R_1^{(W_N)} \\ \vdots & \vdots & \vdots & \vdots & R_2^{(W_N)} \end{bmatrix}. \quad (4.3)$$

5. For last repeated basic matrix of W_N, calculate reducibility number (S_{W_N}).

   (a) Reducibility number (S_{W_i}) is defined as

$$S_{W_i} = \left\lfloor \frac{W_i}{2} \right\rfloor - \left\lfloor \frac{W_{i-1}}{2} \right\rfloor \quad (4.4)$$

      i. Calculated value of S_{W_i} is either 0 or any integer value.
      ii. When $S_{W_i} = 0$, no change is required in basic matrix M_{W_i} .
      iii. When S_{W_i} = integer, reduce S_{W_i} number of columns from left of last repeated M_{W_i}.
      iv. After reduction, last repeated basic matrix is updated as ($R_{1S}^{(W_N)}, R_{2S}^{(W_N)}$).

$$U = \begin{bmatrix} R_1^{(W_N)}.. & .. & & & \\ R_2^{(W_N)}.. & R_{1S}^{(W_N)} & & & \\ .... & R_{2S}^{(W_N)} & R_1^{(W_{N-1})}.. & .. & \\ \vdots & \vdots & R_2^{(W_{N-1})}.. & R_{1S}^{(W_{N-1})} & \\ \vdots & \vdots & \vdots & R_{2S}^{(W_{N-1})} & .. \end{bmatrix}. \quad (4.5)$$

6. Steps 4 and 5 are repeated for weights W_{N-2} to W_1. Basic matrix of

W_{N-2} to W_1 are repeated $N_{W_{N-2}}$ to N_{W_1} times respectively as given in Eq. (6.8).

$$U = \begin{bmatrix} R_1^{(W_N)}.... & & & & & & & \\ R_2^{(W_N)}.. & R_{1S}^{(W_N)} & & & & & & \\ .... & R_{2S}^{(W_N)} & R_1^{(W_{(N-1)})}.. & & & & & \\ \vdots & \vdots & R_2^{(W_{(N-1)})}.. & R_{1S}^{(W_{(N-1)})} & & & & \\ \vdots & \vdots & \vdots & \ddots & & & & \\ \vdots & \vdots & \vdots & \ddots & R_{1S}^{(W_2)} & & & \\ \vdots & \vdots & \vdots & \vdots & R_{2S}^{(W_2)} & R_1^{(W_1)} & & \\ \vdots & \vdots & \vdots & \vdots & \vdots & R_2^{(W_1)} & & \\ \vdots & \vdots & \vdots & \vdots & \vdots & \ddots & & \\ .. & .. & .. & .. & .. & .. & R_2^{(W_1)} & R_1^{(W_1)} \\ .. & .. & .. & .. & .. & .. & .. & R_2^{(W_1)} \end{bmatrix}. \tag{4.6}$$

7. First and last rows of U matrix are removed as shown in Eq. (4.7).

$$U = \begin{bmatrix} R_{2S}^{(W_N)} & .. & R_{1S}^{(W_N)} & & & & & \\ .. & .. & R_{2S}^{(W_N)} & R_1^{(W_{(N-1)})} & & & & \\ \vdots & \vdots & \vdots & R_2^{(W_{(N-1)})} & & & & \\ \vdots & \vdots & \vdots & \vdots & \vdots & \ddots & & \\ \vdots & \vdots & \vdots & \vdots & \ddots & \ddots & R_1^{W_1} & \\ .. & .. & .. & .. & .. & .. & R_2^{W_1} & R_1^{W_1} \end{bmatrix}. \tag{4.7}$$

8. All empty spaces are filled with zeros.

9. Because of Step 7, all columns filled with zeros are deleted from U matrix. $\left(\left\lfloor \frac{W_N}{2} \right\rfloor + 1\right)^{th}$ column to $\left(\left\lfloor \frac{W_N}{2} \right\rfloor + \left\lfloor \frac{W_N-1}{2} \right\rfloor\right)^{th}$ columns from left side, and $\left(\left\lfloor \frac{W_1+1}{2} \right\rfloor + 1\right)^{th}$ column to $\left(\left\lfloor \frac{W_1+1}{2} \right\rfloor + \left\lfloor \frac{W_1-2}{2} \right\rfloor\right)^{th}$ from right

side would be zeros, when W_1 is greater than 3. If W_1 is equal to 3, there are no columns of zeros from right side.

The complete code set is generated after step 9. The total code length (L_T) is the number of wavelengths required by the system for all weights. The total code length is the sum of code lengths 'L_{W_i}' corresponding to weights 'W_i'. Code length calculation for different weights is explained below For N_{W_N} users,

$$L_{W_N} = (W_N - 1) * (N_{W_N} + 1) - S_{W_N} - \left\lfloor \frac{W_N - 1}{2} \right\rfloor. \tag{4.8}$$

For $N_{W_{N-1}}$ users

$$L_{W_{N-1}} = (W_{N-1} - 1) * (N_{W_{N-1}}) - S_{W_{N-1}}. \tag{4.9}$$

Similarly, lengths $L_{W_{N-2}}$ to L_{W_1} for corresponding weights W_{N-2} to W_1 are found as follows. For $N_{W_{N-2}}$ users

$$L_{W_{N-2}} = (W_{N-2} - 1) * (N_{W_{N-2}}) - S_{W_{N-2}}. \tag{4.10}$$

For N_{W_1} users

$$L_{W_1} = (W_1 - 1) * (N_{W_1}) - \left\lfloor \frac{W_1 - 2}{2} \right\rfloor. \tag{4.11}$$

Total code length (L_T) used by the VW code is given as

$$L_T = L_{W_N} + L_{W_{N-1}} + \cdots + L_{W_1}. \tag{4.12}$$

Flow chart of the algorithm indicating code construction steps is shown in Fig. 4.1. The comparison of code properties of proposed code with KS and RD codes is given in Table 4.1.

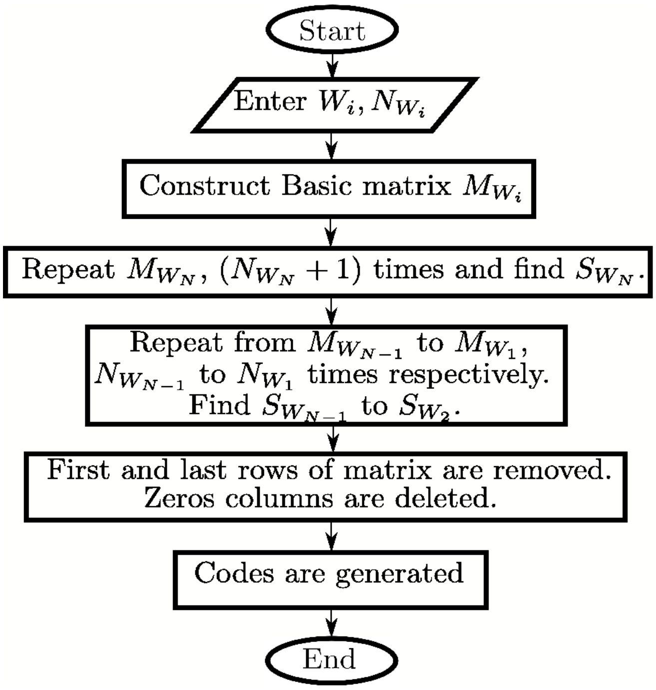

Figure 4.1: Code construction flow chart for proposed VW code.

4.2.2 Code Construction Example

Number of users (N_2) and (N_1) are chosen as 3 each for higher weight ($W_2 = 4$) and lower weight ($W_1 = 3$).

1. Size of basic matrix for weight $W_2 = 4$ is $2 \times (4-1) = 2 \times 3$, and is created as

$$M_{W_2} = \begin{bmatrix} R_1^{(4)} \\ R_2^{(4)} \end{bmatrix} = \begin{bmatrix} \lfloor \frac{4-2}{2} \rfloor 0s & \lfloor \frac{4+1}{2} \rfloor 1s \\ \lfloor \frac{4}{2} \rfloor 1s & \lfloor \frac{4-1}{2} \rfloor 0s \end{bmatrix}_{2\times 3} = \begin{bmatrix} 0 & 1 & 1 \\ 1 & 1 & 0 \end{bmatrix}_{2\times 3}$$

2. Size of basic matrix for weight $W_1 = 3$ is $2 \times (3-1) = 2 \times 2$, and is created as

$$M_{W_1} = \begin{bmatrix} R_1^{(3)} \\ R_2^{(3)} \end{bmatrix} = \begin{bmatrix} \lfloor \frac{3-2}{2} \rfloor 0s & \lfloor \frac{3+1}{2} \rfloor 1s \\ \lfloor \frac{3}{2} \rfloor 1s & \lfloor \frac{3-1}{2} \rfloor 0s \end{bmatrix}_{2\times 2} = \begin{bmatrix} 1 & 1 \\ 1 & 0 \end{bmatrix}_{2\times 2}$$

3. M_{W_2} is repeated $N_2 + 1 = 4$ times to get

$$U = \begin{bmatrix} 011 & .. & .. & .. \\ 110 & 011 & .. & .. \\ .. & 110 & 011 & .. \\ .. & .. & 110 & (0)11 \\ .. & .. & .. & (1)10 \end{bmatrix}.$$

4. Find $S_{W_2} = 2 - 1 = 1$. Reduce a single 1 from $R_2^{(4)}$, and a single 0 from $R_1^{(4)}$ from basic matrix M_{W_2} as shown in steps 3 and 4 of Section 4.2.1. The 1's and 0's reduced in step 4 are indicated in parenthesis in step 3.

$$U = \begin{bmatrix} 011 & .. & .. & .. \\ 110 & 011 & .. & .. \\ .. & 110 & 011 & .. \\ .. & .. & 110 & 11 \\ .. & .. & .. & 10 \end{bmatrix}.$$

5. M_{W_1} is repeated $N_1 = 3$ times as

$$U = \begin{bmatrix} 011 & .. & .. & .. & & & \\ 110 & 011 & .. & .. & & & \\ .. & 110 & 011 & .. & & & \\ .. & .. & 110 & 11 & & & \\ .. & .. & .. & 10 & 11 & .. & .. \\ .. & .. & .. & .. & 10 & 11 & .. \\ .. & .. & .. & .. & .. & 10 & 11 \\ .. & .. & .. & .. & .. & .. & 10 \end{bmatrix}.$$

6. First and last rows of U matrix are removed to get

$$U = \begin{bmatrix} 110 & 011 & .. & .. & & & \\ .. & 110 & 011 & .. & & & \\ .. & .. & 110 & 11 & & & \\ .. & .. & .. & 10 & 11 & .. & .. \\ .. & .. & .. & .. & 10 & 11 & .. \\ .. & .. & .. & .. & .. & 10 & 11 \end{bmatrix}.$$

7. All empty spaces are filled with zeros, and all empty columns are deleted indicated by parenthesis.

$$U = \begin{bmatrix} 11(0) & 011 & 000 & 00 & 00 & 00 & 00 \\ 00(0) & 110 & 011 & 00 & 00 & 00 & 00 \\ 00(0) & 000 & 110 & 11 & 00 & 00 & 00 \\ 00(0) & 000 & 000 & 10 & 11 & 00 & 00 \\ 00(0) & 000 & 000 & 00 & 10 & 11 & 00 \\ 00(0) & 000 & 000 & 00 & 00 & 10 & 11 \end{bmatrix}.$$

8. Code is generated for 6 users using two different weights.

$$\begin{array}{c} C_1 \\ C_2 \\ C_3 \\ C_4 \\ C_5 \\ C_6 \\ BinarySum \end{array} \quad \left[\begin{array}{ccccccc} 11 & 011 & 000 & 00 & 00 & 00 & 00 \\ 00 & 110 & 011 & 00 & 00 & 00 & 00 \\ 00 & 000 & 110 & 11 & 00 & 00 & 00 \\ 00 & 000 & 000 & 10 & 11 & 00 & 00 \\ 00 & 000 & 000 & 00 & 10 & 11 & 00 \\ 00 & 000 & 000 & 00 & 00 & 10 & 11 \\ \hline 11 & 101 & 101 & 01 & 01 & 01 & 11 \end{array}\right]. \tag{4.13}$$

9. Code length for higher weight is $L_{W_2} = (4-1)*(3+1)-1-1 = 10$, and for lower weight is $L_{W_1} = (3-1)*(3) = 6$. The total code length L_T for code is $L_{W_2} + L_{W_1} = 16$.

In the example, we can see that some of the 1's are clubbed together. With increase in weight, more number of 1's would be clubbed together. Hence, for realisation of system, only filter linewidth needs to be changed with respect to number of 1's clubbed together.

4.3 Bit Error Rate calculation

The Gaussian approximation is considered to determine BER along mathematical analysis as given in Section 2.3.1. Coherence time is defined as given in Eq. (2.9). The noise variance of photocurrent as a result of an ideally unpolarized thermal light detection, which is produced due to spontaneous emission, can be given in Eq. (2.10)

Let $C_h(j)$ be the jth element of the hth proposed code. At receiver, PSD is given as

$$r(\upsilon) = \frac{P_{sr}}{\Delta\upsilon} \sum_{h=1}^{N_{max}} d_h \sum_{j=1}^{L_T} C_h(j) rec(j) \tag{4.14}$$

Here effective power of a broadband source P_{sr} is received at receiver, the data bit of hth user is denoted by d_h and the function $rec(i)$ in Eq.(4.14) is given in Eq. (2.15)

4.3.1 Balanced Detection Technique

BD technique is described in Sections 2.3.1, 3.3 and 3.4. Upper arm, correlation function is given as

$$\sum_{j=1}^{L_T} C_h(j) \cdot C_f(j) = \begin{cases} W_i & h = f \quad \text{same user} \\ 1 & h \neq f \quad f = h \pm 1 \\ 0 & h \neq f \quad \text{other users} \end{cases} \tag{4.15}$$

For desired user, all wavelengths are detected by upper arm. To reduce the effect of MAI from undesired user's wavelengths at upper arm, lower arm is used. Correlation function of lower arm is formed by following the steps outlined below.

1. The binary sum of all non-overlapping wavelengths ($C_Y(j)$) for all users is determined as shown in Eq. 4.13.

2. The binary sum of all columns of generated code matrix gives $W_i - 2$ non-overlapping wavelengths. The non-overlapping wavelengths which are not present in desired user are used to eliminate the MAI at lower arm of decoder.

3. The product of $C_Y(j)$ with interfering users code is given as

$$C_Z(j) = \sum_{j=1}^{L_T} (C_Y(j) \cdot C_f(j)). \tag{4.16}$$

   Considering desired user as C_3 and interfering users as C_2 and C_4 from Eq. 4.13. $C_Y(j)$ is the last row of Eq. 4.13. For $C_f(j) = C_2(j)$; $C_{Z2}(j) = [0010000100000000]$. For $C_f(j) = C_4(j)$; $C_{Z4}(j) = [0000000000010000]$.

4. At lower arm, correlation function is written as

$$CF = \sum_{j=1}^{L_T} C_h(j) \cdot C_Z(j) = \begin{cases} 0 & h = f \quad \text{same user} \\ (W_i - 2) & h \neq f \quad f = h \pm 1 \\ 0 & h \neq f \quad \text{other users} \end{cases} \tag{4.17}$$

   Any one of the $(W_i - 2)$ wavelengths from an interfering users' C_Z can be used in the lower arm.

To reduce MAI due to user2; $CF_2 = C_3.C_{Z2} = [0000000100000000]$. Similarly, for user4; $CF_4 = C_3.C_{Z4} = [0000000000010000]$.

Signals from upper arm and lower arm are sent to an electrical subtractor to cancel out the MAI. The correlation function changes to

$$CF' = \begin{cases} W_i & h = f \quad \text{same user} \\ 0 & h \neq f \quad f = h \pm 1 \\ 0 & h \neq f \quad \text{other users} \end{cases} . \tag{4.18}$$

At photodetector (PD_U) of hth receiver, total power incident for one bit period is given below

$$P(PD_U) = \int_0^{\infty} G_1(\upsilon)d\upsilon = \int_0^{\infty} \left[\frac{P_{sr}}{\Delta\upsilon} \sum_{h=1}^{N_{max}} d_h \sum_{j=1}^{L_T} C_h(j)C_f(j)rect(j) \right] d\upsilon.$$

$$= \frac{P_{sr}}{\Delta\upsilon} \frac{\Delta\upsilon}{L_T} \sum_{h=1}^{N_{max}} d_h \sum_{j=1}^{L_T} C_h(j)C_f(j). \tag{4.19}$$

Eq. (4.19) is reduced by using correlation property of upper arm as given in Eq. (4.15), and it is written as

$$P(PD_U) = \frac{P_{sr}W_i}{L_T} + \frac{P_{sr}}{L_T} \sum_{h=1,h\neq f}^{N_{max}} d_h. \tag{4.20}$$

At photodetector (PD_L) of hth receiver, total power incident for one bit period is given below

$$P(PD_L) = \int_0^{\infty} G_2(\upsilon)d\upsilon = \int_0^{\infty} \left[\frac{P_{sr}}{\Delta\upsilon} \sum_{h=1}^{N_{max}} d_h \sum_{j=1}^{L_T} C_h(j)C_Z(j)rect(j) \right] d\upsilon$$

$$P(PD_L) = \frac{P_{sr}}{\Delta\upsilon}\frac{\Delta\upsilon}{L_T}\sum_{h=1}^{N_{max}} d_h CF \tag{4.21}$$

Eq. (4.21) is reduced by using correlation property of lower arm as given in Eq. (4.18), and it is written as

$$P(PD_L) = \frac{P_{sr}}{L_T}\sum_{h=1,h\neq f}^{N_{max}} d_h \tag{4.22}$$

The received signal of desired user is obtained by subtracting the lower arm photocurrent (I_L) from upper arm photocurrent (I_U), which is expressed as $I = I_U - I_L$.

$$I = \mathcal{R}P(PD_U) - \mathcal{R}P(PD_L) \tag{4.23}$$

Here $\mathcal{R} = \eta e/(h\nu_0)$ is the responsivity, and η is the internal quantum efficiency of photodiode, $(h\nu_0)$ is the photon energy, and h is Planck's constant.

Substituting $P(PD_U)$ and $P(PD_L)$ from Eqs. (4.20) and (4.22) into Eq. (4.23), the received signal leads to

$$I = \frac{\mathcal{R}P_{sr}W_i}{L_T} \tag{4.24}$$

The power of shot noise is found as

$$\langle I_{shot}^2\rangle = 2eB(I_U + I_L) = 2eB\mathcal{R}\left[P(PD_U) + P(PD_L)\right] \tag{4.25}$$

On putting the values from Eqs. (4.20) and (4.22) in Eq. (4.25) , shot noise leads to

$$\langle I_{shot}^2\rangle = \frac{2eB\mathcal{R}P_{sr}(W_i + 4)}{L_T} \tag{4.26}$$

The total number of users at a given time is the summation of users with different weights that coexist in a single system [42], denoted by

$$\sum_{h=1}^{N_{max}} C_h = \frac{1}{L_T}\sum_{i=1}^{N} N_{W_i} W_i. \tag{4.27}$$

The power of PIIN is given as

$$\langle I_{PIIN}^2 \rangle = BI_U^2\tau_{c1} + BI_L^2\tau_{c2} = B\mathcal{R}^2\left[\int_0^\infty G_1^2(\upsilon)d\upsilon + \int_0^\infty G_2^2(\upsilon)d\upsilon\right] \tag{4.28}$$

Substituting the expressions from Eqs. (4.20), (4.22) and (4.27) in Eq. (4.28), PIIN leads to

$$\langle I_{PIIN}^2 \rangle = \frac{B\mathcal{R}^2 P_{sr}^2}{L_T^2 \Delta\upsilon}\sum_{i=1}^{N_{max}} N_{W_i} W_i[W_i + 4] \tag{4.29}$$

Substituting the expressions from Eqs. (4.26) and (4.29) in Eq. (2.10), the noise power is expressed as

$$\langle I^2 \rangle = \frac{2eB\mathcal{R}P_{sr}(W_i + 4)}{L_T} + \frac{B\mathcal{R}^2 P_{sr}^2}{L_T^2 \Delta\upsilon}\sum_{i=1}^{N_{max}} N_{W_i} W_i[W_i + 4] + \frac{4K_b T_n B}{R_L}. \tag{4.30}$$

Since the probability for transmitting a bit 1 is half, Eq. (4.30) turns to

$$\langle I^2 \rangle = \frac{P_{sr}eB\mathcal{R}(W_i + 4)}{L_T} + \frac{B\mathcal{R}^2 P_{sr}^2}{2L_T^2 \Delta\upsilon}\sum_{i=1}^{N_{max}} N_{W_i} W_i[W_i + 4] + \frac{4K_b T_n B}{R_L} \tag{4.31}$$

The Signal to Noise Ratio (SNR) is defined in Eq. (2.29). The values from Eqs. (4.24) and (4.31) are put in Eq. (2.29), SNR is given as

$$SNR = \frac{\left(\frac{\mathcal{R}P_{sr}W_i}{L_T}\right)^2}{\frac{P_{sr}eB\mathcal{R}(W_i+4)}{L_T} + \frac{B\mathcal{R}^2 P_{sr}^2}{L_T^2\Delta\upsilon}\sum_{i=1}^{N_{max}} N_{W_i} W_i[W_i + 4] + \frac{4K_b T_n B}{R_L}}. \tag{4.32}$$

The BER is calculated as given in Eq. (2.31).

4.3.2 Direct Detection Technique

In DD, the $(W_i - 2)$ non-overlapping wavelengths $(C_Y(j))$ are incident on photodetector. Correlation function is written as

$$C_Z(j) = \sum_{j=1}^{L_T} (C_Y(j) \cdot C_h(j)) = \begin{cases} W_i - 2 & h = f \quad \text{same user} \\ 0 & h \neq f \quad \text{other users} \end{cases} \tag{4.33}$$

To analysze BER, all the assumptions including Gaussian approximation are similar to that described in Sections 3.4 and 3.5. The variance of photocurrent can be given as [43]

$$\langle I^2 \rangle = \langle I^2_{shot} \rangle + \langle I^2_{thermal} \rangle \tag{4.34}$$

Non-overlapped wavelengths are filtered and sent to the photodiode of hth receiver. For one bit duration, total power at hth receiver is calculated as

$$\int_0^\infty G(\upsilon) d\upsilon = \int_0^\infty \left[\frac{P_{sr}}{\Delta\upsilon} \sum_{h=1}^{N_{max}} d_h \sum_{j=1}^{L_T} C_h(j) C_Z(j) rec(j) \right] d\upsilon. \tag{4.35}$$

$$= \frac{P_{sr}}{\Delta\upsilon} \frac{\Delta\upsilon}{L_T} \sum_{h=1}^{N_{max}} d_h \sum_{j=1}^{L_T} C_c(j) C_Z(j). \tag{4.36}$$

Eq. (4.36) is rewritten in Eq. (4.37) after applying the correlation property from Eq. (4.33) as

$$\int_0^\infty G(\upsilon) d\upsilon = \frac{P_{sr}(W_i - 2)}{L_T}. \tag{4.37}$$

Substituting Eq. (4.37) in Eq. (3.29), photocurrent simplifies to

$$I = \frac{\mathcal{R} P_{sr}(W_i - 2)}{L_T}. \tag{4.38}$$

From Eq. (4.38), shot noise is calculated by putting the value of I in Eq.

Table 4.1: Comparison of properties between different VW codes expressions.

Code	Variable weights	Code Length	λ_c	Mapping
Proposed	W_1 to W_N	L_T (Eq. 12)	≤ 1	not used
VW RD	W_1 to W_N	$L_i = N_i + 2W_i - 3$, $L_T = \sum_1^{W_N} L_i$ $L_T = \sum_1^{W_N} L_i$	≥ 1	used
VW KS	W_1 to W_N	$L_i = 3\lceil(\frac{N_i}{(W_i/2)+1})\rceil \sum_1^{W_i/2} j$, $L_T = \sum_1^{W_N} L_i$ $L_T = \sum_1^{W_N} L_i$	≤ 1	used

(2.12) as

$$\langle I_{shot}^2 \rangle = 2eB\mathcal{R}\left(\frac{P_{sr}(W_i - 2)}{L_T}\right) \tag{4.39}$$

Noise power, $\langle I^2 \rangle$ is given as:

$$\langle I^2 \rangle = 2eB\mathcal{R}\left[\frac{P_{sr}(W_i - 2)}{L_T}\right] + \frac{4K_bT_nB}{R_L} \tag{4.40}$$

Since the probability of transmitting 1 for any user is half, Eq. (4.40) leads to

$$\langle I^2 \rangle = eB\mathcal{R}\left[\frac{P_{sr}(W_i - 2)}{L_T}\right] + \frac{4K_bT_nB}{R_L} \tag{4.41}$$

The SNR according to Eq. (2.29), can be given as,

$$SNR = \frac{(\frac{\mathcal{R}P_{sr}(W_i-2)}{L_T})^2}{eB\mathcal{R}\left[\frac{P_{sr}(W_i-2)}{L_T}\right] + \frac{4K_bT_nB}{R_L}} \tag{4.42}$$

The BER is described as given in Eq. 2.31.

4.4 Numerical Results

Parameters used to obtain numerical results are given in Table 4.2. Higher weight, medium weight, and lower weight are denoted as W_H, W_M and W_L respectively. For each weight, numbers of users are considered to be 50. Data

Table 4.2: The Parameters used to find out the numerical results for VW code.

Parameters	Values
Broadband source linewidth (Δv)	3.75 THz
Electrical bandwidth (B)	311 MHz
Effective power of broadband (P_{sr})	-10 dBm
Quantum efficiency (η)	0.6
Operating wavelength (λ_0)	1550 nm
Receiver noise temperature	300 K
Receiver Load resistor	1030 Ω
Electron charge (e)	$1.6 \times 10^{-19} C$
Planck's constant (h)	$6.66 \times 10^{-34} J/s$
Boltzmann's constant (K_b)	$1.38 \times 10^{-23} J/K$

rate is chosen as 622 Mbps to compare with existing literature.

In Fig. 4.2, BER is plotted against number of users for proposed VW code with ($W_L = 4$ and $W_H = 6$), VW KS code with ($W_L = 4$ and $W_H = 6$) and RD code with ($W_L = 5$ and $W_H = 13$). All the compared codes use BD technique.

BD technique describes reduction of MAI using the IPCC codes [20].

KS code is designed only for even weights. It uses mapping to give more codes for same weight and variable weight. RD code is designed for weight greater than 2. It uses two segments code and data. Data segment has zero cross correlation. The code segment is responsible for cross correlation and its value is high. To obtain the codes for variable weight, RD code uses the mapping technique. Mapping technique can efficiently use the available bandwidth, only if number of requesting users are same as maximum generated users. Otherwise, some portion of the bandwidth may be left unused and result in an increased code length [45].

In comparison to other codes, proposed VW code is applicable for any

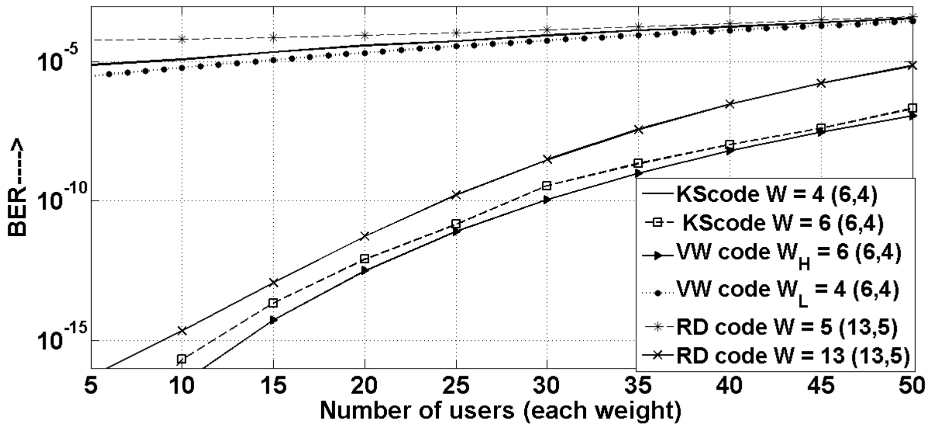

Figure 4.2: Comparison of proposed VW code with other codes using BD technique.

number of users with weight greater than 2. It does not use mapping technique to obtain more codes. A single algorithm is used for variable weights higher than two. It gives comparable, or better BER performance than others, and effect of mapping [86] on BER is eliminated. Supportable number of users for higher weight, at BER of 10^{-9} (data) are 28, 33 and 35 for RD code, KS code, and VW code respectively. Supportable number of users for lower weight, at BER of 10^{-4} (voice) are 23, 31 and 37 for RD code, KS code, and VW code respectively.

Figure 4.3 shows BER versus number of users for VW code by varying the higher weight and keeping lower weight fixed. The combination of two weights (W_H, W_L) is taken as $(6,4), (5,4)$ and $(7,4)$.

The larger value of W_H tends to increase code length and decrease the BER of users. Increasing W_H increases the total code length which leads to higher the BER at fixed W_L. At BER of 10^{-4}, supportable number of users are 50, 36, 16 for $W_L = 4$ when W_H is $7, 6$ and 5 respectively. At BER of 10^{-9}, supportable number of users are 41, 35, 26 for $W_L = 4$ when W_H is $7, 6$

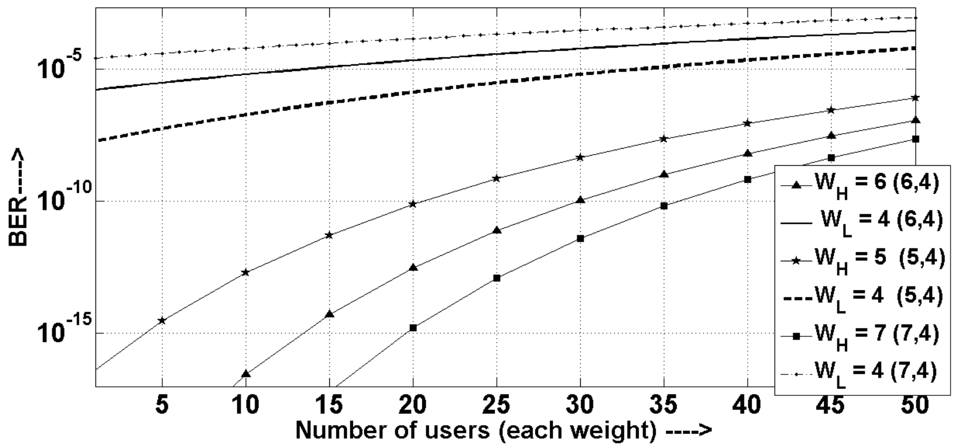

Figure 4.3: Performance of proposed VW code on varying the higher weight (W_H) and fixed lower weight (W_L).

and 5 respectively.

In Fig. 4.4, BER is plotted against number of users for varying W_L and fixed W_H. The combinations of two weights (W_H, W_L) are taken as $(6, 5), (6, 4)$ and $(6, 3)$. As W_L is increased, BER and code length of system decreased and increased respectively. Increasing W_L increases total code length, resulting in higher BER for W_H users.

The higher W_L tends to increase the code length which increases the required total code length of W_H. Hence, lowering the performance of fixed W_H for increasing W_L. The supportable number of users are 50, 36 , and 30 at BER of 10^{-3} for $W_L = 5, 4$ and 3 respectively. The supportable number of users for W_H are 44, 35 and 25 at BER of 10^{-9} on varying $W_L =$ 5, 4 and 3, respectively.

From Eq. (4.32), both numerator and denominator have term $(1/L_T)$. On multiplying L_T^2 to numerator and denominator in Eq. (4.32), denominator varies quadratically with $'L_T'$. Hence, increase in L_T reduces SNR leading to higher BER.

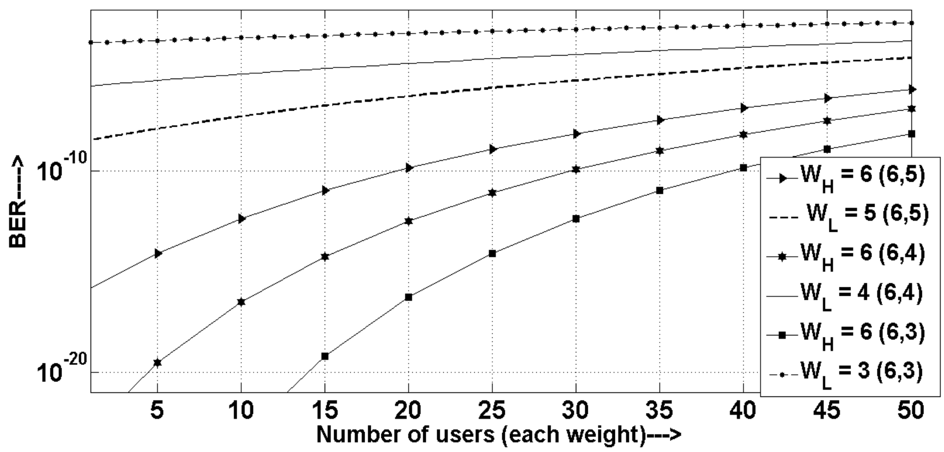

Figure 4.4: Performance variation of proposed VW code on varying the lower weight (W_L) and taking higher weight (W_H) fixed.

Figures 4.5 and 4.6 use three different weights combination corresponding to $W_H = 6$, $W_M = 5$, and $W_L = 3$. Figure 4.5 illustrates the BER for users with W_H, W_M, and W_L versus number of users (each weight) using proposed VW code. The number of users for each weight is chosen as 40. Figure 4.5 also presents the comparison between BD and DD techniques. It is plotted between BER versus number of users. The maximum number of supportable users are 40, 40 and 40 for voice (10^{-3}), data (10^{-9}) and video (10^{-12}), respectively using DD detection. Whereas for BD detection, maximum number of supportable users are 40, 0 and 5 for voice (10^{-3}), data (10^{-9}) and video (10^{-12}), respectively. Since PIIN is not considered in DD, performance is better with respect to BD technique. In DD technique, the receiver is designed with less complexity and its cost is reduced along with better performance [43, 86]. Figure 4.6 illustrates the BER (PIIN, Shot and thermal noise) versus received power using balanced detection for $W_H = 6, W_M = 5, W_L = 3$ with 25 users for each weight. BER of all users decreases with the increase of weight and received power. The application of

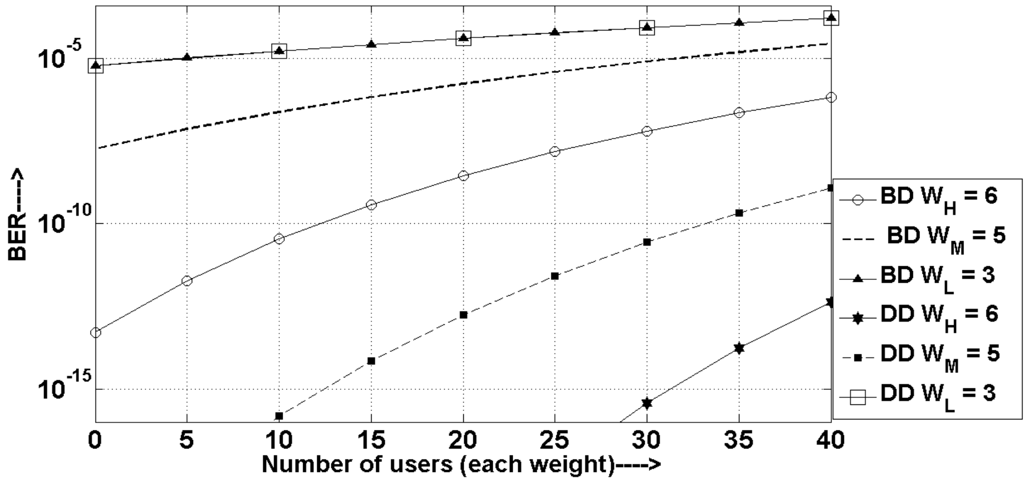

Figure 4.5: Comparison of BD and DD techniques for proposed VW code ($W_H = 6, W_M = 5, W_L = 3$).

proposed VW code to support different services, for average received power of $-20dBm$ has acceptable performance.

It is found that proposed VW code gives comparable and better performance than Generalized Optical Code construction for Enhanced and Modified Double Weight code (Constant weight constant length construction). That is due to lower code length of variable weight codes.

4.5 Summary

VW algorithm is proposed for generalized optical code for enhanced and Modified Double Weight. It is designed for any number of users for weight greater than 2. It does not use mapping technique to obtain more users. The cross correlation of value at most 1 is obtained between any two users. Code construction is begins with the highest weight. On changing number of users of highest weight, code lengths of all lower weight codes are changed. On the other hand, changing number of users of lowest weight, affects its own

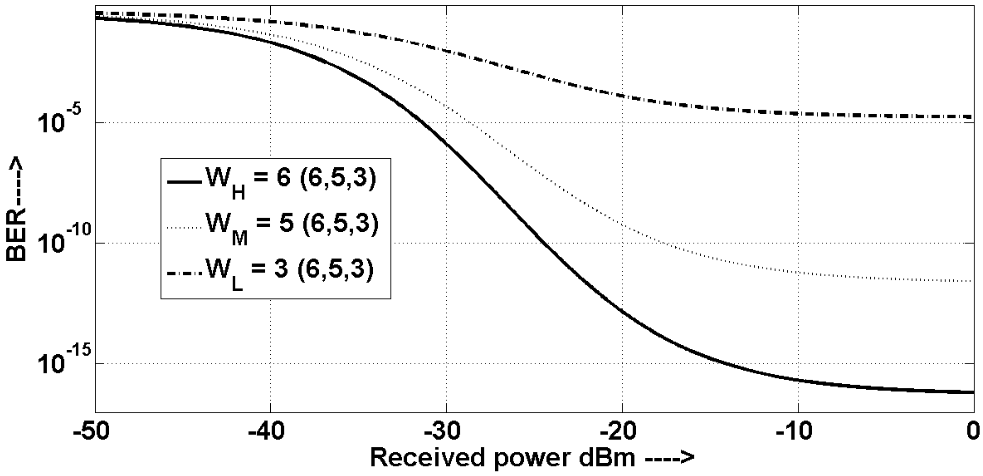

Figure 4.6: Comparison of received power for proposed VW code ($W_H = 6, W_M = 5, W_L = 3$) considering PIIN, shot and thermal noise.

code length and total code length, but does not affect codes of other higher weights. The variation of weights provides different BER. The lowest weight codes have highest BER and highest weight codes have lowest BER.

CHAPTER 5

A new code construction algorithm based on Double Weight Codes with mapping

5.1 Introduction

Reported DW codes algorithms construct the codes on designing different basic matrix of individual weights (odd, even, and 2), and codes for total N number of users are constructed by using mapping. In Chapters 3 and 4, algorithms are proposed without mapping for weights greater than 2. This Chapter describes the effect of mapping and construction of the single code algorithms with mapping for all weights. Like DW code families, basic matrix is first constructed using proposed algorithm. The number of users for basic code matrix depends on the code weight and on a constant value. As size of basic matrix is changed, BER and code length of users are changed. The properties of proposed code are:

- Easy code construction.
- Crosscorreation is $\lambda_c \leq 1$.
- Any positive integer weight can be used for code construction.
- Variety of code set is constructed.
- Size of basic matrix is chosen according to code performance.

2D code construct is also constructed by using 1D code construction. 2D code gives better performance with higher number of users compare to 1D code.

5.2 1D Code Construction

5.2.1 Algorithm

Code construction is starts with constructing the basic matrix (M) of size ($N_B \times L_B$). Here, N_B shows number of users at basic matrix, and it is defined using two conditions for all weights W.

$$N_B = \begin{cases} 3, & \text{A constant value }, \\ W, & \text{Depend on } W \end{cases} . \tag{5.1}$$

L_B is the code length given for basic matrix, defined as

$$L_B = \sum_{i=1}^{W} i = W(W+1)/2. \tag{5.2}$$

As describe in [58], P_n denotes the position of n^{th} pulse in the code sequence for basic matrix and is given by

$$P_n = \begin{cases} 1, & n = 1, \\ P_{n-1} + (n-1), & n > 1 \end{cases}. \tag{5.3}$$

Where, n denotes $n \in 1, 2, ..., W$. Codes for N users are assigned by repeating basic matrix Z times diagonally, where Z is given by

$$Z = \lfloor N/N_B \rfloor. \tag{5.4}$$

As defined in [58], Code length (L) for N users is given by

$$L = Z \times L_B. \tag{5.5}$$

The complete code matrix consisting of N users is written in Eq. (2.2).

Algorithm implementation steps:

Step 1: Define parameters

1. Define W, N_B and N.
2. Calculate L_B and L as defined in Eqs. (5.2) and (5.5) respectively.

Step 2: Construct the basic matrix.

1. Generate a code sequence using Eq. (5.3) and by filling empty spaces with zeros.
2. Rotate code sequence right by one position upto $N_B - 1$ times.
3. Each rotation generates a code sequence.
4. Arrange the generated code sequences in matrix form.

5. After second rotation, find the sum of each column in matrix for each rotation.

6. If all sums are less than 3, codes are generated

7. If sum is greater than 2, interchange the pulse position (P_n) of that column with zero of the column which has sum less than 2 in a same row.

8. Generated matrix is called as basic matrix (M).

Step3 : All N users codes are constructed by using mapping (Z times repetition of basic matrix) as given in Eq. (2.2).

5.2.2 Code construction examples

Example 1 For $W = 2$ and $N_B = 3$ (Constant)

Step 1: Define parameters.

1. $L_B = \sum_{i=1}^{2} i = 3$.

2. Let $N = 12$ and calculated value of $L = 12$.

Step 2: Construction of basic matrix.

1. Calculate the ones positions for given W as

$$P_n = \begin{cases} P_1 = 1, \\ P_2 = P_{2-1} + (2-1) = 2, \end{cases} .$$

2. Arrange these ones to from a code and the empty spaces by zero as

$$\text{Code1} \quad \begin{bmatrix} 1 & 1 & .. \\ 1 & 1 & 0 \\ P_1 & P_2 & \end{bmatrix}.$$

Generated code is denoted by code1.

3. Rotate code1 right by $N_B - 1 = 2$.

4. Rotate code1 right by one position.

$$\text{Code2} \quad \begin{bmatrix} 0 & 1 & 1 \end{bmatrix}.$$

5. Rotate code2 right by one position.

$$\text{Code3} \quad \begin{bmatrix} 1 & 0 & 1 \end{bmatrix}.$$

6. Arrange all the generated codes in matrix form. Check whether all column sums are less than 3 or not.

$$\begin{matrix} \text{Code1} \\ \text{Code2} \\ \text{Code3} \\ \text{Sum} \end{matrix} \begin{bmatrix} 1 & 1 & 0 \\ 0 & 1 & 1 \\ 1 & 0 & 1 \\ \hline 2 & 2 & 2 \end{bmatrix} \quad \text{Basic matrix for } N_B = 3 \text{ is generated.}$$

Step3 : The basic matrix is repeated diagonally for $Z = 4$ as given in Eq. (2.2).

Example 2 for $W = 2$ and $N_B = 2$

Step 1: Define parameters.

1. $L_B = \sum_{i=1}^{2} i = 3$.

2. Let $N = 12$ and calculated $L = 18$.

Step 2: Construction of basic matrix is same as describe in step 2 from 1 to 4.

1. Arrange all the generated codes in matrix form. Check whether all column sums are less than 3 or not. $\begin{matrix} \text{Code1} \\ \text{Code2} \\ \text{Sum} \end{matrix} \begin{bmatrix} 1 & 1 & 0 \\ 0 & 1 & 1 \\ \hline 1 & 2 & 1 \end{bmatrix}$ Basic matrix for $N_B = 2$ is generated.

Step3 : The basic matrix is repeated diagonally for $Z = 3$ as given in Eq. (2.2).

5.2.3 BER analysis

Let $C_k(j)$ be the jth element of the kth proposed code. At balanced receiver, upper part which has same wavelength structure as encoder has correlation function as

$$\sum_{j=1}^{L} C_k(j) \cdot C_l(j) = \begin{cases} W & k = l \quad \text{same user inside } M \\ 1 & k \neq l \quad \text{other users inside } M \\ 0 & k \neq l \quad \text{other users outside } M \end{cases} \tag{5.6}$$

For given user, autocorrelation is W. Cross correlation is 1 and 0 for within M and outside M respectively. In case of lower arm, cross correlation function is defined as

1. Ex-ORing desired user with interfering user.

$$C_Z(j) = \sum_{j=1}^{L} C_k(j) \oplus C_l(j)$$

$\oplus$ denotes the Ex-OR function.

2. C_Z is AND with given interfering user [57].

$$C_Y(j) = C_Z(j) \cdot C_l(j)$$

$\cdot$ denotes the AND function.

3.

$$C_Y(j) = \begin{cases} 0 & k = l \quad \text{same user inside } M \\ (W-1) & k \neq l \quad \text{same users inside } M \\ 0 & k \neq l \quad \text{other users outside } M \end{cases}$$

4. Correlation function is given as

$$\frac{\sum_{j=1}^{L} C_k(j) \cdot C_Y(j)}{(W-1)} = \begin{cases} 0 & k = l \quad \text{same user inside } M \\ 1 & k \neq l \quad \text{same users inside } M \\ 0 & k \neq l \quad \text{other users outside } M \end{cases} \tag{5.7}$$

To analyse BER, the Gaussian approximation with assumptions are taken as per given in [18]. The coherence time of a thermal source [18] is given in Eq. (2.9). The variance of photocurrent [24] can be written as given in Eq. (2.10).

The PSD of the received signals is written as given in Eq. (2.14). The total power at photodetector, PD_1 of kth receiver [25, 58] is

$$P(PD_1) = \int_0^\infty G_1(v)dv = \int_0^\infty \left[\frac{P_{sr}}{\Delta v} \sum_{k=1}^{N_B} d_k \sum_{j=1}^{L} C_k(j) C_l(j) \left\{ u \left[\frac{\Delta v}{L} \right] \right\} \right] dv.$$

$$= \frac{P_{sr}}{\Delta v} \frac{\Delta v}{L} \sum_{k=1}^{N_B} d_k \sum_{j=1}^{L} C_k(j) C_l(j). \tag{5.8}$$

Using correlation function from Eq. (5.6), Eq. (5.8) is written as

$$P(PD_1) = \frac{P_{sr}W}{L} + \frac{P_{sr}}{L}\sum_{k=1,k\neq l}^{N_B} d_k. \tag{5.9}$$

The total power at photodetector, PD_2 [25, 58] is given as

$$P(PD_2) = \int_0^\infty G_2(\upsilon)d\upsilon = \int_0^\infty \left[\frac{P_{sr}}{\Delta\upsilon}\sum_{k=1}^{N_B} d_k \sum_{j=1}^{L} C_k(j)C_X(j)\left\{u\left[\frac{\Delta\upsilon}{L}\right]\right\}\right]d\upsilon$$

$$P(PD_2) = \frac{P_{sr}}{\Delta\upsilon}\frac{\Delta\upsilon}{L}\sum_{k=1}^{N_B} d_k \sum_{j=1}^{L} C_k(j)C_X(j) \tag{5.10}$$

Using correlation property given in Eq. (5.7), Eq. (5.10) lead to

$$P(PD_2) = \frac{P_{sr}}{L}\sum_{k=1,k\neq l}^{N_B} d_k \tag{5.11}$$

The received signal is the difference between photocurrents, which is expressed as $I = I_1 - I_2$. I_1 and I_2 are currents at photodiodes.

$$I = \mathcal{R}P(PD_1) - \mathcal{R}P(PD_2) \tag{5.12}$$

Substituting the expressions of $P(PD_1)$ and $P(PD_2)$ of total power incident at input of PD_1 and PD_2 from Eqs. (5.9) and (5.11) into Eq. (5.12), the received signal is

$$I = \frac{\mathcal{R}P_{sr}W}{L} \tag{5.13}$$

The shot noise is written by substituting Eqs. (5.9) and (5.11) in Eq. (3.17) as

$$\langle I^2_{shot}\rangle = \frac{2eB\mathcal{R}P_{sr}(W + 2(N_B - 1))}{L} \tag{5.14}$$

Using approximation as given in Eq. (3.19) and by substituting Eqs. (5.9) and (5.11) in Eq. (3.20), PIIN is expressed as

$$\langle I_{PIIN}^2 \rangle = \frac{B\mathcal{R}^2 P_{sr}^2 NW}{L^2 \Delta\upsilon}[W + 2(N_B - 1)] \tag{5.15}$$

Noise power, $\langle I^2 \rangle$ as given in Eq. (2.10) is expressed as

$$\langle I^2 \rangle = \frac{2eB\mathcal{R}P_{sr}(W + 2(N_B - 1))}{L} + \frac{B\mathcal{R}^2 P_{sr}^2 NW(W + 2(N_B - 1))}{L^2 \Delta\upsilon} + \frac{4K_b T_n B}{R_L}. \tag{5.16}$$

The probability of sending bit 1 is half [58, 86], Eq. (5.16) leads to

$$\langle I^2 \rangle = \frac{P_{sr} eB\mathcal{R}(W + 2(N_B - 1))}{L} + \frac{B\mathcal{R}^2 P_{sr}^2 NW[W + 2(N_B - 1)]}{2L^2 \Delta\upsilon} + \frac{4K_b T_n B}{R_L} \tag{5.17}$$

The SNR is given in Eq. (2.29). Put values from Eqs. (5.13) and (5.17) in Eq. (2.29), SNR is

$$SNR = \frac{\left(\frac{\mathcal{R}P_{sr}W}{L}\right)^2}{\frac{P_{sr}eB\mathcal{R}(W+2(N_B-1))}{L} + \frac{B\mathcal{R}^2 P_{sr}^2 NW[W+2(N_B-1)]}{2L^2\Delta\upsilon} + \frac{4K_b T_n B}{R_L}}. \tag{5.18}$$

The BER is explained in Eq. (2.31).

5.2.4 Numerical Results

Numerical results are simulated using Matlab software. The parameters are given in Table 2.2 to calculate the numerical results. The data rate and maximum number of users are chosen to 622 Mbps and 100 for all simulations respectively.

Figure 5.1 depicts the BER versus code length for EDW code ($W = 3$), proposed code for ($W = 2$ and 3) for a condition of $N_B = 3$ using balanced detection. Proposed code ($W = 2, N_B = 3, L_B = 3$) require less code length

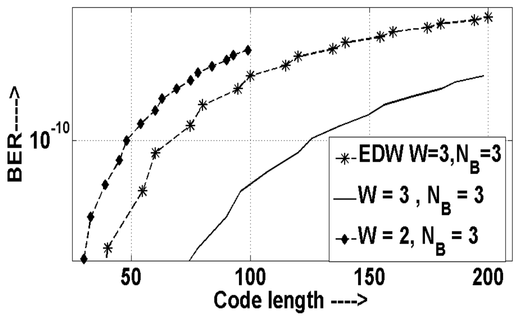

Figure 5.1: BER versus code length for proposed code ($W = 2, 3$) and EDW code ($W = 3$) for $N_B = 3$ upto 100 users.

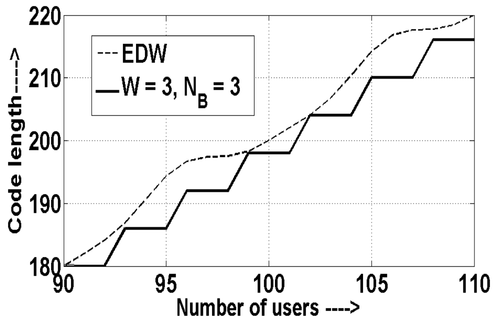

Figure 5.2: Code length against number of users for proposed code and EDW code for $N_B = 3, W = 3$.

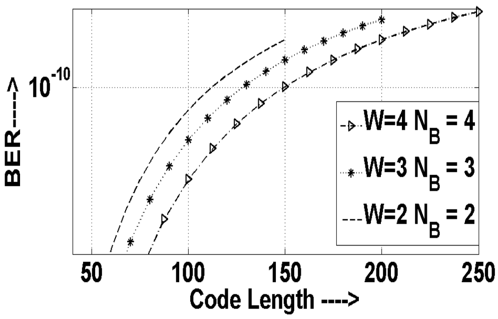

Figure 5.3: BER against code length for proposed code when weight is varied from 2 to 4 for $N_B = W$ upto 100 users.

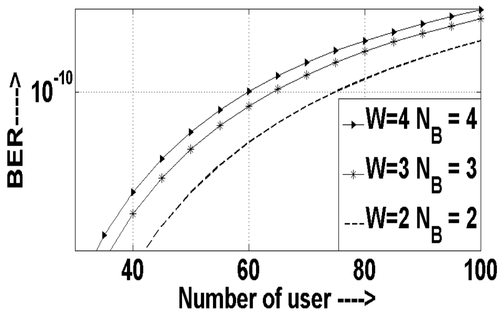

Figure 5.4: BER against number of users for proposed code when weight is varied from 2 to 4 for $N_B = W$ upto 100 users.

compare to EDW and proposed code ($W = 3, N_B = 3, L_B = 6$). Reason behind is lower size of basic matrix in case of proposed code ($W = 2, N_B = 3, L_B = 3$) compare to others Code length of 200, 198 and 99 is required by EDW code, proposed code ($W = 3, N_B = 3, L_B = 6$) and proposed code ($W = 2, N_B = 3, L_B = 3$) respectively.

Code length increment of EDW code is differing from proposed code. The difference is shown in Fig. 5.2, for weight ($W = 3$) and basic matrix of ($N_B = 3, L_B = 6$). Difference in the length is due to different techniques used to calculate code length (L) for N users. For EDW, it involves a sine relation between L and N [31]. Proposed code follows constant variation of code length defined in eq. 5.27. These code length variations effect the BER performance of codes which depend on N and L.

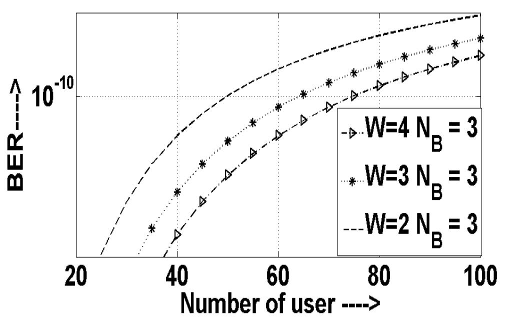

Figure 5.5: BER against number of users for proposed code when weight is varied from 2 to 4 for N_B=3 upto 100 users.

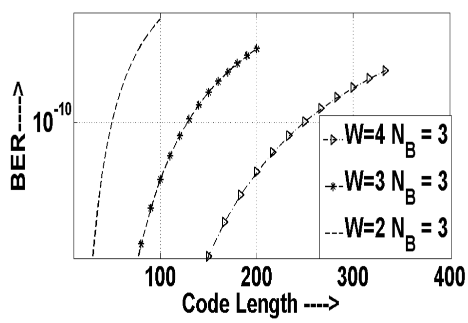

Figure 5.6: BER against code length for proposed code when weight is varied from 2 to 4 for N_B=3 upto 100 users.

BER is plotted against code length for proposed code when weight is varied from 2 to 4 for a condition of $N_B = W$ as shown in Fig.5.3. As the weight W of the proposed code is increased, N_B and L_B is increased which further increases the size of the basic matrix (in term of N_B and L_B). Due to these reasons, code length require for N users are increased as W is increased. Required code length (L) for W = 2, 3 and 4 are 150, 198 and 250 respectively.

Figure 5.4 depicts the BER againstnumber of users for proposed code when weight is varied from 2 to 4 for a condition of $N_B = W$. As W of proposed code is increased, the number of users (N_B) at basic matrix is increased. Increase in N_B, increase the interfering users at basic matrix which decreases the BER performances. For proposed code with W = 2, 3 and 4, number of users are 87, 75 and 70 respectively.

Figure 5.5 depicts BER against number of users for proposed code when $W = 4$, 3 and 2 at constant value of $N_B = 3$. L_B of basic matrix is increased as W is increased and N_B is fixed to value 3 for all weights. Because of above reason interfering users in basic matrix is fixed and on other hand weight and code length of each user is increased. Due to these facts, BER performance is improved as weight increases.

Figure 5.6 illustrates the BER against code length for proposed code when $W = 4$, 3 and 2 for $N_B = 3$. The code length L depends on L_B, N_B and N. L_B increases as weight W of code increases. For $N_B = 3$ condition, code length for $W = 2$, 3 and 4 are 99, 198 and 330 respectively.

As weight (W) of proposed code is changed, M and L are changed in a two ways. First way is the N_B is constant ($N_B = 3$) and L_B is increased as W is increased. Second way is both $N_B = W$ and L_B are increased as W is increased. Due to above conditions, repetition of basic matrix (M) is changed. Resultant code length required for N users is changed.

5.3 2D code construction

5.3.1 Algorithm

2D Code construction begins with construction of basic matrix of size ($N_g \times L_x$) for 1D code. N_g is the number of users in basic matrix, and is equal to W_x. W_x is code weight of spectral dimension. L_x is the code length for basic matrix, and it is defined as

$$L_x = W_x(W_x + 1)/2. \tag{5.19}$$

As described in [58], P_n denotes the position of n^{th} pulse in the code sequence for basic matrix and as given in Eq. (5.3).

Spatial dimension is derived as. The basic matrix of size $(N_h \times L_y)$. Where N_h is the number of users in basic matrix, and is equal to N_g. Code weight W_y is given as

$$W_y = W_x - 1. \tag{5.20}$$

Code length (L_y) is given as

$$L_y = N_h \times W_y. \tag{5.21}$$

For second dimension, code construction is explained as Subtracting the positions of P_{n+1} from P_1 code as

$$P_m = P_{n+1} - P_1. \tag{5.22}$$

Where P_m is the position of ones in spatial dimension and, n=1,2,...

Total number of codes for N users is given as

$$N = g \times h. \tag{5.23}$$

Where g and h are number of codes used for each dimension. These codes are assigned by repeating basic matrix diagonally M_g and M_h times. M_g and M_h are given as

$$M_g = \lfloor g/N_g \rfloor \tag{5.24}$$

and

$$M_h = \lfloor h/N_h \rfloor. \tag{5.25}$$

As defined in [58], code length (L_g and L_h) for g and h codes are given by

$$L_g = M_g \times L_x \tag{5.26}$$

and

$$L_h = M_h \times L_y. \tag{5.27}$$

Algorithm implementation steps:

Step 1: Define parameters

1. Choose W_x.
2. Calculate L_x, W_y, L_y, and N as defined in Eqs. (5.19), (5.20), (5.21) and (5.23) respectively.
3. N_h and N_g are equal to W_x.

Step 2: Construct the code for spectral dimension.

1. Generate code sequence using Eq. (5.3) and by filling empty spaces with zeros.
2. Rotate code sequence right by one position upto $N_g - 1$ times and each rotation generates a code sequence.
3. Arrange the generated code sequences in matrix form.
4. After second rotation, find the sum of each column in matrix for each rotation.
5. If all sums are less than 3, codes are generated
6. If sum is greater than 2, interchange the pulse position (P_n) of that column with zero of the column which has sum less than 2 in a same row.

Table 5.1: 2D code construction using DW codes.

	[1 1 0]	[0 1 1]
1	1 1 0	0 1 1
1	1 1 0	0 1 1
0	0 0 0	0 0 0
0	0 0 0	0 0 0
1	1 1 0	0 1 1
1	1 1 0	0 1 1

Table 5.2: 2D code cross corelation values.

	$R^0(g,h)$	$R^1(g,h)$	$R^2(g,h)$	$R^3(g,h)$
$g=0 \bigcap h=0$	W_xW_y	0	0	0
$g=0 \bigcap h\neq 0$	W_x	W_x	0	0
$g\neq 0 \bigcap h=0$	0	0	W_y	0
$g\neq 0 \bigcap h\neq 0$	0	0	1	1

7. Generated matrix is called as basic matrix (C_g), and is repeated diagonally M_g times, to construct the code for all g.

Step 3: Construct the code for second dimension.

1. Generate code sequence using Eq. (5.22) and filling empty spaces with zeros.
2. Rotate code sequence right by one position upto $N_g - 1$ times. Each rotation generates a code sequence.
3. After second rotation, find the sum of each column in matrix for each rotation.
4. If all sums are one, codes are generated
5. If sum is greater than 1, interchange the pulse position (P_m) of that column with zero of the column in same row.
6. Generated matrix is called as basic matrix (C_h), and is repeated diagonally M_h times, to construct the code for all h.

Example-

Step 1: Define parameters-

1. $W_x = 2$.
2. $W_y = W_x - 1 = 1$, $N_g = 2 = N_h$, $L_x = (2*3)/2 = 3$ and $L_y = 2$.

Step 2:

1. $P_1 = 1$, (first one is at position 1)
2. $P_2 = P_{2-1} + (2-1) = 2$, (second one is at position 2)
3. Arrange these ones to from a code as

   1 1 ... .
4. Fill the empty spaces by zero [1 1 0].
5. Generated code for user1 is denoted by code 1.
6. Rotate code 1 right by one position upto given number of $(N_g - 1 = 1)$. Code 2 is generated [0 1 1].
7. Put all the generated codes in matrix form to find the sum of each column, and check whether it is greater than two or not. If it is greater than 2, interchange the 1 of that column with zero of the column for same row which has sum less than 2 as shown below

$$\left[\begin{array}{ccc} 1 & 1 & 0 \\ 0 & 1 & 1 \\ \hline 1 & 2 & 1 \end{array}\right] \begin{array}{c} \text{Code 1} \\ \text{Code 2} \\ \text{Sum} \end{array}$$

Step 3:

1. From code 1, on subtracting the positions of $n+1$ from P_1 code for another dimension is drived. $P_{n+1} - P_1 = P_m$

$$P_1 = P_2 - P_1 = 1$$

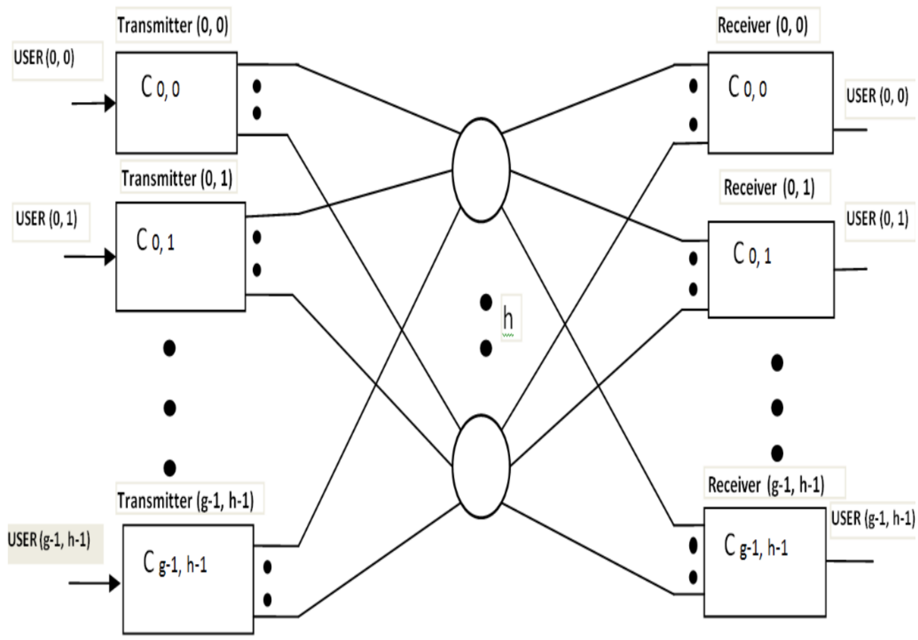

Figure 5.7: SAC-OCDMA network design using 2D code.

2. Arrange these ones to from a code as 1 ... .

3. Fill the empty spaces by zeros

   1 0 code 1 .

4. Rotate code 1 right by one position upto given number of $(N_g - 1 = 2)$. Code 2 is generated [0 1].

$$\begin{bmatrix} 1 & 0 \\ 0 & 1 \\ \hline 1 & 1 \end{bmatrix} \begin{matrix} \text{Code 1} \\ \text{Code 2} \\ \text{Sum} \end{matrix}$$

The cross correlation of 2D code is calculated as

$$R_{gh}^{(d)} = \sum_{i=o}^{L_g-1} \sum_{j=0}^{L_h-1} C^{(d)} C_{gh}. \tag{5.28}$$

Where $C^{(d)}$ denotes characteristic matrices $d(0,1,2,3)$, $C^0 = X_g^T Y_h$, $C^1 = \overline{X_g^T} Y_h$, $C^2 = X_g^T \overline{Y_h}$, and $C^3 = \overline{X_g^T}\,\overline{Y_h}$. T denotes the transpose function. $\overline{X_g^T}$ and $\overline{Y_h}$ are complement of X_g and Y_h. C_{gh} is total number of codes, given as $X_g^T Y_h$. Here, X_g and Y_h are 1D codes in spectral and spatial domain respectively. Codes are represented as $X = x_0, x_1, x_2, ..., x_{L_g-1}$ and $Y = y_0, y_1, y_2, ..., y_{L_h-1}$. L_g and L_h are code lengths of 1D code.

The MAI elimination is obtained as follows using Table 5.2

$$R^{(0)}_{g,h} - \frac{R^{(1)}_{g,h}}{(W_x - 1)} = \begin{cases} W_x W_y & \text{same user or g=0, h=0} \\ 0 & \text{other users} \end{cases} \tag{5.29}$$

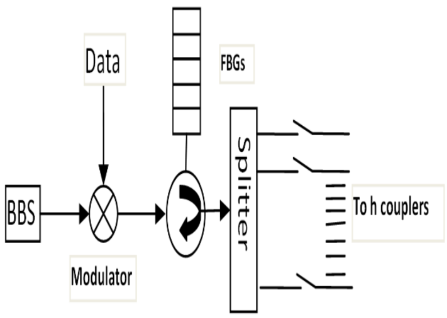

Figure 5.8: Encoder design using 2D code.

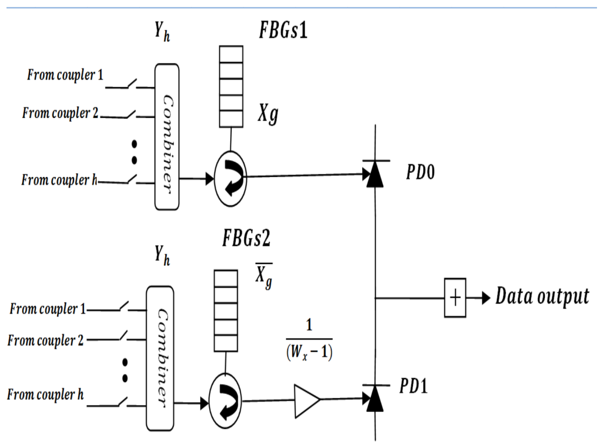

Figure 5.9: Decoder structure using 2D code.

5.3.2 System Description

Figure 5.7 shows the SAC-OCDMA system implementation using 2D code. System consists of $g \times h$ pairs of transmitters and receivers. There are h star couplers with $g \times h$ inputs and $g \times h$ outputs. The structure of transmitter for each user is shown in Fig. 5.8. At the transmitter, Broadband Source (BBS) is modulated according to incoming data. The spectral encoding of code is done by selecting wavelengths using Fiber Bragg Grating (FBGs) according to the spectral code. Optical splitter is used to provide spatial encoding after spectral encoding. It divides each spectral component equally. Output of splitter is sent towards the h star couplers.

Figure 5.9 shows the structure of the receiver. Output from h star couplers are received and combined by two combiners. Upper and lower combiners outputs correspond to the spatial code. FBGs are designed according to the spectral code sequence. Upper FBG is used to obtain the spectral components, which are matched to 1s of the spectral code sequence. Lower FBG is used to obtain the spectral components, which are matched to 0s of the spectral code sequence means complement of code. The optical attenuator with the value of $1/W_x - 1$ is used to adjust the power level of the optical pulses.

$PD0$ and $PD1$ convert the optical signals to electronic signals and then pass them to the integrator. The output current from $PD0$ and $PD1$ are proportional to $R^{(0)}_{g,h}$ and $R^{(1)}_{g,h}/(W_x - 1)$ respectively. The output current at the integrator is proportional to $R^{(0)}_{g,h} - R^{(1)}_{g,h}/(W_x - 1)$. The value of output current is equal to W_xW_y for same user $g = h = 0$, or zero for other users, according to Eq. 5.29.

5.3.3 BER analysis

To analyse BER of the system, the Gaussian approximation as in Section 2.3.1, the coherence time of a thermal source [18] as given in Eq. (2.9) and The variance of photocurrent [24] as given in Eq. (2.10) are considered for analysis. The PSD of the received optical signals can be written as

$$r(f) = \frac{P_{sr}}{K_y \Delta f} \sum_{U=1}^{U} d(u) \sum_{i=0}^{(L_x-1)} \sum_{j=0}^{(L_y-1)} a_{ij}(u) F(f,i) \quad (5.30)$$

Here $d(u)$ is the data bit of the uth user, P_{sr} is effective power of a BLS at the receiver, $a_{i,j}(u)$ is element of uth user code and $F(f,i)$ is explained in terms of unit step function $u(f)$ as shown in Eqs.(5.31).

$$F(f,i) = u\left[f - f_0 - \frac{\Delta f}{2L_x}(-L_x + 2i)\right] - u\left[f - f_0 - \frac{\Delta f}{2L_x}(-L_x + 2i + 2)\right] \quad (5.31)$$

PSDs of received signals at PDs of each user can be written as

$$S_0(f) = \frac{P_{sr}}{W_h \Delta f} \sum_{n=1}^{N} d(n) \sum_{i=0}^{L_g-1} \sum_{j=0}^{L_h-1} a_{ij}^{(0)} a_{ij}(u) * F(f,i) \quad (5.32)$$

$$S_1(f) = \frac{P_{sr}}{W_h \Delta f} \sum_{n=1}^{N} d(n) \sum_{i=0}^{L_g-1} \sum_{j=0}^{L_h-1} a_{ij}^{(1)} a_{ij}(u) * F(f,i) \quad (5.33)$$

Calculate the output currents of each PDs as

$$I_0 = \mathcal{R} \int_0^\infty S_0(f) df = \frac{\mathcal{R} P_{sr}}{W_h L_g} \left[W_g W_h + \frac{W_h(N-1)(N_g-1)}{(gh-1)}\right] \quad (5.34)$$

$$I_1 = \mathcal{R} \int_0^\infty S_1(f) df = \frac{\mathcal{R} P_{sr}}{W_h L_g} \left[\frac{W_h(N-1)(N_g-1)}{(gh-1)}\right] \quad (5.35)$$

The average photo current of receiver is given as

$$I = \mathcal{R}\int_0^\infty (S_0(f) - S_1(f)) = I_0 - I_1 = \frac{\mathcal{R}P_{sr}W_g}{L_g} \tag{5.36}$$

The shot noise is

$$I_{shot} = 2eBI_{total} = 2eB(I_0 + I_1) \tag{5.37}$$

The PIIN is

$$I_{PIIN} = BI^2\tau = B\mathcal{R}^2\int_0^\infty [S_0 - S_1]^2 df \tag{5.38}$$

$$I_{PIIN} = B\mathcal{R}^2\int_0^\infty \left[S_0^2(f) - 2S_0(f)S_1(f) + S_1^2(f)\right] df = \frac{B\mathcal{R}^2P_{sr}W_x^2}{\Delta f L_x} \tag{5.39}$$

Each user transmits 1s and 0s with equal probability.

$$I_{shot} = eB\frac{\mathcal{R}P_{sr}}{W_hL_g}\left[W_gW_h + \frac{2W_h(N-1)(N_g-1)}{(gh-1)}\right] \tag{5.40}$$

$$I_{PIIN} = \frac{B\mathcal{R}^2P_{sr}W_x^2}{2\Delta f L_x} \tag{5.41}$$

The SNR is defined in Eq. (2.29). The BER is calculated by using Gaussian approximation from SNR as expressed in Eq. (2.31).

5.3.4 Numerical results

The relevant parameters as given in Table 2.2 are used to obtain numerical results. Figure 5.10 depicts the BER versus number of users for 1D code for $W = 2$, 2D hybrid code ($m_s = 21, P = 7$) and 2D code for ($g = 7, h = 21$) at a data rate of 5 Gbps using balanced detection. The total number of users for 1D and 2D codes are set to 150. The total number of users for hybrid code is 147 dependent on (m_s, P). The BER of 4×10^{-6} and 9×10^{-15} are obtained using 2D hybrid code and proposed 2D code respectively. The 2D hybrid code is using values of weights $K_l = 20$ for spectral and $K_p = 3$ for spatial dimension.

The proposed 2D code is using $W_x = 2$ for spectral and $W_y = 1$ for spatial. The 2D hybrid code requires more bandwidth of source compared to proposed 2D code due to higher value of spectral weight. Degradation of BER performance of 1D code is fast compared to proposed 2D code as shown in Fig. 5.10.

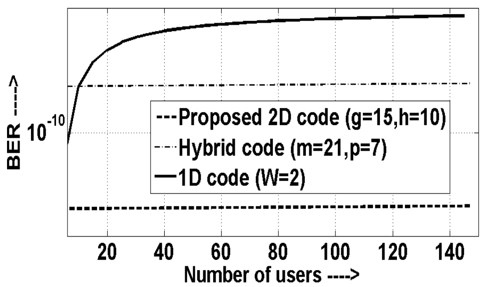

Figure 5.10: Comparison of 2D Hybrid code and 1D code with designed 2D code for BER versus number of active users.

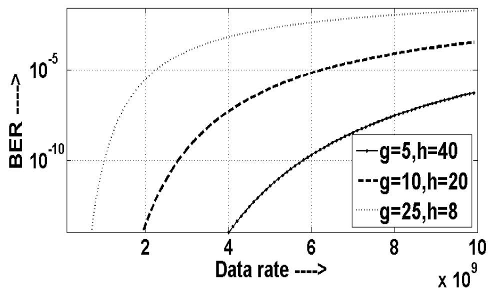

Figure 5.11: BER versus data rate comparison for different value of g and h of 2D code.

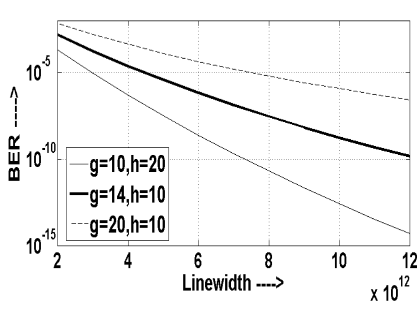

Figure 5.12: BER versus Line width of BBS for different value of g and h for 2D code.

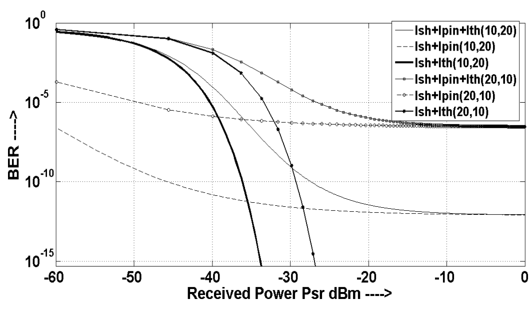

Figure 5.13: BER versus received power when active number of users are 140 and data rate is 5 Gps.

Figure 5.11 depicts the effect of data rate on BER. The weight of the code is set by values $W_x = 2, W_y = 1$. The number of users are chosen to be 200. The number of codes for both dimension are taken as $(g = 25, h = 8)$, $(g = 10, h = 20)$, and $(g = 5, h = 40)$. These codes attain a BER of 10^{-9} at data rate of 6.54 *Gbps* for $(g = 5, h = 40)$, 3.15 *Gbps* for $(g = 10, h = 20)$, and 1.14 *Gbps* for $(g = 25, h = 8)$. As the value of spatial codes h is increased and spectral codes g is decreased, BER performance is improved. This is due to orthogonal property of h codes.

Figure 5.12 shows the BER versus Line width of BBS for different values of g and h for 2D code. The values of g and h are taken as $(g = 10, h = 20)$, $(g = 14, h = 10)$, and $(g = 20, h = 10)$. Data rate of 10 *Gbps* is set for numerical result. The code size $(g = 10, h = 20)$ requires less line width of source than other two code values. This is due to lower value of spectral code g. Lower value of g requires less amount of BBS. Figure 5.13 shows BER versus received power when active number of users are 200 and data rate is 5 *Gbps*. The code size of $(g = 10, h = 20)$ and $(g = 20, h = 10)$ are used to have 200 users. The lower value of spectral code g require less power compared to higher value of g.

5.4 Summary

A new and single code construction algorithm is proposed for DW code families for all weights using mapping. Proposed code algorithm is analysed for BER and compared with EDW code. A other 2D code is proposed for SAC-OCDMA systems. The code is having a low value of IPCC for spectral dimension and orthogonal in spatial dimension. In comparison with 1D code, it offers greater number of users along with better BER performance.

CHAPTER 6

Development of ZCCC for Constant and Variable Weight

6.1 Introduction

The codes proposed in Chapters 2, 3, 4 and 5, suffer from PIIN. PIIN is eliminated theoretically by using the codes with zero cross correlation (ZCC) property. The code with the property of zero cross correlation is called Zero Cross Correlation Code (ZCCC). The code structure of ZCCC does not have any overlapping of wavelengths between any users. The ZCC code is reported with Constant Weight (CW) code construction in [36]. Codes are using mapping technique to provide codes for the higher number of users. Basic matrix is constructed by using code transformation technique which needs the basic matrix of all lower weights.

A new ZCCC is proposed without mapping. Code construction algorithm is designed with any weight for any number of users having constant or variable weights. Variable weight (VW) codes give different QoS, and are suitable, and useful for multimedia applications.

6.2 Constant Weight Code Construction

Construction of code is as follows

1. Define weight W and number of users N for code.

2. Basic matrix M of size $2 \times W$ for W is constructed as

$$M = \begin{bmatrix} S_1 \\ S_2 \end{bmatrix} = \begin{bmatrix} \lfloor \frac{W}{2} \rfloor 0s & \lfloor \frac{W+1}{2} \rfloor 1s \\ \lfloor \frac{W}{2} \rfloor 1s & \lfloor \frac{W+1}{2} \rfloor 0s \end{bmatrix}_{2 \times W} \tag{6.1}$$

3. Basic matrix of weight W is repeated $N_W + 1$ times as

$$U = \begin{bmatrix} S_1 & .. & .. & .. & .. \\ S_2 & S_1 & .. & .. & .. \\ .. & S_2 & S_1 & .. & .. \\ .. & .. & \ddots & .. & .. \\ .. & .. & \ddots & S_2 & S_1 \\ \vdots & \vdots & \vdots & \vdots & S_2 \end{bmatrix}. \tag{6.2}$$

4. First and last rows along with unused columns of U matrix are removed. Unused columns are equal to $\lfloor \frac{W+1}{2} \rfloor + \lfloor \frac{W}{2} \rfloor$.

5. Code length is calculated as $N * W$.

6.2.1 Example

CW-ZCCC (Proposed)

$W = 3$ for $N = 3$ are chosen for explanation of code construction and is described below

1. Basic matrix M of size 2×3 for $W = 2$ is constructed as

$$M = \begin{bmatrix} S_1 \\ S_2 \end{bmatrix} = \begin{bmatrix} \lfloor \frac{3}{2} \rfloor 0s & \lfloor \frac{3+1}{2} \rfloor 1s \\ \lfloor \frac{3}{2} \rfloor 1s & \lfloor \frac{3+1}{2} \rfloor 0s \end{bmatrix}_{2\times 3} = \begin{bmatrix} 0 & 1 & 1 \\ 1 & 0 & 0 \end{bmatrix}_{2\times 3} \tag{6.3}$$

2. Basic matrix is repeated 4 times as

$$U = \begin{bmatrix} 011 & .. & .. & .. \\ 100 & 011 & .. & .. \\ .. & 100 & 011 & .. \\ .. & .. & 100 & 011 \\ .. & .. & .. & 100 \end{bmatrix}.$$

3. Empty spaces are filled with zeros. First and last rows along with unused columns of U matrix are removed. Unused columns are equal to 3 (shown by parenthesis).

$$U = \begin{bmatrix} 1(00) & 011 & 000 & (0)00 \\ 0(00) & 100 & 011 & (0)00 \\ 0(00) & 000 & 100 & (0)11 \end{bmatrix} = \begin{bmatrix} 1 & 011 & 000 & 00 \\ 0 & 100 & 011 & 00 \\ 0 & 000 & 100 & 11 \end{bmatrix}.$$

ZCC Code (reported)

Basic matrix of size $((W+1)\times W(W+1))$ is first constructed. Basic matrix is repeated diagonally to obtain higher number of users called as mapping. Due to mapping it has a stepwise increase in code length. Basic matrix is obtained by using code transformation technique which need the code of all lower weights [36] e.g. Basic matrix of $(W=3)$ needs basic matrix of $W=1$ and $W=2$.

$$\text{Basic matrix of } (W=3) = \begin{bmatrix} 000 & 000 & 010 & 101 \\ 000 & 101 & 000 & 010 \\ 010 & 010 & 001 & 000 \\ 101 & 000 & 100 & 000 \end{bmatrix}.$$

Proposed ZCCC construct any weight code without any information about lower weight codes. It constructs the code without mapping. It has a linear increase in code length.

6.3 Variable Weight Code Construction

Construction of code is as follows

1. The total number of users are defined as

$$\Psi = \sum_{i=1}^{M} N_{W_i}. \tag{6.4}$$

   Where N_{W_i} users with weight W_i. Total number of weights are from W_1 to W_M.

2. Basic matrix (M_{W_i}) of size $2\times W_i$ for W_i is constructed as

$$M_{W_i} = \begin{bmatrix} S_1^{(W_i)} \\ S_2^{(W_i)} \end{bmatrix} = \begin{bmatrix} \lfloor \frac{W_i}{2} \rfloor 0s & \lfloor \frac{W_i+1}{2} \rfloor 1s \\ \lfloor \frac{W_i}{2} \rfloor 1s & \lfloor \frac{W_i+1}{2} \rfloor 0s \end{bmatrix}_{2\times W_i} \tag{6.5}$$

3. Construction of code begins from highest weight (W_M) to lowest weight (W_1).

4. Basic matrix of highest weight W_M is repeated $N_{W_M}+1$ times as

$$U = \begin{bmatrix} S_1^{(W_M)} & .. & .. & .. & .. \\ S_2^{(W_M)} & S_1^{(W_M)} & .. & .. & .. \\ .. & S_2^{(W_M)} & S_1^{(W_M)} & .. & .. \\ .. & .. & \ddots & .. & .. \\ .. & .. & \ddots & S_2^{(W_M)} & S_1^{(W_M)} \\ \vdots & \vdots & \vdots & \vdots & S_2^{(W_M)} \end{bmatrix}. \tag{6.6}$$

5. For last repeated basic matrix of W_M, calculate reducibility number (R_{W_M}).

   (a) Reducibility number (R_{W_i}) is defined as given below

$$R_{W_i} = \left\lfloor \frac{W_{i-1}+1}{2} \right\rfloor - \left\lfloor \frac{W_i}{2} \right\rfloor \tag{6.7}$$

   where W_i varies from W_M to W_1.

      i. Calculated value of R_{W_i} is either 0 or any negative integer value. This is due to code construction which starts from highest weight to lowest weight.

      ii. When $R_{W_i}=0$, no change is required in basic matrix M_{W_i} .

iii. When R_{W_i} = negative integer, reduce R_{W_i} number of 1s from $S_2^{(W_i)}$ and 0s from $S_1^{(W_i)}$ of basic matrix M_{W_i}.

iv. After reduction, last repeated basic matrix is shown as $(S_{1R}^{(W_i)}, S_{2R}^{(W_i)})$.

6. Step 4 and 5 are repeated for weights W_{M-1} to W_1. Basic matrix of W_{M-1} to W_1 are repeated $N_{W_{M-1}}$ to N_{W_1} times respectively as per eq. (6.8).

$$U = \begin{bmatrix}
S_1^{(W_M)}.. & .. & & & & & & \\
S_2^{(W_M)}.. & S_{1R}^{(W_M)} & & & & & & \\
.... & S_{2R}^{(W_M)} & S_1^{(W_{(M-1)})}.. & & & & & \\
\vdots & \vdots & S_2^{(W_{(M-1)})}.. & S_{1R}^{(W_{(M-1)})} & & & & \\
\vdots & \vdots & \vdots & \ddots & & & & \\
\vdots & \vdots & \vdots & \ddots & S_{1R}^{(W_2)} & & & \\
\vdots & \vdots & \vdots & \vdots & S_{2R}^{(W_2)} & S_1^{(W_1)} & & \\
\vdots & \vdots & \vdots & \vdots & \vdots & S_2^{(W_1)} & & \\
\vdots & \vdots & \vdots & \vdots & \vdots & \ddots & & \\
.. & .. & .. & .. & .. & .. & S_2^{(W_1)} & S_1^{(W_1)} \\
.. & .. & .. & .. & .. & .. & .. & S_2^{(W_1)}
\end{bmatrix}. \tag{6.8}$$

7. First row and last row of U matrix is removed as shown in eq.(6.9).

$$U = \begin{bmatrix}
S_{2R}^{(W_M)} & .. & S_{1R}^{(W_M)} & & & & & \\
.. & .. & S_{2R}^{(W_M)} & S_1^{(W_{(M-1)})} & & & & \\
\vdots & \vdots & \vdots & S_2^{(W_{(M-1)})} & & & & \\
\vdots & \vdots & \vdots & \vdots & \vdots & \ddots & & \\
\vdots & \vdots & \vdots & \vdots & \ddots & \ddots & S_1^{W_1} & \\
.. & .. & .. & .. & .. & .. & S_2^{W_1} & S_1^{W_1}
\end{bmatrix}. \tag{6.9}$$

8. Empty spaces are filled with zeros.

$$U = \begin{bmatrix} S_2^{(W_M)}.. & S_1^{(W_M)} R_{W_M} & & & & \\ 0 & S_2^{(W_M)} R_{W_M} & S_1^{(W_{(M-1)})}..0 & & & \\ \vdots & \vdots & S_2^{(W_{(M-1)})}..0 & & & \\ \vdots & \vdots & \vdots & \ddots & & \\ 0 & 0 & 0 & 0 & S_2^{W_1} & S_1^{W_2} \end{bmatrix} \quad (6.10)$$

9. All 0s columns are deleted. Number of all 0s columns are $\lfloor \frac{W_M+1}{2} \rfloor 0s$ from left side and $\lfloor \frac{W_1}{2} \rfloor 0s$ from right side.

10. The complete code set is generated as shown in eq.(6.10).

11. At each transition of weight, code length is changed. The code length is amount of Broad Band Source (BBS) (wavelengths) required by a particular weight. Code length L_{W_M} is amount of BBS required by W_M. For W_{M-1}, code length ($L_{W_{M-1}}$) is (L_{W_M}+ BBS required by W_{M-1}). This is so on upto weight W_1. Total code length used by the code is L_n which is given as

$$L_n = L_{W_1} \quad (6.11)$$

where L_{W_1} is code length required by weight W_1.

12. Code lengths are defined as

For N_{W_M} users, code length is

$$L_{W_M} = W_M * (N_{W_M} + 1) + R_{W_M} - \left\lfloor \frac{W_M + 1}{2} \right\rfloor \quad (6.12)$$

For $N_{W_{N-1}}$ users, code length is

$$L_{W_{M-1}} = L_{W_M} + W_{M-1} * (N_{W_{M-1}}) + R_{W_{M-1}} \quad (6.13)$$

For $N_{W_{N-2}}$ users, code length is

$$L_{W_{M-2}} = L_{W_{M-1}} + W_{M-2} * (N_{W_{M-2}}) + R_{W_{M-2}} \tag{6.14}$$

.....

For N_{W_1} users, code length is

$$L_{W_1} = L_{W_2} + W_1 * (N_{W_1}) - \left\lfloor \frac{W_1}{2} \right\rfloor \tag{6.15}$$

6.3.1 Example

$W_H = 3$ for $N_H = 3$ and $W_L = 2$ for $N_L = 3$ are chosen for explanation of code construction and is described below

1. Size of basic matrix of $W_H = 3$ is defined as 2×3 and it is created as

$$M_{W_H} = \begin{bmatrix} S_1^{(3)} \\ S_2^{(3)} \end{bmatrix} = \begin{bmatrix} \lfloor \frac{3}{2} \rfloor 0s & \lfloor \frac{3+1}{2} \rfloor 1s \\ \lfloor \frac{3}{2} \rfloor 1s & \lfloor \frac{3+1}{2} \rfloor 0s \end{bmatrix}_{2\times 3} = \begin{bmatrix} 0 & 1 & 1 \\ 1 & 0 & 0 \end{bmatrix}_{2\times 3}.$$

2. Size of basic matrix of $W_L = 2$ is defined as 2×2 and it is created as

$$M_{W_L} = \begin{bmatrix} S_1^{(2)} \\ S_2^{(2)} \end{bmatrix} = \begin{bmatrix} \lfloor \frac{2}{2} \rfloor 0s & \lfloor \frac{2+1}{2} \rfloor 1s \\ \lfloor \frac{2}{2} \rfloor 1s & \lfloor \frac{2+1}{2} \rfloor 0s \end{bmatrix}_{2\times 2} = \begin{bmatrix} 0 & 1 \\ 1 & 0 \end{bmatrix}_{2\times 2}.$$

3. M_{W_H} is repeated $N_H + 1 = 4$ times as

$$U = \begin{bmatrix} 011 & .. & .. & .. \\ 100 & 011 & .. & .. \\ .. & 100 & 011 & .. \\ .. & .. & 100 & 011 \\ .. & .. & .. & 100 \end{bmatrix}.$$

4. Find $R_{W_H} = 1 - 1 = 0$

5. M_{W_L} is repeated $N_L = 3$ times as

$$U = \begin{bmatrix} 011 & .. & .. & .. & & & \\ 100 & 011 & .. & .. & & & \\ .. & 100 & 011 & .. & & & \\ .. & .. & 100 & 011 & & & \\ .. & .. & .. & 100 & 01 & & \\ .. & .. & .. & .. & 10 & 01 & \\ .. & .. & .. & .. & .. & 10 & 01 \\ .. & .. & .. & .. & .. & .. & 10 \end{bmatrix}.$$

6. First and last row of U matrix is removed.

$$U = \begin{bmatrix} 100 & 011 & .. & .. & & & \\ .. & 100 & 011 & .. & & & \\ .. & .. & 100 & 011 & & & \\ .. & .. & .. & 100 & 01 & .. & .. \\ .. & .. & .. & .. & 10 & 01 & .. \\ .. & .. & .. & .. & .. & 10 & 01 \end{bmatrix}.$$

7. Empty spaces are filled with zeros.

$$U = \begin{bmatrix} 1 & 00 & 011 & 000 & 000 & & & & \\ 0 & 00 & 100 & 011 & 000 & & & & \\ 0 & 00 & 000 & 100 & 011 & & & & \\ 0 & 00 & 000 & 000 & 100 & 01 & 00 & 0 & 0 \\ 0 & 00 & 000 & 000 & 000 & 10 & 01 & 0 & 0 \\ 0 & 00 & 000 & 000 & 00 & 00 & 10 & 0 & 1 \end{bmatrix}.$$

8. Remove all columns which have only 0s from U. Above matrix contains $\lfloor \frac{W_M+1}{2} \rfloor 0s = \lfloor \frac{3+1}{2} \rfloor = 2$ columns of 0s towards left side and $\lfloor \frac{W_1}{2} \rfloor 0s = \lfloor \frac{2}{2} \rfloor = 1$ column of 0s towards right side.

$$U = \begin{bmatrix} 1 & 011 & 000 & 000 & & & \\ 0 & 100 & 011 & 000 & & & \\ 0 & 000 & 100 & 011 & & & \\ 0 & 000 & 000 & 100 & 01 & 00 & 0 \\ 0 & 000 & 000 & 000 & 10 & 01 & 0 \\ 0 & 000 & 000 & 00 & 00 & 10 & 1 \end{bmatrix}.$$

9. Code lengths are $L_{W_H} = W_M * (N_{W_M} + 1) + R_{W_M} - \lfloor \frac{W_M+1}{2} \rfloor = 3 * (3 + 1) - 2 = 10$ and $L_{W_L} = L_{W_H} + W_L * (N_{W_L}) - \lfloor \frac{W_L}{2} \rfloor = 10 + 2 * (3) - 1 = 15$. Total code length used by code is 15.

6.4 Performance analysis

Performance metric evaluated for analysis is BER. Let $F_C(j)$ be the jth component of the Cth proposed code. Correlation function is given as

$$F_X(j) = \sum_{j=1}^{L_n} (F_C(j) \cdot F_Z(j)) = \begin{cases} W_i & C = Z \quad \text{same user with same weight} \\ 0 & C \neq Z \quad \text{other users with same weight} \\ 0 & C \neq Z \quad \text{other users with different weight} \end{cases} \tag{6.16}$$

The variance of photocurrent due to the detection of an ideally unpolarized thermal light, which is generated by spontaneous emission, can be written as shown in Eq. (2.10).

The W_i unique wavelengths are incident upon a photo detector. The coherence time of a thermal source is given in Eq. (2.9).

The PSD of optical signals at receiver is given in Eq. (4.14).

6.4.1 CW-ZCCC BER analysis

Filtered wavelengths are incident upon the input of photodiode of Cth receiver. For one bit duration, total power at Cth receiver for constant weight is calculated as

$$\int_0^{\infty} G(v)dv = \int_0^{\infty} \left[\frac{P_{sr}}{\Delta v} \sum_{k=1}^{N} d_C \sum_{j=1}^{L} F_C(j) F_X(j) \left\{ u \left[\frac{\Delta v}{L} \right] \right\} \right] dv \tag{6.17}$$

$$= \frac{P_{sr}}{\Delta v} \frac{\Delta v}{L} \sum_{k=1}^{N} d_C \sum_{j=1}^{L} F_C(j) F_X(j). \tag{6.18}$$

For CW-ZCCC, the total code length L_n is denoted as L and W_i becomes W due to constant weight. Applying the correlation property from Eq. (6.16) for same weight condition in Eq. (6.18) gives

$$\int_0^{\infty} G(v)dv = \frac{P_{sr} W}{L}. \tag{6.19}$$

The photo current created due to incident optical power at photo diode, is written as

$$I = \mathcal{R} \int_0^{\infty} G(v)dv. \tag{6.20}$$

The resultant photo current from Eq. (6.20) is obtained by putting the value from Eq. (6.19) as

$$I = \frac{\mathcal{R} P_{sr} W}{L}. \tag{6.21}$$

From Eq. (6.21), shot noise is calculated by putting the values of I in

Eq. (2.10) as

$$\langle I_{shot}^2 \rangle = 2eB\mathcal{R}\left(\frac{P_{sr}W}{L}\right) \tag{6.22}$$

The PIIN power is given as

$$\langle I_{PIIN}^2 \rangle = I^2 B\tau_c = B\mathcal{R}^2 \int_0^\infty G^2(\upsilon)d\upsilon \tag{6.23}$$

The approximation is used as per the Eq. (3.19) and by substituting the values in Eq. (6.23) from Eqs. (6.17), PIIN is

$$\langle I_{PIIN}^2 \rangle = \frac{B\mathcal{R}^2 P_{sr}^2 N W^2}{L^2 \Delta\upsilon} \tag{6.24}$$

Noise power, $\langle I^2 \rangle$ is given as:

$$\langle I^2 \rangle = \frac{B\mathcal{R}^2 P_{sr}^2 N W^2}{L^2 \Delta\upsilon} + 2eB\mathcal{R}\left[\frac{P_{sr}W}{L}\right] + \frac{4K_b T_n B}{R_L} \tag{6.25}$$

Let at any time, the probability of transmitting bit 1 for each user is half, Eq. (6.26) leads to

$$\langle I^2 \rangle = \frac{B\mathcal{R}^2 P_{sr}^2 N W^2}{2L^2 \Delta\upsilon} + eB\mathcal{R}\left[\frac{P_{sr}W}{L}\right] + \frac{4K_b T_n B}{R_L} \tag{6.26}$$

The SNR is calculated on substituting Eqs. (6.21), (6.26) in Eq. (2.29) as

$$SNR = \frac{\left(\frac{\mathcal{R}P_{sr}W}{L}\right)^2}{\frac{B\mathcal{R}^2 P_{sr}^2 N W^2}{2L^2 \Delta\upsilon} + eB\mathcal{R}\left[\frac{P_{sr}W}{L_n}\right] + \frac{4K_b T_n B}{R_L}} \tag{6.27}$$

The BER using Gaussian approximation from SNR is expressed as given in Eq. (2.31).

6.4.2 VW-ZCCC BER analysis

For one bit duration, total power at Cth receiver for variable weight is calculated as

$$\int_0^\infty G(\upsilon)d\upsilon = \int_0^\infty \left[\frac{P_{sr}}{\Delta\upsilon}\sum_{k=1}^{N} d_C \sum_{j=1}^{L_n} F_C(j)F_X(j)\left\{u\left[\frac{\Delta\upsilon}{L_n}\right]\right\}\right] d\upsilon \quad (6.28)$$

$$= \frac{P_{sr}}{\Delta\upsilon}\frac{\Delta\upsilon}{L_n}\sum_{k=1}^{N} d_C \sum_{j=1}^{L_n} F_C(j)F_X(j). \quad (6.29)$$

Applying the correlation property from Eq. (6.16) in Eq. (6.29) gives

$$\int_0^\infty G(\upsilon)d\upsilon = \frac{P_{sr}W_i}{L_n}. \quad (6.30)$$

The photo current created due to incident optical power at photo diode, is written as

$$I = \mathcal{R}\int_0^\infty G(\upsilon)d\upsilon. \quad (6.31)$$

The resultant photo current from Eq. (6.31) is obtained by putting the value from Eq. (6.30) as

$$I = \frac{\mathcal{R}P_{sr}W_i}{L_n}. \quad (6.32)$$

From Eq. (6.32), shot noise is calculated by putting the values of I in Eq. (3.17) as

$$\langle I_{shot}^2\rangle = 2eB\mathcal{R}\left(\frac{P_{sr}W_i}{L_n}\right) \quad (6.33)$$

The PIIN nosie power is given as

$$\langle I_{PIIN}^2\rangle = I^2B\tau_c = B\mathcal{R}^2\int_0^\infty G^2(\upsilon)d\upsilon \quad (6.34)$$

The total number of users at a given time is the summation of users with different weights that coexist in a single system [42], denoted by

$$\sum_{h=1}^{N_{max}} C_h = \frac{1}{L_T}\sum_{i=1}^{N} N_{W_i} W_i. \tag{6.35}$$

By substituting the values in Eq. (6.34) from Eqs. (6.17), PIIN noise is

$$\langle I^2_{PIIN}\rangle = \frac{B\mathcal{R}^2 P^2_{sr}}{L^2_T \Delta\upsilon} \sum_{i=1}^{N_{max}} N_{W_i} W_i [W_i] \tag{6.36}$$

Noise power, $\langle I^2\rangle$ is given as:

$$\langle I^2\rangle = \frac{B\mathcal{R}^2 P^2_{sr}}{L^2_T \Delta\upsilon} \sum_{i=1}^{N_{max}} N_{W_i} W_i [W_i] + 2eB\mathcal{R}\left[\frac{P_{sr} W_i}{L_n}\right] + \frac{4K_b T_n B}{R_L} \tag{6.37}$$

Let at any time, the probability of transmitting bit 1 for each user is half, Eq. (6.37) leads to

$$\langle I^2\rangle = \frac{B\mathcal{R}^2 P^2_{sr}}{2L^2_T \Delta\upsilon} \sum_{i=1}^{N_{max}} N_{W_i} W_i [W_i] + eB\mathcal{R}\left[\frac{P_{sr} W_i}{L_n}\right] + \frac{4K_b T_n B}{R_L} \tag{6.38}$$

Substituting Eqs. (6.32), (6.38) in Eq. (2.29), SNR is expressed as

$$SNR = \frac{(\frac{\mathcal{R}P_{sr}W_i}{L})^2}{\frac{B\mathcal{R}^2 P^2_{sr}}{2L^2_T \Delta\upsilon} \sum_{i=1}^{N_{max}} N_{W_i} W_i [W_i] + eB\mathcal{R}\left[\frac{P_{sr} W_i}{L_n}\right] + \frac{4K_b T_n B}{R_L}} \tag{6.39}$$

The BER is computed as given in Eq. (2.31).

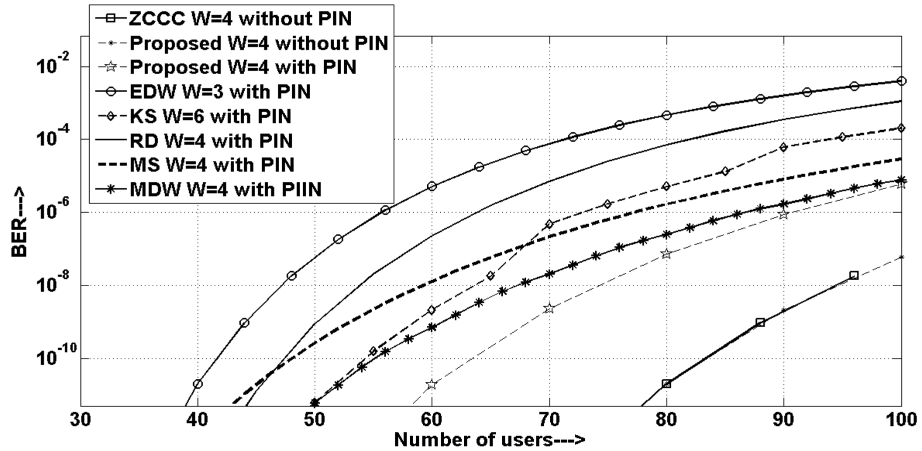

Figure 6.1: Comparison of ZCC, KS, EDW, RD, MS, MDW and proposed codes for BER versus number of users.

6.5 Numerical Results

Proposed code is compared with the previously reported ZCC Code, KS [42], RD [87], MS [47], MDW [59] and EDW [88] codes in Figure 6.1. KS code [42] was reported with variable weight code construction. Its cross-correlation is given by ($\lambda_c \leq 1$). It was designed with even weights only. EDW code [88] was designed with odd weights only and it was used for multirate transmission. MDW code [30] was designed with even weights only. MS code was designed for variable number of users in basic code with fixed weight. All above described codes are using mapping technique to provide codes for greater number of users. RD code [87] divide code sequence into two parts (code, and data) segments. Code segment exhibits ZCC property. Proposed code does not use the mapping technique to provide codes. The parameters used for numerical comparison are listed in Table 2.2.

Figure 6.1 is plotted for BER versus number of users. Proposed code is constructed with weight 4 and 100 users. KS code, ZCCC, RD code, MS code and EDW code are designed with weights 6, 4, 4, 4 and 3 respectively

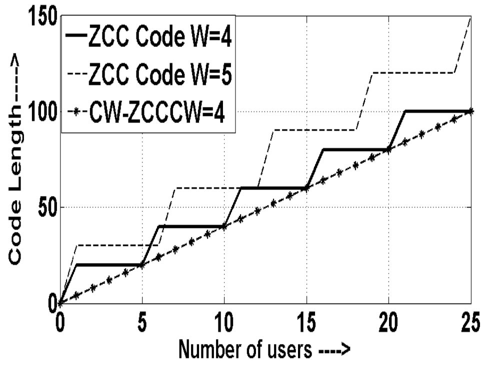

Figure 6.2: Comparison between the previously reported ZCC code and proposed ZCCC for constant weight (CW).

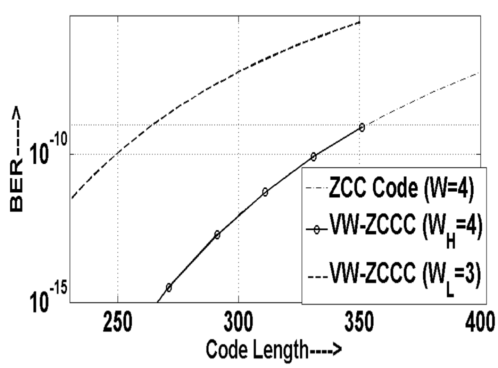

Figure 6.3: Comparison between the previously reported ZCC code and proposed ZCCC for variable weight (VW) without PIIN consideration.

with 100 users each. Proposed code has almost same BER as compare to ZCCC without PIIN consideration for weight 4. That is because of same zero cross-correlation, code length, weight, noise consideration, and number of users. All codes except ZCCC give higher BER as compared to proposed code ($W = 4$). That is due to cross-correlation property of these codes. The number of users for EDW code ($W = 3$), KS code ($W = 6$), MS code ($W = 4$), RD code ($W = 4$) and proposed ZCCC ($W = 4$) are 41, 54, 47, 48 and 64 respectively at BER of 10^{-10} with PIIN consideration. The number of users for proposed code and ZCCC is 83 users at 10^{-10} without PIIN consideration.

Comparison between the previously reported ZCC code and proposed ZCCC is shown in Figures 6.2 and 6.3. Figure 6.2 shows variation of code length as a function of number of users. Reported ZCC code used the mapping technique to assign codes for higher number of users. Variation of code length depends on basic matrix size which is determined by code weight. As weight is increased, size of basic matrix increases which leads to higher step size, whereas proposed ZCCC has a linear increment of code length.

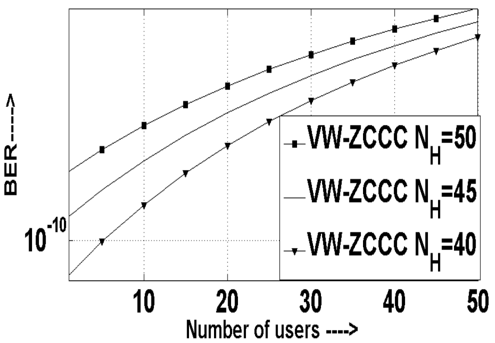

Figure 6.4: Comparison of BER versus number of users on varying N_H of weight (W_H) with PIIN consideration.

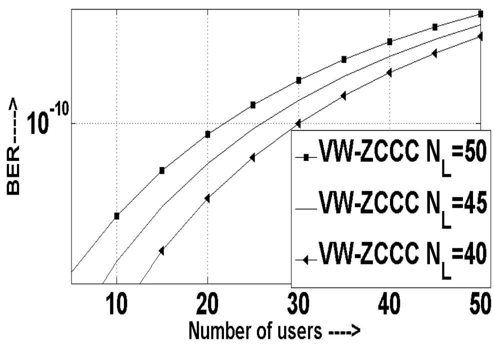

Figure 6.5: Comparison of BER versus number of users on varying N_L of weight (W_L) with PIIN consideration.

Reported ZCC code used code transformation technique, which converts the lower weight code to higher weight code [36], whereas proposed ZCCC has no restriction to construct codes of any weight. Proposed ZCCC require less number of filtering elements compare to reported ZCC code. For reported ZCC code, numbers of filtering elements are equal to number of weight. Proposed ZCCC requires two filtering elements irrespective to weight.

Figure 6.3 shows the BER comparison of ZCC code and VW ZCCC as a function of code length without PIIN consideration. (W_H) and (W_L) are used to indicate higher weight, and lower weight respectively. N_H and N_L represent number of users for higher weight (W_H) and lower weight (W_L) respectively. The values of N_H and N_L are 50 for each weight. Total number of users are 100 for VW-ZCCC. For reported ZCC code, weight and number of users are 4 and 100 respectively. VW-ZCCC and ZCC code are required 350 and 400 code lengths respectively. VW ZCCC requires less code length compare to ZCC code. It is due to variable weight code construction. Variable BER is obtained by using VW ZCCC compare to ZCC code.

Figures 6.4 and 6.5 illustrate the BER versus number of users with PIIN

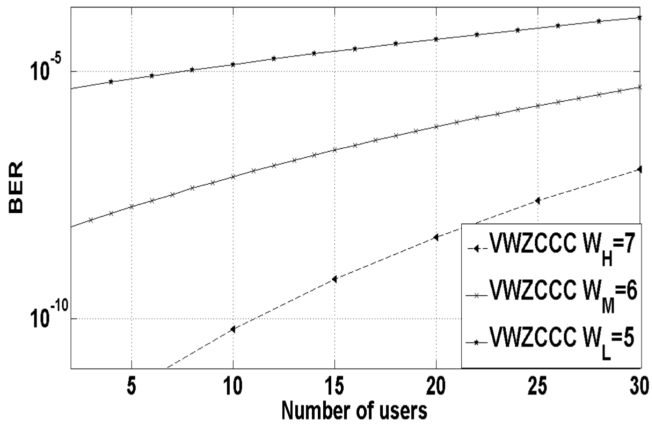

Figure 6.6: Comparison of BER versus number of users for three different weights with PIIN consideration.

consideration. The combination of weights ($W_H = 7, W_L = 6$) are chosen for Figs. 6.4 and 6.5.

For Fig. 6.4, number of users N_L for W_L are set to 50 users. The number of users N_H is varied and it is set to 50, 45 and 40 users. Higher number of users leads to longer code length and vice versa. Change in code length affect the BER of system. On increasing / decreasing the value of N_H, BER increases / decreases. The variation in BER is due to different weights which further change the code length. Results indicate lowest weight codes have highest BER and highest weight codes have lowest BER.

For Fig. 6.5, number of users N_L is varied and it is set to 50, 45 and 40 users. The number of users N_H is set to 50 users. As the number of users of N_L decreases, code length decreases which tends to decrease BER. The W_L does not affect the code length of W_H but the total code length is decreased thus BER of W_H is decreased.

Figure 6.6 is plotted between the BER versus number of users with PIIN consideration. The (W_H), (W_M) and (W_L) are used to indicate different

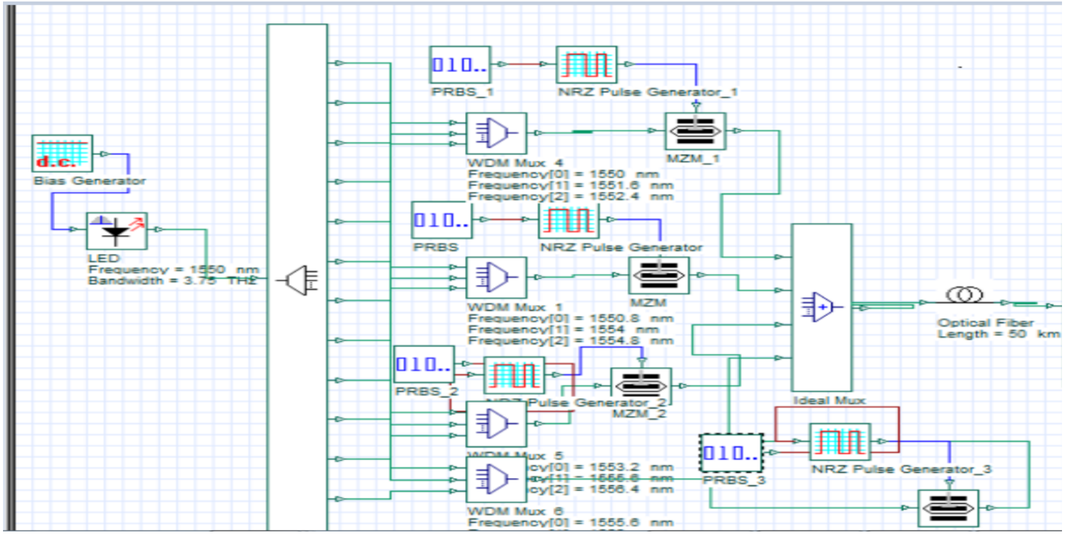

Figure 6.7: Simulation setup of encoder with optical fiber using OptiSystem 13. is designed for 4 users of weight 3.

weights as higher weight, medium weight and lower weight respectively. The combination of weights $(W_H = 7, W_M = 6, W_L = 5)$ is chosen. The N_H, N_M and N_L are denoted as number of users for higher weight (W_H), medium weight (W_M) and lower weight (W_L) respectively. The number of users are set to 30 users for each weight. N_L effect the total code length not the code length of N_H and N_M.

On changing N_H, code lengths of all lower weight codes are changed. On the other hand, changing N_L, effects its own code length and total code length, but does not effect codes of other weights. Different weights provide variable BER. Resultant code is suitable for multimedia service.

6.6 Simulation Setup and Results

The simulation setup with LED as a broadband light source is shown in Figs. 6.7 and 6.8, using OptiSystem 13.

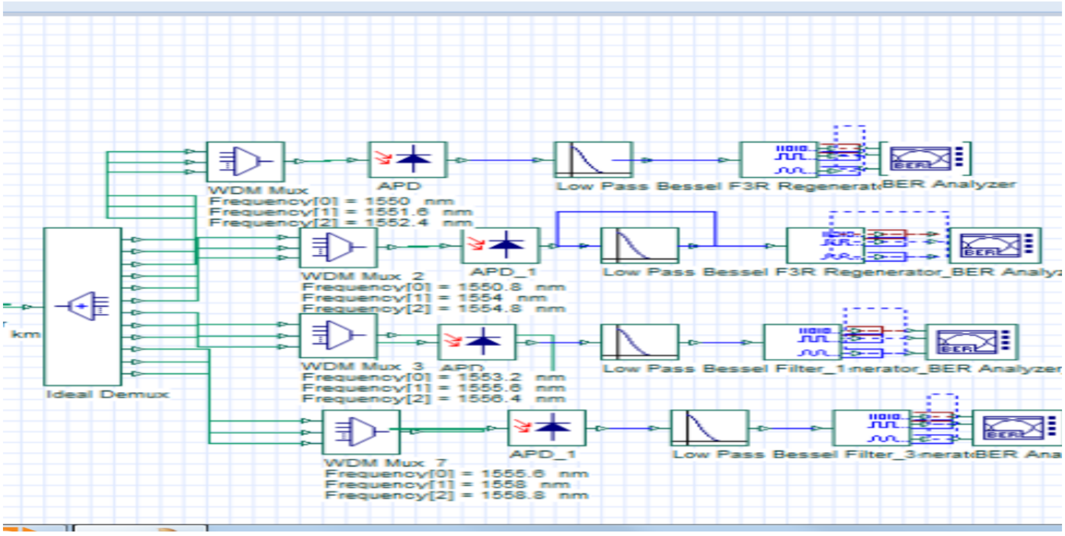

Figure 6.8: Simulation setup of decoder with optical fiber using OptiSystem 13. is designed for 4 users of weight 3.

Simulation setup for proposed ZCCC is designed for 4 users of weight 3. Data rate for simulation is set to 622 Mbps. Spectral width is set to $.8nm$ for each chip. The transmitter side consists of five components: a pseudo random bit sequence (PRBS) generator, a non-return-zero (NRZ) pulse generator, LED with bias generator, WDM demux and mux (for filtering wavelength), and an external modulator. The simulation parameters of LED are set as wavelength of 1550 nm, bandwidth of 3.75 THz (30 nm), external quantum efficiency is 0.05, and transmitted Power is -10 dBm. Spectrum slicing of LED is elaborated as per [37]. The external intensity modulators used are MachZehnder modulators. All signals from all users are combined and launched into a single fiber. Fiber length is chosen to be $9Km$ with dispersion of $16.75ps/nm-km$, and attenuation of $0.2dB/km$.

Direct detection technique is used to detect signals. This technique requires only one photodiode to detect unique wavelengths of each user. At recevier, the incoming signal was split and sent to wavelength mux to detect

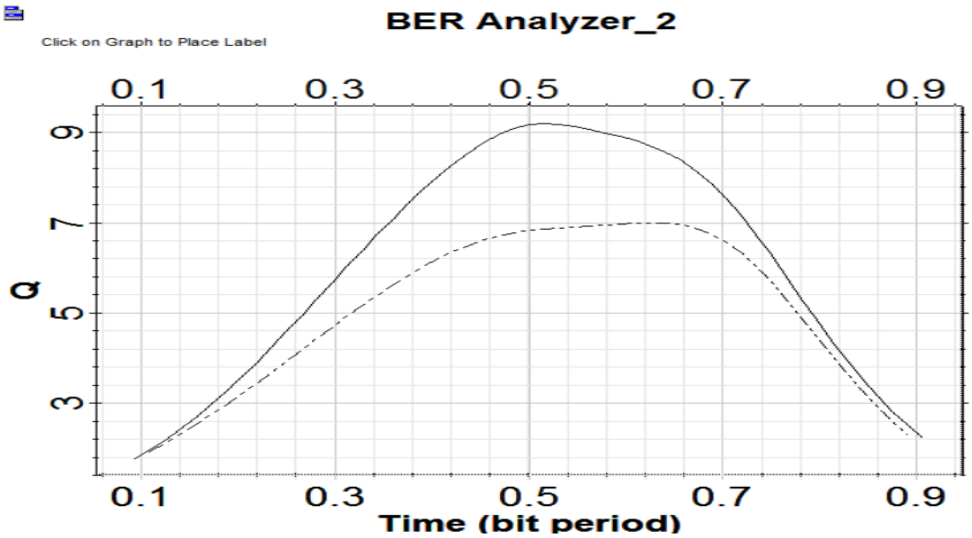

Figure 6.9: The comparison of Q factors between reported ZCC code and proposed ZCCC.

required wavelengths. Photodiode parameters are set as dark current of $5nA$, responsivity of $1A/W$, thermal noise of $100 \times 10^{-24} W/Hz$, and with gain of 10.

Simulation setup for previously reported ZCC code is designed for 4 users of weight 3. The minimum possible users for weight 3 is 4. Reported ZCC code has dependence on basic matrix. Proposed ZCCC has not basic matrix limitation. Simulation setup for reported ZCC code has same parameters values as defined for setup in Figs. 6.7 and 6.8. The trasmitter side has same components as per shown in Fig. 6.7. Q factor and BER of 9.22 and 7.64×10^{-21} are achieved by proposed ZCCC. Q factor and BER of 6.99 and 7.77×10^{-13} are achieved by reported ZCC code. The comparison of Q factors between reported ZCC code and proposed ZCCC are shown in Fig. ??.

6.7 Summary

ZCCC is proposed without mapping. Code algorithm is designed with any integer value of weight for any number of users. Algorithm is explained for both constant and variable weight code construction.

CW ZCCC is compared with reported ZCC code. Proposed ZCCC construct any weight code without any information about lower weight codes. It construct the code without mapping. It has a linear increase in code length. Variable weight (VW) codes give different quality of service, and are suitable, and useful for multimedia applications. Construction of code for variable weight is begins with the highest weight. On changing number of users of highest weight, code length of all lower weight codes are changed. On the other hand, changing number of users of lower weight, effects its own code length and total code length, but does not effect codes of other weights. The variation of weights provides different BER and code length.

CHAPTER 7

Conclusions and Future Directions

7.1 Concluding Remarks

The thesis proposes some new algorithms to construct codes for SAC-OCDMA systems. The main purpose of algorithms are to support higher cardinality with better performance, to simplify code construction with variety of code sets and, good properties like auto-correlation, cross-correlation and to support multimedia applications and fill the gaps in reported code constructions.

The outcomes obtained from these studies are summarized below:

7.1.1 DW code families for SAC-OCDMA systems

Chapter 2 presents the review on code construction algorithms of 1D codes DW code families and a gap between the reported works. Using reported codes, odd weight construction of KS code and 2D code construction from 1D DW code families are proposed.

The odd weight code construction for KS code is a combination of previously proposed KS code (for even weight) and identity matrix. It provides an extension of KS code by implementing for all weight construction. Application of proposed KS code for FSO channel and multi media service can be explored. The 2D code is proposed which is constructed using 1D DW code families for weight greater than 1. The proposed 2D code provides higher cardinality at lower BER on comparing with 1D code. Hence, it provides a solution for limited bandwidth of BBS. On comparing with other 2D codes, proposed 2D code has lower BER. BER is decreased as h is maximized and g is minimized. Hence, a solution is provided by incresing the dimensions of code to enchance number of users, and lower BER.

7.1.2 Generalized Optical Code construction for EDW and MDW like Codes without mapping

Chapter 3 introduces an algorithm named as Generalized Optical Code construction for EDW and MDW like Codes without mapping. The BER analysis is same for all weights greater than 2. Comparison with EDW and MDW codes shows proposed code is having lower BER. At BER of 10^{-9}, number of users are 61 and 58 for $W = 3$ and $W = 4$ respectively for generalized code. The number of users for EDW ($W = 3$) and MDW ($W = 4$) are 34 and 61 respectively. The variation of results are due to difference in code length which depends on the number of users and its dependency on mapping for EDW and MDW which affects the BER performance. Compared to the BD, DD does not require power splitter, two photodiodes and subtractor at decoder of each user. Due to the use of less components, the cost of the system is lower [56, 85].

7.1.3 VW code construction using Generalized code

In Chapter 4, VW algorithm based on Chapter 3 is proposed without mapping. Proposed code requires two filtering elements irrespective of weight. The variation of weights provides different BER. The lowest weight codes have highest BER and highest weight codes have lowest BER. It is observed that supportable number of users for higher weight, at BER of 10^{-9} (data) are 28, 33 and 35 for RD code, KS code, and VW code respectively using BD. Supportable number of users for lower weight, at BER of 10^{-4} (voice) are 23, 31 and 37 for RD code, KS code, and VW code respectively using BD. Results show that code is suitable for multimedia application. By using DD technique, receiver is designed with less complexity and its cost is reduced along with better performance. Figure 4.6 illustrates the BER (PIIN, Shot and thermal noise) versus received power using balanced detection for $W_H = 6, W_M = 5, W_L = 3$ with 25 users for each weight. BER of all users decreases with the increase of weight and received power. The application of proposed VW code to support different services, for average received power of $-20dBm$ has acceptable performance. It is found that proposed VW code gives comparable and better performance than Generalized Optical Code construction for Enhanced and Modified Double Weight code (CW and CL construction). That is due to lower code length of variable weight codes.

7.1.4 A new code construction algorithm based on DW Codes

A new and single code construction algorithm with mapping is proposed for DW code families in Chapter 5. The code design has several advantages such as simplicity of code construction, the weight of any positive number can be used for the code design and variety of code set for different code length and weight. Code length increment of EDW code is differ from proposed code. The difference is shown in Fig. 5.2, for weight ($W = 3$) and basic matrix of ($N_B = 3, L_B = 6$). Difference in the length is due to different techniques used to calculate code length (L) for N users. For EDW, it involve a sine relation between L and N [31]. Proposed code follows constant variation of code length defined in Eq. 5.27. These code length variations effect the BER performance of codes which depend on N and L.

A 2D code is proposed for SAC-OCDMA systems. The code is having a low value of IPCC for spectral dimension and orthogonal in spatial dimension. In comparison with 1D code, it offers greater number of users along with better BER performance. On comparing with hybrid code, it gives lower BER.

7.1.5 Development of ZCCC for Constant and Variable Weight

An algorithm is proposed for CW and VW using zero cross correlation property without mapping in Chapter 6. Code algorithm is designed with any integer value of weight for any number of users. Comparison between the previously reported ZCC code and proposed ZCCC is shown in Figures 6.2 and 6.3. Reported ZCC code used the mapping technique to assign codes for higher number of users. Variation of code length depends on basic matrix size which is determined by code weight. As weight is increased, size of basic matrix increases which leads to higher step size, whereas proposed ZCCC has a linear increment of code length. Reported ZCC code used code transformation technique, which converts the lower weight code to higher weight code [36], whereas proposed ZCCC has no restriction to construct codes of any weight. Proposed ZCCC require less number of filtering elements compare to reported ZCC code. For reported ZCC code, number of filtering elements are equal to number of weight. Proposed ZCCC require two filtering elements irrespective to weight.

Construction of code for variable weight is begins with the highest weight. On changing number of users of highest weight, code length of all lower weight codes are changed. On the other hand, changing number of users of lower weight, effects its own code length and total code length, but does not effect codes of other weights. The variation of weights provides different BER and code length. Results indicate that lowest weight codes have highest BER and highest weight codes have lowest BER. Resultan, code is suitable for multimedia service.

7.2 Scope for Further Study

Proposed algorithms are analyzed by taking the effects of PIIN, shot noise and thermal noise. Therefore, the performance of codes can be analyzed by considering the other noise. For mathematical simplification, some assumptions are taken such as LED spectrum is flat. But, spectrum has a Gaussian shape, means different wavelengths on spectrum have different amplitude. So, to analyse BER some practical consideration is may be taken for further extension to BER equation. Optical power budget analysis is also estimated due to various components in systems as an further extension of work. Extension of codes to design it in multi-dimension, to enhance cardinality by reducing BER. Lower and upper bounds of these codes are also investigated. The experimental and simulation results are also demonstrated. Application of these codes can be tested for other domain of OCDMA, wireless optical systems, Free Space Optics, and Visible Light Communication.

Also, since spectrum slicing plays an important role in encoding of the spectrum, new methods can be studied for use in SAC-OCDMA systems. The analysis of encoder/decoder circuit with suitable optical devices can be introduced to reduce the PIIN and to improve the system performance.

References

[1] A. Stok and E. Sargent, "System performance comparison of optical CDMA and WDMA in a broadcast local area network," *Communications Letters, IEEE*, vol. 6, no. 9, pp. 409–411, Sep 2002.

[2] W. Huang, M. Nizam, I. Andonovic, and M. Tur, "Coherent optical CDMA (OCDMA) systems used for high-capacity optical fiber networks-system description, OTDMA comparison, and OCDMA/WDMA networking," *Lightwave Technology, Journal of*, vol. 18, no. 6, pp. 765–778, Jun 2000.

[3] P. Prucnal, M. Santoro, and T. Fan, "Spread spectrum fiber-optic local area network using optical processing," *Lightwave Technology, Journal of*, vol. 4, no. 5, pp. 547 – 554, may 1986.

[4] K.-i. Kitayama, X. Wang, and N. Wada, "Ocdma over wdm ponsolution path to gigabit-symmetric ftth," *Journal of Lightwave Technology*, vol. 24, no. 4, p. 1654, 2006.

[5] R. Pickholtz, L. Milstein, and D. Schilling, "Spread spectrum for mobile communications," *Vehicular Technology, IEEE Transactions on*, vol. 40, no. 2, pp. 313 –322, may 1991.

[6] K. Fouli and M. Maier, "Ocdma and optical coding: Principles, applications, and challenges [topics in optical communications]," *IEEE Communications Magazine*, vol. 45, no. 8, pp. 27–34, 2007.

[7] G. Cincotti, "Design of optical full encoders/decoders for code-based photonic routers," *Journal of lightwave technology*, vol. 22, no. 7, p. 1642, 2004.

[8] D. Leaird, Z. Jiang, and A. Weiner, "Experimental investigation of security issues in ocdma: a code-switching scheme," *Electronics letters*, vol. 41, no. 14, p. 1, 2005.

[9] B. K. Kim, S. Park, Y. Yeon, and B. W. Kim, "Radio-over-fiber system using fiber-grating-based optical cdma with modified pn codes," *IEEE Photonics Technology Letters*, vol. 15, no. 10, pp. 1485–1487, 2003.

[10] J. A. Salehi, "Code division multiple-access techniques in optical fiber networks–part I: fundamental principles," *IEEE Transactions on Communications*, vol. 37, no. 8, pp. 824–833, August 1989.

[11] J. A. Salehi and C. A. Brackett, "Code division multiple-access techniques in optical fiber networks–part II: systems performance analysis," *IEEE Transactions on Communications*, vol. 37, no. 8, pp. 834–842, August 1989.

[12] D. Zaccarin and M. Kavehrad, "An optical cdma system based on spectral encoding of led," *Photonics Technology Letters, IEEE*, vol. 5, no. 4, pp. 479–482, April 1993.

[13] J. P. Heritage and A. M. Weiner, "Advances in spectral optical code-division multiple-access communications," *IEEE journal of selected topics in quantum electronics*, vol. 13, no. 5, pp. 1351–1369, 2007.

[14] Z. Wei, H. Ghafouri-Shiraz, and H. Shalaby, "New code families for fiber-bragg-grating-based spectral-amplitude-coding optical cdma systems," *Photonics Technology Letters, IEEE*, vol. 13, no. 8, pp. 890–892, Aug 2001.

[15] M. Kavehrad and D. Zaccarin, "Optical code-division-multiplexed systems based on spectral encoding of noncoherent sources," *Lightwave Technology, Journal of*, vol. 13, no. 3, pp. 534–545, Mar 1995.

[16] L. Adam, E. S. Simova, and M. Kavehrad, "Experimental optical cdma system based on spectral amplitude encoding of noncoherent broadband sources," pp. 122–132, 1995. [Online]. Available: http://dx.doi.org/10.1117/12.227823

[17] D. Zaccarin and M. Kavehrad, "Optical cdma by spectral encoding of led for ultrafast atm switching," in *Communications, 1994. ICC '94, SUPERCOMM/ICC '94, Conference Record, 'Serving Humanity Through Communications.' IEEE International Conference on*, May 1994, pp. 1369–1373 vol.3.

[18] Z. Wei, H. Shalaby, and H. Ghafouri-Shiraz, "Modified quadratic congruence codes for fiber bragg-grating-based spectral-amplitude-coding

optical cdma systems," *Lightwave Technology, Journal of*, vol. 19, no. 9, pp. 1274–1281, Sep 2001.

[19] Z. Wei and H. Ghafouri-Shiraz, "Proposal of a novel code for spectral amplitude-coding optical cdma systems," *IEEE Photonics Technology Letters*, vol. 14, no. 3, pp. 414–416, March 2002.

[20] ——, "Codes for spectral-amplitude-coding optical cdma systems," *Lightwave Technology, Journal of*, vol. 20, no. 8, pp. 1284–1291, Aug 2002.

[21] I. B. Djordjevic and B. Vasic, "Novel combinatorial constructions of optical orthogonal codes for incoherent optical cdma systems," *Journal of Lightwave Technology*, vol. 21, no. 9, pp. 1869–1875, Sept 2003.

[22] S. p. Tseng and J. Wu, "A new code family suitable for high-rate sac ocdma pons applications," *IEEE Journal on Selected Areas in Communications*, vol. 28, no. 6, pp. 827–837, Aug 2010.

[23] H. Y. Ahmed, Z. M. Gharsseldien, and S. A. ALJUNID, "Performance analysis of diagonal permutation shifting (dps) codes for sac-ocdma systems," *JOURNAL OF INFORMATION SCIENCE AND ENGINEERING*, vol. 33, no. 2, pp. 429–444, 2017.

[24] T. Abd, S. Aljunid, H. Fadhil, R. Ahmad, and M. Rashid, "New approach for evaluation of the performance of spectral amplitude coding-optical code division multiple access system on high-speed data rate," *Communications, IET*, vol. 6, no. 12, pp. 1742–1749, August 2012.

[25] H. Y. Ahmed and K. Nisar, "Diagonal eigenvalue unity (deu) code for spectral amplitude coding-optical code division multiple access," *Optical Fiber Technology*, vol. 19, no. 4, pp. 335 – 347, 2013.

[26] M. Z. Hassan Yousif Ahmed, "An efficient spectral amplitude coding (sac) technique for optical cdma system using wavelength division multiplexing (wdm) concepts," *(IJACSA) International Journal of Advanced Computer Science and Applications*, vol. 8, no. 7, pp. 36–44, 2017.

[27] H. Y. Ahmed, M. Zeghid, K. S. Nisar, and S. A. Aljunid, "Numerical method for constructing fixed right shift (frs) code for sac-ocdma systems," in *International Journal of Advanced Computer Science and Applications (IJACSA)*, vol. 8, no. 1, 2017, pp. 1546–1550.

[28] H. Y. Ahmed, "Matrix partitioning code family for spectral amplitude coding ocdma," *Photonic Network Communications*, vol. 28, no. 1, pp. 102–111, 2014. [Online]. Available: http://dx.doi.org/10.1007/s11107-014-0439-1

[29] K. Nisar, "Numerical construction of generalized matrix partitioning code for spectral amplitude coding optical {CDMA} systems," *Optik - International Journal for Light and Electron Optics*, vol. 130, pp. 619 – 632, 2017.

[30] S. Aljunid, M. Ismail, A. Ramli, B. Ali, and M. Abdullah, "A new family of optical code sequences for spectral-amplitude-coding optical cdma systems," *Photonics Technology Letters, IEEE*, vol. 16, no. 10, pp. 2383–2385, Oct 2004.

[31] M. A. S. S. F.N. HASOON, S.A. ALJUNID, "Spectralamplitude coding ocdma systems using enhanced double weight code," *Journal of Engineering Science and Technology*, vol. 1, no. 2, pp. 192–202, 2006.

[32] M. Abdullah, S. Aljunid, S. Anas, R. Sahbudin, and M. Mokhtar, "A new optical spectral amplitude coding sequence: Khazani-syed (ks) code," in *Information and Communication Technology, 2007. ICICT'07. International Conference on.* IEEE, 2007, pp. 266–278.

[33] H. A. Fadhil, S. Aljunid, and R. Badlisha, "Random diagonal code for spectral amplitude-coding optical cdma system," *Int. J. Comput. Sci. Network Secur*, vol. 7, pp. 258–262, 2007.

[34] C. Rashidi, S. Aljunid, F. Ghani, H. A. Fadhil, and M. Anuar, "New design of flexible cross correlation (fcc) code for sac-ocdma system," *Procedia Engineering*, vol. 53, pp. 420–427, 2013.

[35] C. A. S. Fazlina, C. B. M. Rashidi, A. K. Rahman, S. A. Aljunid, and R. Endut, "Enhanced performance of bit error rate by utilizing sequential algorithm (seq) code in optical cdma network systems," *International Journal of Applied Engineering Research*, vol. 12, no. 7, pp. 1411 – 1415, 2017.

[36] M. Anuar, S. Aljunid, N. Saad, and S. Hamzah, "New design of spectral amplitude coding in {OCDMA} with zero cross-correlation," *Optics Communications*, vol. 282, no. 14, pp. 2659 – 2664, 2009. [Online]. Available: http://www.sciencedirect.com/science/article/pii/S0030401809003216

[37] M. S. Anuar, S. A. Aljunid, A. R. Arief, and N. M. Saad, "Led spectrum slicing for zcc sac-ocdma coding system," in *7th International Symposium on High-capacity Optical Networks and Enabling Technologies*, Dec 2010, pp. 128–132.

[38] T. H. Abd, S. Aljunid, H. A. Fadhil, R. Ahmad, and N. Saad, "Development of a new code family based on sac-ocdma system with large cardinality for {OCDMA} network," *Optical Fiber Technology*, vol. 17, no. 4, pp. 273 – 280, 2011. [Online]. Available: http://www.sciencedirect.com/science/article/pii/S1068520011000526

[39] C. B. M. Rashidi, S. A. Aljunid, F. Ghani, and M. S. Anuar, "Development of modified zero cross correlation code for ocdma network," in *International Conference On Photonics 2010*, 2010, pp. 1–6.

[40] W. A. Imtiaz, M. Ilyas, and Y. Khan, "Performance optimization of spectral amplitude coding ocdma system using new enhanced multi diagonal code," *Infrared Physics & Technology*, vol. 79, pp. 36–44, 2016.

[41] I. B. Djordjevic, B. Vasic, and J. Rorison, "Multi-weight unipolar codes for multimedia spectral-amplitude-coding optical cdma systems," *IEEE Communications Letters*, vol. 8, no. 4, pp. 259–261, April 2004.

[42] S. A. Anas, M. Abdullah, M. Mokhtar, S. Aljunid, and S. Walker, "Optical domain service differentiation using spectral-amplitude-coding," *Optical Fiber Technology*, vol. 15, no. 1, pp. 26 – 32, 2009.

[43] "Experimental demonstration of variable weight sac-ocdma system for qos differentiation," *Optical Fiber Technology*, vol. 20, no. 5, pp. 495 – 500, 2014.

[44] S. Seyedzadeh, M. Moghaddasi, and S. B. Anas, "Variable-weight optical code division multiple access system using different detection schemes," *Journal of Telecommunications and Information Technology*, no. 3, pp. 50–59, 2016.

[45] ——, "Variable-weight optical code division multiple access system using different detection schemes," *Journal of Telecommunications and Information Technology*, no. 3, pp. 50–59, 2016.

[46] F. Hilal Adnan, S. J. Syed Alwee Aljunid, and A. R Badlishah, "Multirate transmissions on spectral amplitude coding optical code division multiple access system using random diagonal codes," 2009.

[47] M. H. Kakaee, S. I. Essa, S. Seyedzadeh, M. Mokhtar, S. B. Anas, and R. K. Sahbudin, “Proposal of multi-service (ms) code to differentiate quality of services for ocdma systems,” in *2014 IEEE 5th International Conference on Photonics (ICP)*, Sept 2014, pp. 176–178.

[48] C.-C. Yang and J.-F. Huang, “Two-dimensional m-matrices coding in spatial/frequency optical cdma networks,” *IEEE Photonics Technology Letters*, vol. 15, no. 1, pp. 168–170, Jan 2003.

[49] J.-F. Huang and C.-C. Yang, “Permuted m-matrices for the reduction of phase-induced intensity noise in optical cdma network,” *IEEE Transactions on Communications*, vol. 54, no. 1, pp. 150–158, Jan 2006.

[50] C.-H. Lin, J. Wu, and C.-L. Yang, “Noncoherent spatial/spectral optical cdma system with two-dimensional perfect difference codes,” *Journal of Lightwave Technology*, vol. 23, no. 12, pp. 3966–3980, Dec 2005.

[51] B. C. Yeh, C. H. Lin, C. L. Yang, and J. Wu, “Noncoherent spectral/spatial optical cdma system using 2-d diluted perfect difference codes,” *Journal of Lightwave Technology*, vol. 27, no. 13, pp. 2420–2432, July 2009.

[52] C.-M. Tsai, “Optical wavelength/spatial coding system based on quadratic congruence code matrices,” *Photonics Technology Letters, IEEE*, vol. 18, no. 17, pp. 1843–1845, Sept 2006.

[53] C.-C. Yang, “The application of spectral-amplitude-coding optical cdma in passive optical networks,” *Optical Fiber Technology*, vol. 14, no. 2, pp. 134 – 142, 2008. [Online]. Available: http://www.sciencedirect.com/science/article/pii/S1068520007000612

[54] S. P. Tseng, J. Wu, and W. H. Yang, “Two-dimensional spectral/spatial fiber-optic cdma pon with ems/epd codes,” *IEEE Transactions on Communications*, vol. 60, no. 11, pp. 3451–3460, November 2012.

[55] B. C. Yeh, C. H. Lin, and J. Wu, “Noncoherent spectral/spatial ocdma system using two-dimensional hybrid codes,” *IEEE/OSA Journal of Optical Communications and Networking*, vol. 2, no. 9, pp. 653–661, September 2010.

[56] M. K. Abdullah, F. N. Hasoon, S. Aljunid, and S. Shaari, “Performance of {OCDMA} systems with new spectral direct detection (sdd) technique using enhanced double weight (edw) code,” *Optics Communications*, vol. 281, no. 18, pp. 4658 – 4662, 2008.

[57] H. Y. Ahmed, M. Almaleeh, H. Fadhil, S. Aljunid, A. Elyass, and N. Saad, "Performance analysis of spectral-amplitude-coding optical {CDMA} systems with new subtract exclusive {OR} detection (sed) using vectors combinatorial (vc) code," *Optik - International Journal for Light and Electron Optics*, vol. 123, no. 15, pp. 1352 – 1359, 2012.

[58] M. H. Kakaee, S. Seyedzadeh, H. A. Fadhil, S. B. A. Anas, and M. Mokhtar, "Development of multi-service (ms) for sac-ocdma systems," *Optics & Laser Technology*, vol. 60, no. 0, pp. 49 – 55, 2014.

[59] S. A. Aljunid, Z. Zan, A. Anas, S. Barirah, M. Abdullah *et al.*, "A new code for optical code division multiple access systems," *Malaysian Journal of Science*, vol. 17, no. 2, pp. 30–39, 2004.

[60] A. Mohammed, N. Saad, S. A. Aljunid, A. Safar, and M. Abdullah, "Optical spectrum cdma: a new code construction for double weight code family," in *Communications and Information Technologies, 2006. ISCIT'06. International Symposium on.* IEEE, 2006, pp. 812–815.

[61] A. Zahid, F. Hasoon, and S. Shaari, "New code structure for enhanced double weight (edw) code for spectral amplitude coding ocdma system," in *Future Computer and Communication, 2009. ICFCC 2009. International Conference on*, April 2009, pp. 658–661.

[62] F. Hasoon, S. Aljunid, M. Abdullah, and S. Shaari, "Enhanced double weight code implementation in multi-rate transmission," *International jornal of computer science and network security*, vol. 7, no. 11, 2007.

[63] I. S. Hmud, F. N. Hasoon, and S. Shaari, "Optical cdma system parameters limitations for and subtraction detection scheme under enhanced double weight (edw) code based on simulation experiment," *Optica Applicata*, vol. 40, no. 3, pp. 669–676, 2010.

[64] A. Z. G. Zahid, F. N. Hasoon, H. Bakarman, and S. Shaari, "Implementing edw in point to multipoint optical access network for ftth applications," in *Communications (MICC), 2009 IEEE 9th Malaysia International Conference on.* IEEE, 2009, pp. 371–375.

[65] F. A. Hatim, F. N. Hasoon, and S. Shaari, "Effects of nonlinear stimulated brillouin scattering on performance analysis of an optical cdma transmission system," *Journal of optical communications*, vol. 30, no. 2, pp. 104–108, 2009.

[66] S. Aljunid, M. Samad, M. Othman, M. Hisham, A. Kasiman, and M. Abdullah, "Development of modified double-weight code and its implementation in multi-rate transmissions," in *Networks, 2005. Jointly held with the 2005 IEEE 7th Malaysia International Conference on Communication., 2005 13th IEEE International Conference on*, vol. 1. IEEE, 2005, pp. 5–pp.

[67] H. Dayang and S. A. Aljunid, "Optical code division multiple access (ocdma) using double weight (dw) codes for local area network," in *Computer and Communication Engineering (ICCCE), 2010 International Conference on.* IEEE, 2010, pp. 1–3.

[68] Z. Zan, S. Aljunid, M. Yaacob, M. Abdullah, and S. Shaari, "Design configuration of encoder and decoder modules for modified double weight (mdw) code spectral amplitude coding (sac) optical code division multiple access (ocdma) based on fiber bragg gratings," in *Advanced Optoelectronics and Lasers, 2005. Proceedings of CAOL 2005. Second International Conference on*, vol. 2. IEEE, 2005, pp. 249–252.

[69] I. S. Hmud, F. N. Hasoon, and S. Shaari, "And subtraction detection scheme performance analysis based on enhanced double weight code."

[70] S. Aljunid, R. B. Ahmad, and H. A. Fadhil, "Complementary detection technique to performance analysis of rz&nrz on mdw code in ftth network," *International Journal of Computer Applications*, vol. 21, no. 10, pp. 9 – 13, 2011.

[71] M. Norazimah, S. Aljunid, H. Fadhil, and A. Md Zain, "Analytical comparison of various sac-ocdma detection techniques," in *Photonics (ICP), 2011 IEEE 2nd International Conference on*, Oct 2011, pp. 1–5.

[72] H. M. R. Al-Khafaji, S. A. Aljunid, A. Amphawan, and H. A. Fadhil, "Improving spectral efficiency of sac-ocdma systems by spd scheme," *IEICE Electronics Express*, vol. 9, no. 24, pp. 1829–1834, 2012.

[73] H. M. Al-Khafaji, A. SA, A. Amphawan, and H. A. Fadhil, "Soa/spd-based incoherent sac-ocdma system at 9× 5gbps," *IEICE Electronics Express*, vol. 10, no. 5, pp. 20 130 044–20 130 044, 2013.

[74] A. Arief, S. A. Aljunid, M. Anuar, M. Junita, R. Ahmad, and F. Ghani, "Enhanced performance of new family modified double weight codes spectral amplitude coding optical cdma system network," in *Control System, Computing and Engineering (ICCSCE), 2011 IEEE International Conference on.* IEEE, 2011, pp. 488–494.

[75] A. Arief, S. Aljunid, M. Anuar, M. Junita, and R. Ahmad, "Cardinality enhancement of spectral/spatial modified double weight code optical code division multi-access system by {PIIN} suppression," *Optik - International Journal for Light and Electron Optics*, vol. 124, no. 19, pp. 3786 – 3793, 2013. [Online]. Available: http://www.sciencedirect.com/science/article/pii/S0030402613000375

[76] A. Arief, S. Aljunid, M. Anuar, M. Junita, R. Ahmad, and F. Ghani, "Apd impact on spatial/spectra modified double weight codes optical code division multiple access systems," in *Photonics (ICP), 2012 IEEE 3rd International Conference on*. IEEE, 2012, pp. 307–311.

[77] A. Arief, S. AlJunid, M. Anuar, M. Junita, R. Ahmad, and F. Ghani, "Phase-induced intensity noise suppression wavelength-time modified double weight codes optical code division multiple access systems," in *Photonics (ICP), 2012 IEEE 3rd International Conference on*. IEEE, 2012, pp. 275–279.

[78] N. D. Keraf, S. Aljunid, A. Arief, M. Anuar, C. Rashidi, P. Ehkan, and M. Nurol, "An optimal cardinality of wavelength/time incoherent ocdma system using 2-d hybrid fcc-mdw code," in *Electronic Design (ICED), 2014 2nd International Conference on*. IEEE, 2014, pp. 356–361.

[79] N. D. Keraf, S. Aljunid, A. Arief, M. Nurol, M. Anuar, C. Rashidi, and P. Ehkan, "Noise mitigation for ocdma system with wavelength/time 2d hybrid code," in *Photonics (ICP), 2014 IEEE 5th International Conference on*. IEEE, 2014, pp. 166–168.

[80] I. S. Ahmed, S. A. Aljunid, C. B. M. Rashidi, and L. A. K. A. Dulaimi, "Performance analysis of 2-d mdw ocdma code with nrz and rz data formats," in *2016 3rd International Conference on Electronic Design (ICED)*, Aug 2016, pp. 159–163.

[81] H. A. Bakarman, F. N. Hasoon, S. Shaari, and M. Ismail, "Security enhancement for spectral amplitude coding ocdma based on hybrid edw/m seq. code systems," in *Computer and Communication Engineering (ICCCE), 2010 International Conference on*, May 2010, pp. 1–5.

[82] M. Nurol, A. Arief, M. Anuar, S. Aljunid, N. Din Keraf, and S. Arif, "Performance analysis of 2-d extended-edw code for optical cdma system," in *Electronic Design (ICED), 2014 2nd International Conference on*, Aug 2014, pp. 287–292.

[83] A. Z. G. Zahid, J. Mandeep, P. S. Menon, H. Bakarman, F. N. Hasoon, A. A. A. Bakar, and M. A. M. Ali, "Performance analysis of multi-weight 2d-ocdma tedw," in *Photonics (ICP), 2012 IEEE 3rd International Conference on.* IEEE, 2012, pp. 204–209.

[84] M. Noshad and K. Jamshidi, "Code family for modified spectral-amplitude-coding ocdma systems and performance analysis," *Optical Communications and Networking, IEEE/OSA Journal of*, vol. 2, no. 6, pp. 344–354, June 2010.

[85] H. A. Fadhil, S. Aljunid, and R. Ahmad, "Performance of random diagonal code for {OCDMA} systems using new spectral direct detection technique," *Optical Fiber Technology*, vol. 15, no. 3, pp. 283 – 289, 2009.

[86] S. Kumawat and M. R. Kumar, "Generalized optical code construction for enhanced and modified double weight like codes without mapping for sacocdma systems," *Optical Fiber Technology*, vol. 30, pp. 72 – 80, 2016.

[87] H. FADHIL, S. A. Aljunid, and R. AHMAD, "Multi-rate transmissions on spectral amplitude coding optical code division multiple access system using random diagonal codes," in *Optica Applicata*, vol. XXXIX, no. 2, 2009, pp. 225–232.

[88] F. N. Hasoon, S. A. Aljunid, M. K. Abdullah, and S. Shaari, "Multi-rate transmissions on sac-ocdma system using new enhancement double-weight (edw) codes," in *2006 2nd International Conference on Information Communication Technologies*, vol. 2, 2006, pp. 2047–2050.

Publications from the Thesis Work

Journals (Accepted/Communicated)

1. Soma Kumawat, M. Ravi Kumar, "Generalized Optical Code construction for Enhanced and Modified Double Weight like Codes without mapping for SAC-OCDMA systems," Optical Fiber Technology, vol. 30, pp. 72-80, 2016.

2. Soma Kumawat, M. Ravi Kumar, "Development of ZCCC for multimedia service using SAC-OCDMA systems," Optical Fiber Technology, vol. 39, pp. 12-20, 2017.

3. Soma Kumawat, M. Ravi Kumar, "Design of Variable Weight code for multimedia service in SAC-OCDMA systems," IET Optoelectronics, vol.12 (2), pp. 56-64, 2018.

Conference Proceedings

1. Soma Kumawat, M. Ravi Kumar, "Design and Analysis of Different Decoders for SAC-OCDMA Systems.," Proceedings of the International Conference on Recent Cognizance in Wireless Communication & Image Processing (ICRCWIP-2014), Springer, New Delhi DOI:doi.org/10.1007/978-81-322-2638-3$_{49}$.

2. Soma Kumawat, M. Ravi Kumar, "Analysis of Diagonal Eigenvalue Unity (DEU) code for Spectral Amplitude Coding OCDMA systems using Direct Detection technique," 2015 International Conference on Microwave, Optical and Communication Engineering (ICMOCE), Bhubaneswar, 2015, pp. 45-48. DOI: 10.1109/ICMOCE.2015.7489687

3. Soma Kumawat, M. Ravi Kumar, "A new code construction algorithm based on Double Weight codes for SAC-OCDMA systems," 2017 International Conference on Computer, Communications and Electronics (Comptelix), Jaipur, 2017, pp. 1-6. DOI: 10.1109/COMPTELIX.2017.8003927.

4. Soma Kumawat, M. Ravi Kumar, "A new technique to construct Zero cross correlation code for SAC-OCDMA," Optical and Wireless Technologies (OWT), Jaipur, 2017. DOI: 10.1007/978-981-10-7395-3_4.

5. Soma Kumawat, M. Ravi Kumar, "2D code construction using DW code families for SAC-OCDMA systems," TENCON, Malaysia, 2017. DOI: 10.1109/TENCON.2017.8228273

6. Soma Kumawat, M. Ravi Kumar, "A review on code families for a SAC-OCDMA systems," Optical and Wireless Technologies (OWT), Jaipur, 2018.

7. Soma Kumawat, M. Ravi Kumar, "2D Spectral/Spatial code construction for SAC-OCDMA system," ICRAIE, Jaipur, 2018, communicated.

Author's Resume

S. Kumawat received B.E. degree in Electronics & communication in 2004 from MAIET Jaipur, MTech degree in communication in 2011 from MNIT Jaipur. She is pursuing her Phd on Optical CDMA codes from MNIT Jaipur. Her research interests include optical communication, Coding, visible light communication and free space communication.